European air quality maps for 2015

PM_{10}, $PM_{2.5}$, Ozone, NO_2 and NO_x spatial estimates and their uncertainties

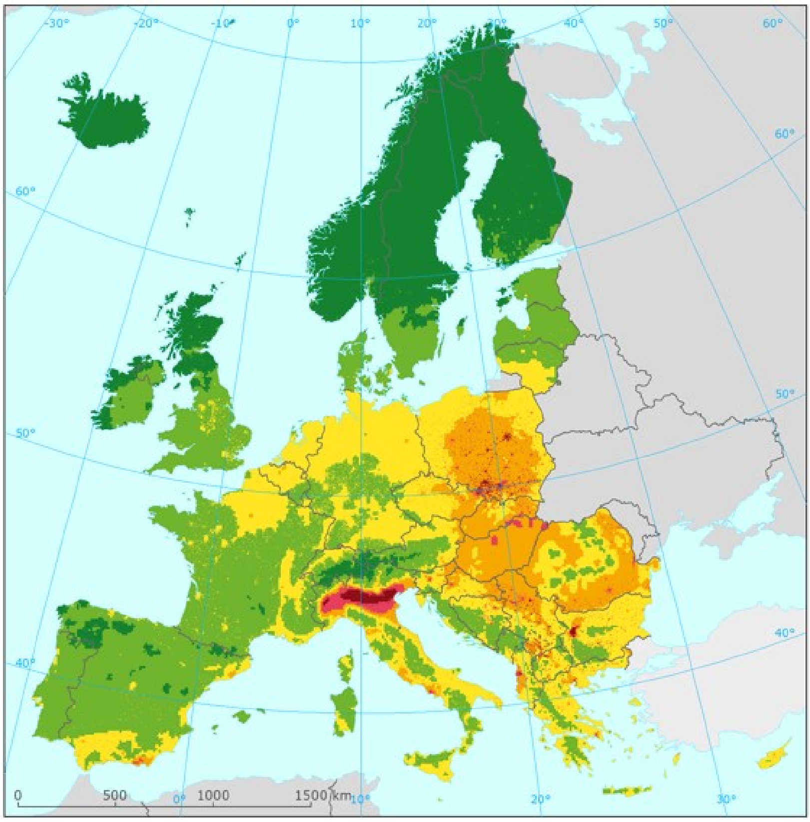

ETC/ACM Technical Paper 2017/7

February 2018

Jan Horálek, Peter de Smet, Frank de Leeuw,
Pavel Kurfürst, Nina Benešová

The European Topic Centre on Air Pollution and Climate Change Mitigation (ETC/ACM)
is a consortium of European institutes under contract of the European Environment Agency
RIVM Aether CHMI CSIC EMISIA INERIS NILU ÖKO-Institut ÖKO-Recherche PBL UAB UBA-V VITO 4Sfera

Front page picture:
Concentration map of $PM_{2.5}$ annual average for the year 2015. Spatially interpolated concentration field. Units: $\mu g \cdot m^{-3}$. (Map 3.1 of this paper.)

Author affiliation:
Jan Horálek, Pavel Kurfürst, Nina Benešová: Czech Hydrometeorological Institute (CHMI), Prague, Czech Republic
Peter de Smet, Frank de Leeuw: National Institute for Public Health and the Environment (RIVM), Bilthoven, The Netherlands

Refer to this document as:
Horálek J, De Smet P, De Leeuw F, Kurfürst P, Benešová N (2018). European air quality maps for 2014. ETC/ACM Technical paper 2017/7.
http://acm.eionet.europa.eu/reports/ETCACM_TP_2017_7_AQMaps2015

DISCLAIMER

ETC/ACM Technical Paper 2017/7
European Topic Centre on Air Pollution and Climate Change Mitigation
PO Box 1
3720 BA Bilthoven
The Netherlands
Phone +31 30 2748562
Fax +31 30 2744433
Email etcacm@rivm.nl
Website http://acm.eionet.europa.eu/

Contents

Executive summary

European air quality concentrations maps have been prepared for the year 2015. The maps are based on air quality data as reported under the air quality directive by EEA member and cooperating countries. Concentration maps have been produced to assess the situation with respect to the most stringent air quality limit values and indicators most relevant for the assessment of impacts on human health and vegetation.

The mapping method follows the methodology developed earlier (Horálek et al, 2017b, 2017c, and reference citied therein); it combines the monitoring data with supplementary data (such as the results from a chemical dispersion model, meteorological and geographical data). The method ('residual kriging') is a linear regression model followed by kriging of the residuals produced from that model. This methodology has been applied systematically during the past 10 years which enable the evaluation of changes in exposure over time.

Population exposure

Concentrations of particulate matter continued to exceed the EU and WHO standards in large parts of Europe. 6.3% of the European population is exposed to levels above the EU $PM_{2.5}$ limit value of 25 $\mu g \cdot m^{-3}$; 80.8% of the European population is exposed to levels above the WHO $PM_{2.5}$ Air Quality Guideline of 10 $\mu g \cdot m^{-3}$ (Table 3.1). Figure ES.1 indicates that in 7 (eastern European) countries more than 50% of the population is exposed to concentrations above the PM_{10} daily limit value. The concentrations of $PM_{2.5}$ and PM_{10} are often highly correlated, the highest $PM_{2.5}$ exposures are also found in the eastern parts.

Figure ES.1 PM_{10} concentrations in relation to the daily limit value (50 $\mu g \cdot m^{-3}$) in 2015. The box plots show for each country, the concentration to which 2, 25, 75 and 98% of the population is exposed. The marker corresponds to the concentration to which 50% of the population is exposed.

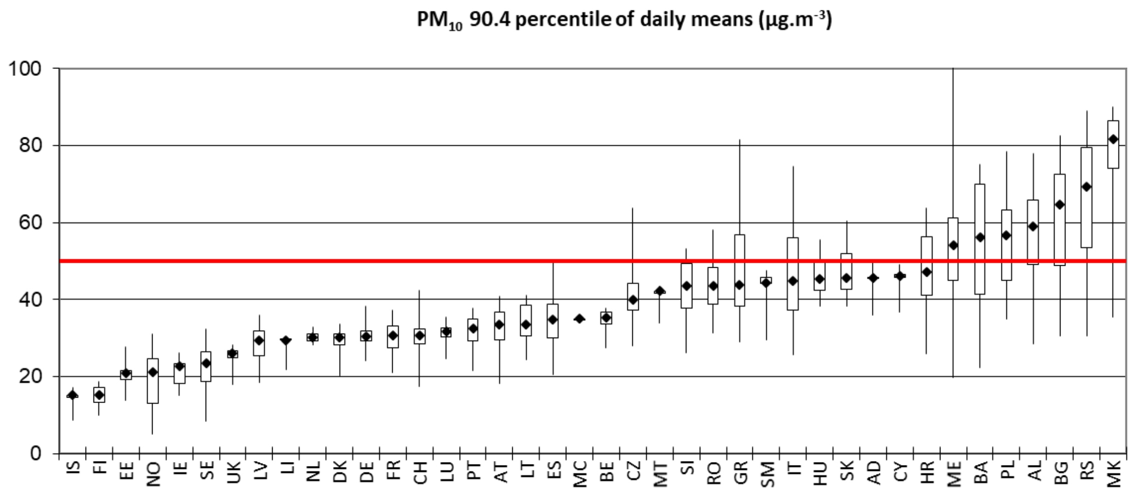

The NO_2 annual mean concentration map shows a different spatial distribution than the PM-maps. Table 5.1 indicates that in 25 countries a limited fraction of the population (3.2% in total) is exposed to concentrations above the annual limit value of 40 $\mu g \cdot m^{-3}$. Figure ES.2 shows that with the exception of 5 countries, the median exposure is less than half the limit value. High exposures are observed in the larger conurbations (e.g. greater London, the Benelux-Ruhr area, Po valley, Naples, Paris, Madrid).

Figure ES.2 NO_2 concentrations in relation to the annual limit value (40 µg·m^{-3}) in 2015. The box plots show for each country, the concentration to which 2, 25, 75 and 98% of the population is exposed. The marker corresponds to the concentration to which 50% of the population is exposed.

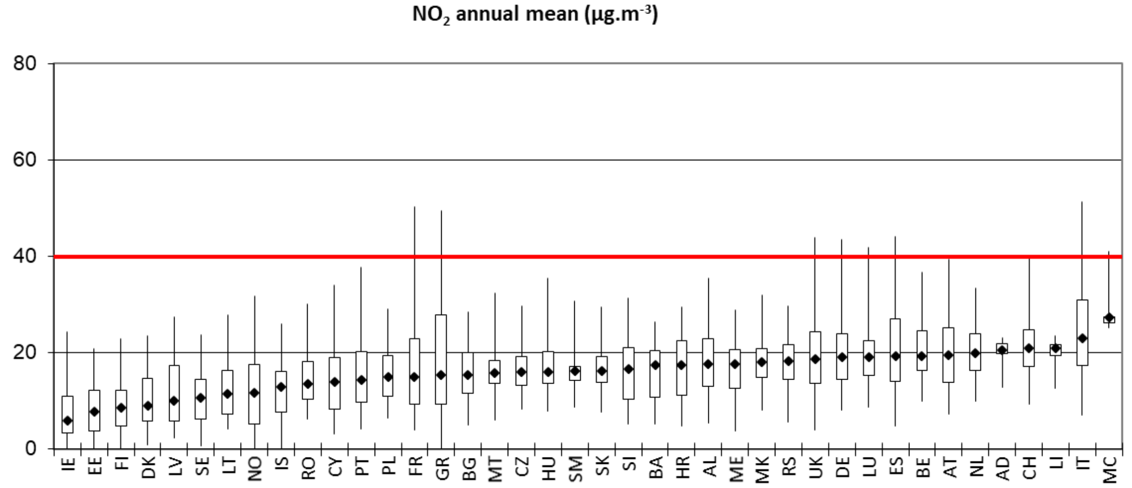

Exposure to ozone concentrations above the EU target value (a maximum daily 8-hour average value of 120 µg·m^{-3} not to be exceeded on more than 25 days per year is widespread (Figure ES.3). 34% of the Europeans live in areas where the ozone TV is exceeded. The highest ozone concentrations are observed in southern Europe.

Figure ES.3 Ozone concentrations in relation to the daily target value (120 µg·m^{-3}) in 2015. The box plots show for each country, the concentration to which 2, 25, 75 and 98% of the population is exposed. The marker corresponds to the concentration to which 50% of the population is exposed.

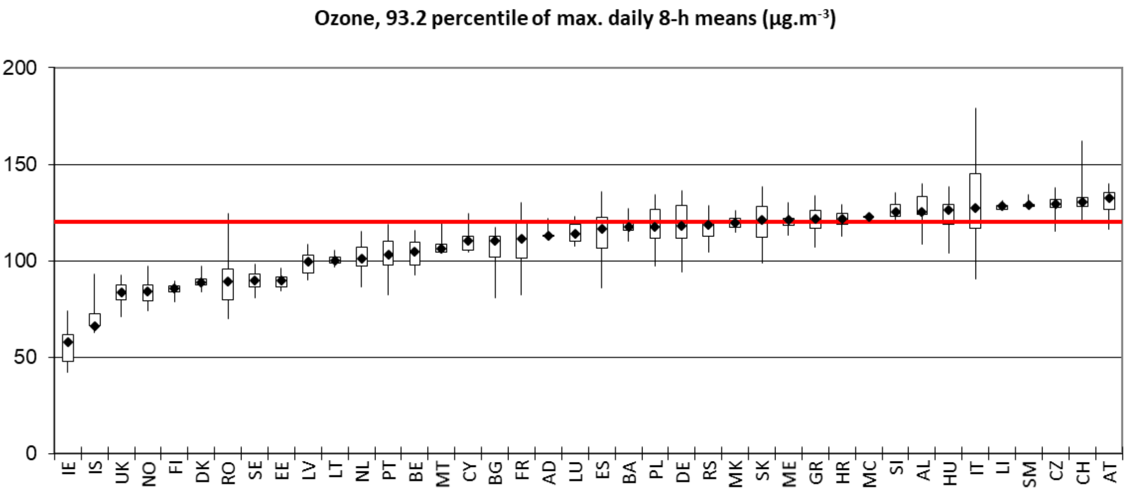

Accumulated risks

Although the spatial distributions of PM, NO_2 and ozone concentrations differs widely, the possibility of an accumulation of risk resulting from high exposures to all three pollutants cannot be excluded. Combining the maps of the three most frequently exceeded standards (PM_{10} daily limit value, NO_2 annual limit value and ozone target value) shows that out of the total population of 536 million in the model area, 8.9% (47.5 million) lives in areas where 2 or 3 air quality standards are exceeded; 3.9

million people live in areas where all three standards are exceeded. The worst situation is observed in Italy (Po valley): 3.7 million inhabitants live in areas where the three standards are breached.

Changes over time

Since 2005 the maps have been prepared in a consistent way. This enables an analysis of changes in exposure over time. The PM concentrations show a steady decrease of about 0.7 µg·m^{-3} per year (PM_{10} annual average) and 0.3 µg·m^{-3} per year ($PM_{2.5}$ annual average, Figure ES.4). For the ozone concentration (expressed as SOMO35, Figure ES.4) a small decreasing trend is observed, in spite of the year-to-year variability.

Figure ES.4 Changes in population averaged concentrations of $PM_{2.5}$ (annual mean) and ozone (SOMO35)

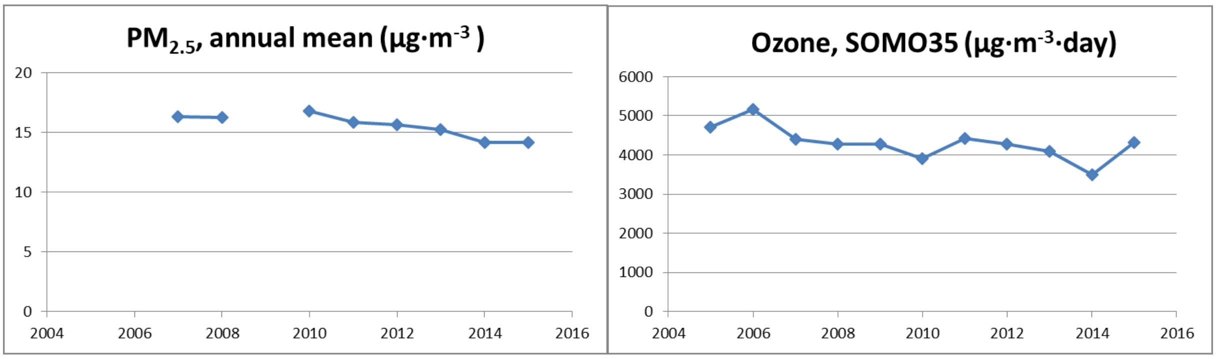

Vegetation exposure

Standards for the protection of vegetation have been set, among others, for NO_x and ozone. In a limited number of cases the NO_x critical level has been exceeded. A larger impact on vegetation can be expected from the direct exposure to ozone. The target value for the protection of vegetation (AOT40) is exceeded in about 30% of the agricultural areas. The long-term objective is exceeded in 80% of the agricultural area. The vegetation-weighted concentration tends to decrease over the period 2005–2015.

1 Introduction

This paper provides an update of European air quality concentration maps, population exposure and vegetation exposure estimates and probabilities of exceeding relevant thresholds for 2015. The analysis is based on interpolation of annual statistics of monitoring data from 2015, reported by EEA member and cooperating countries in 2016. The paper presents mapping results and includes an uncertainty analysis of the interpolated maps, adopting the latest methodological developments, see Horálek et al. (2017b, 2017c) and reference citied therein.

We consider in this paper PM_{10}, $PM_{2.5}$, ozone, NO_2 and NO_x for 2015, being the most relevant pollutants for annual updating. The analysis method applied is similar to that of previous years. Another potentially relevant pollutant, benzo[a]pyrene (BaP), is not presented, as the station coverage is not dense enough for enabling the regular mapping. The current status of mapping the BaP concentrations in Europe was discussed by Guerreiro et al. (2015) and Horálek et al. (2017a).

The mapping method is based primarily on air quality measurements. It combines monitoring data, chemical transport model results and other supplementary data (such as altitude and meteorology). The method is a linear regression model followed by kriging of the residuals produced from that model ('residual kriging'). It should be noted that the applied methodology does not allow for formal compliance checking with limit or target values in line with the air quality directive.

The maps of health related indicators of PM_{10}, $PM_{2.5}$, and ozone are created for the rural and urban (including suburban) background areas separately on a grid at 10x10 km resolution. Subsequently, the rural and urban background maps are merged into one final combined air quality indicator map using a 1x1 km population density grid, following a weighting criterion applied per grid cell. This fine resolution takes into account the smaller urbanisations in the European context that are not resolved at the 10x10 km grid resolution. The map of health related indicator of NO_2 is constructed by improved methodology developed in Horálek et al. (2017c): next to the rural and urban background map layers, the urban traffic map layer is constructed and incorporated into the final merged map using the road data; all separate map layers are created just at 1x1 km resolution; land cover and road data are included in the mapping process as supplementary data. The maps of vegetation related ozone and NO_x indicators are at a grid resolution of 2x2 km and based on rural background measurements; in the case of ozone they serve as input to EEA's core set indicator CSI005 (EEA, 2017d).

Next to the annual indicator maps, we present in tables the population exposure to PM_{10}, $PM_{2.5}$, ozone, and NO_2, and the exposure of vegetation to ozone. Tables of population exposure are prepared using the final combined maps and the population density map of 1x1 km grid resolution. For NO_2, the population exposure in each grid cell is calculated separately for urban areas directly influenced by traffic and for the background (both rural and urban) areas, in order to better reflect the population exposed to traffic emissions. The tables of the vegetation exposure are prepared with a 2x2 km grid resolution based on the Corine Land Cover 2006.

Chapters 2, 3, 4 and 5 present the concentration maps and exposure estimates for PM_{10}, $PM_{2.5}$, ozone and NO_2, respectively. Chapter 5 presents the concentration map for NO_x; exceedances of the critical level for the protection of vegetation occur in very limited areas and, as such, it is considered not to provide relevant information from the European scale perspective. Chapter 6 summarizes the trends in exposure estimates in the period 2005 – 2015 (2007 – 2015 for $PM_{2.5}$).

Annex 1 describes briefly the different methodological aspects. Annex 2 documents the input data applied in the 2015 mapping and exposure analysis. Annex 3 presents the technical details of the maps and their uncertainty analysis including the cross-validation results and the maps of probability of exceedance of limit/target values. Annex 4 shows the inter-annual changes including the inter-annual difference maps between 2014 and 2015, the variations in population exposure in the period 2005 –

2015 for PM_{10} and ozone, resp. 2007 – 2015 for $PM_{2.5}$ and 2013 – 2015 for NO_2, and the results of the trend analysis for these relevant periods. Annex 5 presents the concentration maps including the station points, in order to provide more complete information of the air quality in 2015 across Europe.

2 PM_{10}

The Ambient Air Quality Directive (EU, 2008) sets limit values for long-term and for short-term PM_{10} concentrations. The long-term annual PM_{10} limit value is set at 40 µg·m^{-3}. The short-term limit value is that the daily average PM_{10} concentration should not exceed 50 µg·m^{-3} during more than 35 days per year. This daily limit value is most frequently exceeded in Europe. It corresponds to the 90.4 percentile of daily PM_{10} concentrations in one year. The Air Quality Guideline recommended by the World Health Organization (WHO, 2005) for the PM_{10} annual average is 20 µg.m^{-3}.

This chapter presents the 2015 updates of the two PM_{10} indicators: annual average and the 90.4 percentile of the daily averages. The latter is a more relevant indicator in the context of the AQ Directive (EU, 2008) than the formerly used 36th highest daily mean (Horálek et al., 2016b). The separate rural and urban background concentration maps are calculated on the 10x10 km resolution grid and the subsequent final combined concentration map is based on the 1x1 km gridded population density map. All maps here are presented in this 1x1 km grid resolution. The population exposure tables are calculated based on these maps in this resolution.

Annex 3 provides details on the regression and kriging parameters applied for deriving the maps of the two PM_{10} indicators, as well as the uncertainty analysis of the maps. Annex 4 discusses briefly the inter-annual changes observed in the concentration maps and the relevant population exposure.

2.1 PM_{10} annual average

2.1.1 Concentration map

Map 2.1 presents the final combined concentration map for the 2015 PM_{10} annual average as the result of interpolation and merging of the separate maps as described in Annex 1 (for a more detailed description see Horálek et al., 2007, and De Smet et al 2011). Red and purple areas indicate exceedances of the limit value (LV) of 40 µg·m^{-3}.

The most relevant linear regression submodel for the use of the PM_{10} mapping has been identified earlier in Horálek et al. (2008) and De Smet et al. (2009, 2010, 2011). Supplementary data used in the linear regression for rural areas consisted of EMEP model output, altitude, wind speed and surface solar radiation and for urban background areas it was EMEP model output only (Annex 3, Section A3.1). The linear regression and ordinary kriging on its residuals is applied on the logarithmically transformed data of both measurement and modelled PM_{10} values.

The final combined concentration map presented in Map 2.1 is presented on a 1x1 km grid resolution (Annex 1). The station points are not presented in the map, in order to better visualise the urban areas. However, concentration values from measurements at the station points used in the kriging interpolation methodology (Annex 3) are considered to provide relevant information. In Map A5.1 of Annex 5 these point values are presented on top of Map 2.1 and illustrate the smoothing effect the interpolation methodology can have on the gridded concentration fields.

Map 2.1 shows LV exceedances in southern Spain near Almeria, in some urban areas of Bulgaria with high concentrations at Sofia, in urban areas of northern FYR of Macedonia, Kosovo[1] and the

[1] In this paper references to Kosovo shall be understood to be in the context of UN Security Council Resolution 1244/99.

agglomerations Thessaloniki and Athens in Greece. The extent of the exceeded area near Almeria and at Sofia is larger in 2015 compared to 2014. Contrary to that, one may observe a clear reduction at the Ostrava–Katowice region of southern Poland and north-eastern Czech Republic. Overall, there are slight improvements in northern Europe, slight increases in concentrations observed in the Po Valley and Spain, with rather similar patterns in western, south-western, eastern and south-eastern Europe.

The uncertainty of the concentration map can be expressed in relative terms of the absolute Root Mean Square Error (RMSE) uncertainty related to the mean air pollution indicator value for all stations (see Annex 1). This *relative mean uncertainty* (RRMSE) of the final combined map of PM_{10} annual average is 19.4 % for rural areas and 19.2 % for urban areas (Annex 3).

Map 2.1 Concentration map of PM_{10} annual average, 2015

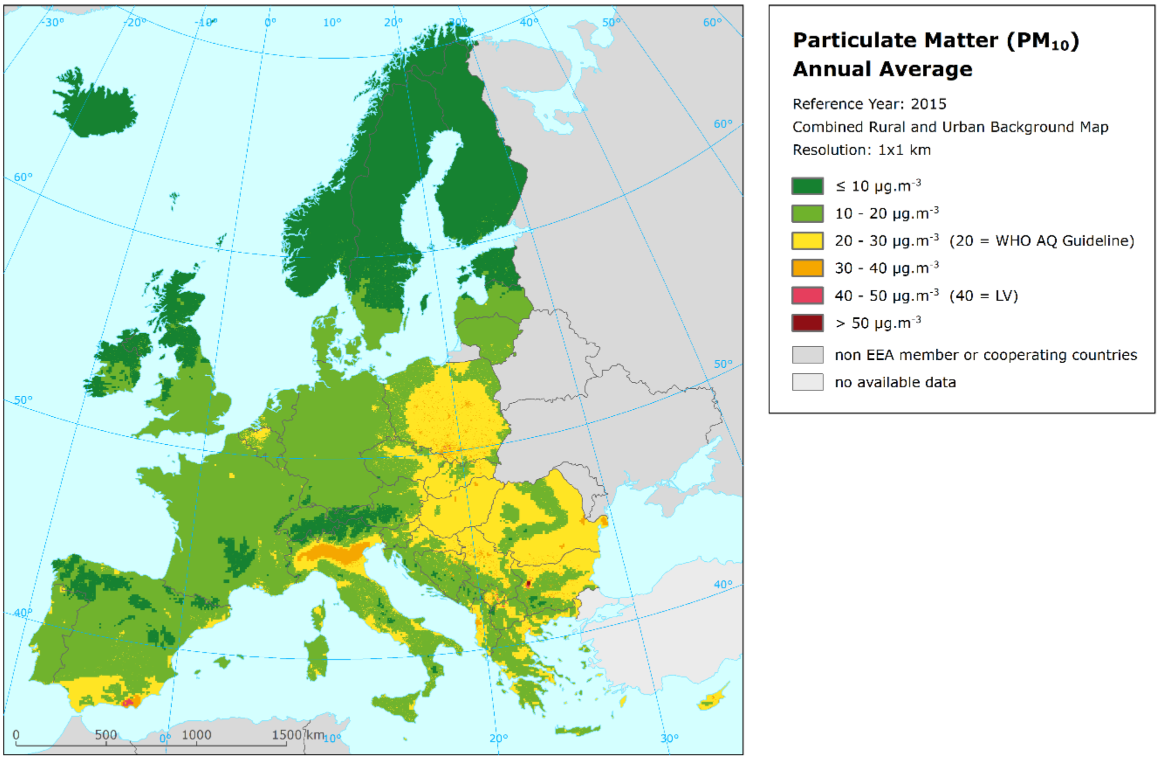

2.1.2 Population exposure

Table 2.1 gives the population frequency distribution for a limited number of exposure classes, as well as the population weighted concentration for individual countries and for Europe as a whole according to Equation A1.7. Annex 4 shows details on the eleven years evolution of population exposure.

About 46 % of the European population (and 45 % of the EU-28 population) has been exposed to annual average concentrations above the Air Quality Guideline of 20 μg.m^{-3} recommended by the World Health Organization (WHO, 2005). CSI004 (EEA, 2017c) estimates that about 53% of the population in urban agglomerations in the EU-28 was exposed in 2015 to levels above the WHO guideline. The latter estimate accounts for the urban population of the EU-28. It therefore represents areas where, in general, considerably higher PM_{10} concentrations occur. The estimates in Table 2.1 account for the total European and EU-28 population, *including* the population in rural areas, smaller cities and villages that are in general exposed to lower levels of PM_{10}.

Table 2.1 Population exposure and population-weighted concentration, PM_{10} annual average, 2015

Country		Population	PM_{10} annual average, exposed population [%]						Population weighted conc.
			< LV				> LV		
		[inhbs . 1000]	< 10 $\mu g.m^{-3}$	10 - 20 $\mu g.m^{-3}$	20 - 30 $\mu g.m^{-3}$	30 - 40 $\mu g.m^{-3}$	40 - 45 $\mu g.m^{-3}$	> 45 $\mu g.m^{-3}$	[$\mu g.m^{-3}$]
Albania	AL	2 892	0.0	6.2	29.3	63.8	0.6		30.2
Andorra	AD	78	0.2	1.6	98.2				24.7
Austria	AT	8 576	2.3	55.2	42.6				18.7
Belgium	BE	11 237		34.4	65.6				20.4
Bosnia & Herzegovina	BA	3 825	0.1	18.7	41.5	39.7	0.0		26.8
Bulgaria	BG	7 202	0.0	4.2	27.8	52.9	14.5	0.7	33.1
Croatia	HR	4 225	0.0	12.6	79.1	8.4			25.1
Cyprus	CY	1 173		0.6	18.8	80.6			31.4
Czech Republic	CZ	10 538	0.0	17.8	74.0	8.2			23.3
Denmark	DK	5 660	0.4	99.6					17.1
Estonia	EE	1 315	21.0	79.0					12.1
Finland	FI	5 472	61.8	38.2					9.1
France (metropolitan)	FR	64 344	0.5	74.4	25.2	0.0			18.2
Germany	DE	81 198	0.1	92.9	7.0				17.8
Greece	GR	10 858		5.6	53.9	35.1	5.4		28.7
Hungary	HU	9 856		0.1	90.2	9.7			26.3
Iceland	IS	329	31.8	68.2					9.7
Ireland	IE	4 629	19.9	80.1					11.9
Italy	IT	60 796	0.2	9.0	65.7	25.2			26.6
Latvia	LV	1 986	1.3	80.0	18.7				16.5
Liechtenstein	LI	37	0.1	99.9					16.3
Lithuania	LT	2 921		64.8	35.2				18.5
Luxembourg	LU	563		92.3	7.7				18.5
Macedonia, FYR of	MK	2 069	0.0	1.7	4.9	63.5	29.9	0.0	37.3
Malta	MT	429		1.3	98.7				26.4
Monaco	MC	38			100.0				23.2
Montenegro	ME	622	0.3	17.0	57.7	22.0	3.0		26.7
Netherlands	NL	16 901		85.1	14.9				18.7
Norway	NO	5 166	40.7	59.3					11.1
Poland	PL	38 006		4.4	44.1	50.1	1.3		29.5
Portugal (excl. Az., Mad.)	PT	9 870	0.3	64.2	35.5				18.7
Romania	RO	19 871		5.5	76.8	17.7			25.7
San Marino	SM	33		7.0	93.0				24.6
Serbia (incl. Kosovo*)	RS	8 919	0.0	3.8	25.9	67.4	2.9	0.0	32.7
Slovakia	SK	5 421		1.1	81.7	17.2			26.3
Slovenia	SI	2 063	0.0	19.8	80.2				23.3
Spain (excl. Canarias)	ES	44 323	0.7	38.3	59.1	1.8	0.1		21.6
Sweden	SE	9 747	20.9	79.1					13.3
Switzerland	CH	8 238	2.5	91.1	6.5				17.4
United Kingdom (& dep.)	UK	64 875	1.9	98.1	0.0				15.1
Total		**536 303**	**2.1**	**52.3**	**33.6**	**11.5**	**0.6**	**0.0**	**21.2**
			54.3				**0.6**		
EU-28		**504 055**	**1.7**	**53.2**	**34.5**	**10.1**	**0.4**	**0.0**	**20.9**
			55.0				**0.4**		

Kosovo*	KS	1 805	0.0	4.0	18.6	64.8	12.6	0.1	34.8
Serbia (excl. Kosovo*)	RS	7 114		3.7	27.6	68.1	0.6		32.2

*) under the UN Security Council Resolution 1244/99

Note 1: Turkey is not included in the calculation due to the lack of air quality data.
Note 2: The percentage value "0.0" indicates that an exposed population exists, but it is small and estimated lesser than 0.05 %. Empty cells mean: no population in exposure.

The population exposure exceeding the EU limit value of 40 µg.m^{-3} is about 0.5 % for the population of the total of European area considered and the EU-28. In Bulgaria and FYR of Macedonia more than 10 % of the population is exposed to concentrations above the LV. A limited fraction of the population (0.1 – 5.9 %) is exposed to concentrations above the LV in Albania, Greece, Montenegro, Poland, Serbia (including Kosovo) and Spain. However, as the current mapping methodology tends to underestimate high values (see Annex 3, Section A3.1), the exceedance percentage will most likely be underestimated. Additional exceedances could therefore be expected in countries like Albania, Bosnia & Herzegovina, Bulgaria, Cyprus, Greece, Italy, Montenegro, Poland, Romania and Slovakia, as a relatively large fraction of the population lives in areas with concentration levels above 30 µg·m^{-3}.

The European-wide population-weighted concentration of the annual average for 2015 is estimated to be about 21 µg·m^{-3}, the same as for the EU-28 only. This is together with year 2014 the lowest level of the eleven years period 2005 – 2015 (Tables 6.1 and A4.1).

Figure 2.1 shows, for the whole mapped area, the population frequency distribution for exposure classes of 1 µg·m^{-3}. One can see the highest population frequency for classes between 16 and 20 µg·m^{-3}. And continuous decline of population frequency for classes between 20 and 40 µg·m^{-3}.

Figure 2.1 Population frequency distribution, PM_{10} annual average, 2015

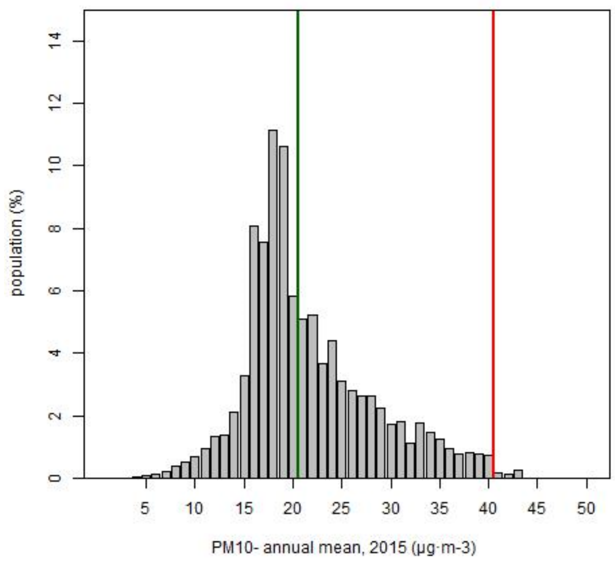

2.2 *PM_{10} – 90.4 percentile of daily means*

The AQ Directive (EU, 2008) describes the PM_{10} daily limit as "daily average 50 µg·m^{-3} not to be exceeded more than 35 times a calendar year". This requirement can be evaluated by the indicator 36th highest daily mean, which is in principle equivalent to the indicator 90.4 percentile of daily means. However, for measurement data these two indicators are equivalent only if no data is missing, which is in general not the case. As shown in de Leeuw (2012), the additional uncertainty related to incomplete time series is substantially smaller when using percentile values instead of the x-th highest value. Furthermore, the AQ Directive requires the use of the 90.4 percentile when random measurements are used to assess the requirements of the PM_{10} daily limit value. As in the previous ETC/ACM Technical Paper 2016/6 with its 2014 maps, we express the PM_{10} daily means as the 90.4 percentile instead of the formerly used 36th highest daily mean.

2.2.1 Concentration map

Map 2.2 presents the final combined map, where red and purple marked areas indicate exceedances of the limit value (LV) of 50 µg·m^{-3} on more than 35 measurement days. The similar mapping procedure as in the case of the annual average is used. The mapping details and the uncertainty analysis are presented in Annex 3. Large areas above the daily LV are observed in northern Italy (i.e. the Po Valley) with elevated values in the region around Venice, in the region with the agglomerations Ostrava – Katowice - Krakow, in north-eastern Hungary, the Almeria region in Spain, southern Romania and northern Serbia. Urban areas with concentrations above the LV are observed in Poland, southern and eastern Romania, Bulgaria, Greece, Albania, FYR of Macedonia, Serbia (including Kosovo), Croatia and Slovenia. In general, the central and the eastern parts of Europe appear with higher concentrations than the western and the northern parts. The intensity of urban areas in exceedance has increased slightly in 2015 compared to 2014.

The *relative mean uncertainty* (relative RMSE) of the final combined map of the 90.4 percentile of PM_{10} daily means is 21.1 % for rural areas and 25.6 % for urban areas (Annex 3).

The final combined map *including* the indicator 90.4 percentile of daily means based on the actual measurement data at station points is presented in Map A5.2 of Annex 5.

Map 2.2 Concentration map of PM_{10} indicator 90.4 percentile of daily means, 2015

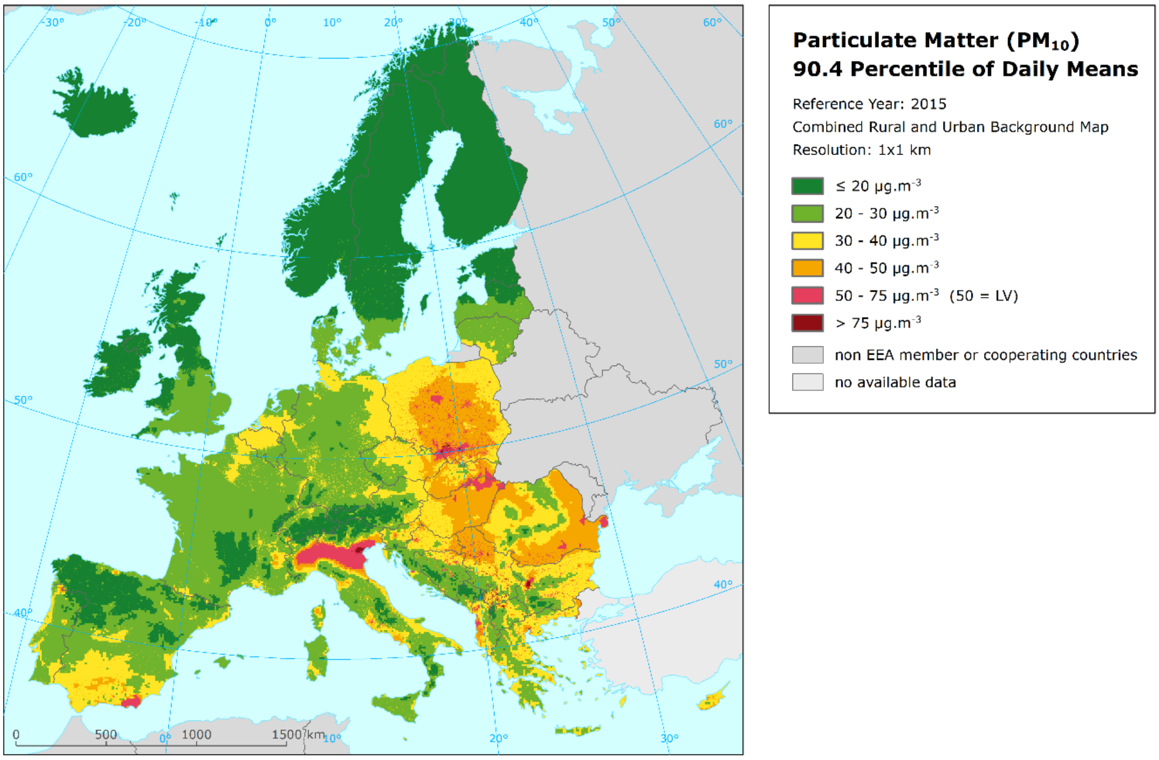

2.2.2 Population exposure

Table 2.2 gives the population frequency distribution for a limited number of exposure classes calculated at 1x1 km grid resolution, as well as the population-weighted concentration for individual countries and for Europe as a whole. Annex 4 shows details on the eleven years evolution of population exposure.

Table 2.2 Population exposure and population-weighted concentrations, PM_{10} indicator 90.4 percentile of daily means, 2015

Country		Population	PM_{10}, 90.4 percentile of daily means, exposed population [%]						Pop. weighted conc.
			< LV				> LV		
			< 20	20 - 30	30 - 40	40 - 50	50 - 75	> 75	
		[inhbs . 1000]	µg.m^{-3}	µg.m^{-3}	µg.m^{-3}	µg.m^{-3}	µg.m^{-3}	µg.m^{-3}	[µg.m^{-3}]
Albania	AL	2 892	0.1	2.8	8.4	15.2	69.7	3.8	56.6
Andorra	AD	78	0.1	0.1	1.6	88.5	9.7		45.7
Austria	AT	8 576	3.3	23.8	68.7	4.2			32.4
Belgium	BE	11 237		4.6	95.4				34.6
Bosnia & Herzegovina	BA	3 825	0.5	9.3	13.5	12.3	62.3	2.1	54.5
Bulgaria	BG	7 202	0.1	1.7	7.7	19.2	54.5	16.9	62.2
Croatia	HR	4 225	0.1	5.4	16.7	35.2	42.5		46.8
Cyprus	CY	1 173		0.3	10.3	89.4			45.2
Czech Republic	CZ	10 538	0.0	4.0	45.3	38.6	12.1		41.6
Denmark	DK	5 660	1.9	45.3	52.8				29.3
Estonia	EE	1 315	28.1	71.9					20.7
Finland	FI	5 472	100.0						15.0
France (metropolitan)	FR	64 344	1.2	43.5	55.1	0.2	0.0		30.2
Germany	DE	81 198	0.2	41.9	57.5	0.4	0.1		30.6
Greece	GR	10 858	0.0	2.6	26.8	41.0	22.8	6.7	48.2
Hungary	HU	9 856			6.1	74.6	19.3		46.2
Iceland	IS	329	98.9	1.1					14.5
Ireland	IE	4 629	34.1	65.9	0.0				21.3
Italy	IT	60 796	0.3	5.6	30.5	31.0	30.8	1.8	47.4
Latvia	LV	1 986	5.6	48.5	45.9				29.0
Liechtenstein	LI	37	0.1	99.9					28.9
Lithuania	LT	2 921		21.1	75.9	3.0			34.0
Luxembourg	LU	563		21.2	78.8				31.1
Macedonia, FYR of	MK	2 069	0.0	1.0	2.2	1.9	24.5	70.4	78.1
Malta	MT	429		0.9	2.7	96			41.7
Monaco	MC	38			100.0				35.0
Montenegro	ME	622	2.5	10.6	8.4	11.1	59.2	8.2	52.9
Netherlands	NL	16 901		47.2	52.8				30.2
Norway	NO	5 166	46.1	47.5	6.4				19.3
Poland	PL	38 006		0.0	9.2	27.7	53.5	9.6	55.7
Portugal (excl. Az., Mad.)	PT	9 870	1.1	29.2	68.5	1.2	0.0		31.8
Romania	RO	19 871		1.3	28.9	50.7	19.2		43.8
San Marino	SM	33		1.9	11.6	86			43.7
Serbia (incl. Kosovo*)	RS	8 919	0.0	1.7	6.4	11.7	45.7	34.5	65.7
Slovakia	SK	5 421		0.1	8.7	58.5	32.8		47.4
Slovenia	SI	2 063	0.0	6.7	28.1	42.6	22.5		42.6
Spain (excl. Canarias)	ES	44 323	1.8	22.2	54.7	19.3	1.9		34.9
Sweden	SE	9 747	27.5	64.2	8.3				22.4
Switzerland	CH	8 238	3.5	36.8	57.6	1.6	0.5		30.1
United Kingdom (& dep.)	UK	64 875	4.9	94.7	0.4	0.0			25.3
Total		**536 303**	**3.5**	**31.9**	**35.7**	**14.2**	**12.6**	**2.2**	**36.9**
			85.3				**14.7**		
EU-28		**504 055**	**3.1**	**32.8**	**36.6**	**14.7**	**11.5**	**1.4**	**36.2**
			87.1				**12.9**		

Note 1: Turkey is not included in the calculation due to the lack of air quality data.
Note 2: The percentage value "0.0" indicates an exposed population exists, but it is small and estimated less than 0.05 %. Empty cells mean: no population in exposure.

It has been estimated that in 2015 almost 15 % of the European population lived in areas where the 90.4 percentile of the PM_{10} daily means exceeded the EU limit value of 50 µg·m^{-3}. In Albania, Bosnia & Herzegovina, Bulgaria, FYR of Macedonia, Montenegro, Poland and Serbia (including Kosovo) the population-weighted indicator concentration was above the LV and more than half of the population was exposed to concentrations exceeding the LV. In Croatia, Greece, Italy and Slovakia the portion of the population living in areas with concentrations above the LV was between 25 and 50 percent.

For the EU-28 around 13% lived in areas where the 90.4 percentile of the PM_{10} daily mean exceeded the EU limit value of 50 µg·m^{-3}. According to CSI004 (EEA, 2017c), in 2015 almost 19 % of the urban population in the EU-28 was exposed to PM_{10} above this limit value. The difference between the two estimates is because the EEA accounts for the urban population of the larger agglomerations only, while Table 2.2 provides estimates also including inhabitants in rural areas, smaller cities and villages.

The European-wide population-weighted concentration of the 90.4 percentile of PM_{10} daily means is estimated for 2015 at about 37 µg·m^{-3}, and 36 µg·m^{-3} for the EU-28. This is the lowest level of the eleven years period 2005 – 2015 (Tables 6.1 and A4.2).

Figure 2.2 shows, for the whole mapped area, the population frequency distribution for exposure classes of 1 µg·m^{-3}. One can see the highest population frequency for classes between 25 and 35 µg·m^{-3}, and continuous decline of population frequency for classes between 35 and 55 µg·m^{-3}.

Like in previous years, also in 2015 the daily limit value is more widely exceeded than the annual limit value.

Figure 2.2 Population frequency distribution, PM_{10} indicator 90.4 percentile of daily means, 2015

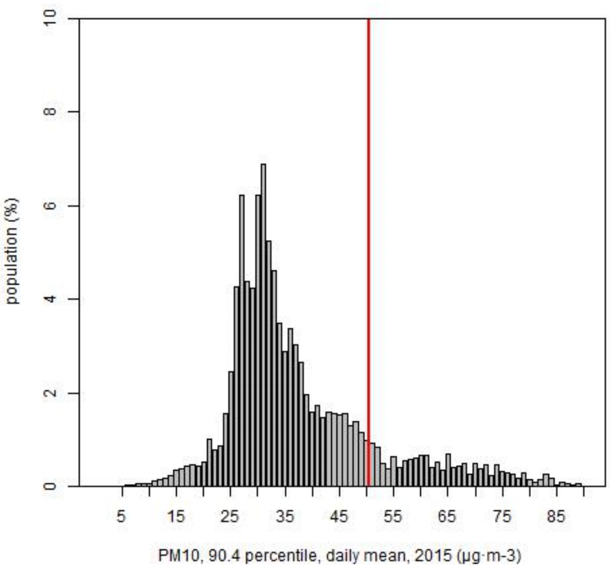

3 $PM_{2.5}$

In the Ambient Air Quality Directive (EU, 2008), the limit value (LV) for the annual average $PM_{2.5}$ concentrations was set at 25 $\mu g \cdot m^{-3}$. In the AQ directive there is also an indicative LV of 20 $\mu g \cdot m^{-3}$ defined as Stage 2 that should become potentially into force in 2020. The Air Quality Guideline recommended by the World Health Organization (WHO, 2005) for the $PM_{2.5}$ annual average is 10 $\mu g.m^{-3}$.

The current number of $PM_{2.5}$ measurement stations is yet limited and its spatial distribution is irregular over Europe. Deriving a reasonably reliable European wide spatially interpolated $PM_{2.5}$ annual average map on the basis of these $PM_{2.5}$ measurement data alone is not feasible. The resulting map would not be suitable for being used in population exposure assessments.

Therefore, in this paper the mapping of the health-related indicator $PM_{2.5}$ annual average is based on a mapping methodology developed in Denby et al. (2011a, 2011b). This methodology derives additional *pseudo* $PM_{2.5}$ annual mean concentrations from PM_{10} annual mean measurement concentrations. As such, it increases the number and spatial coverage of $PM_{2.5}$ 'data points' and these data is used to derive a European wide map of annual mean $PM_{2.5}$. Pseudo $PM_{2.5}$ stations data are estimated using PM_{10} measurement data, surface solar radiation, latitude and longitude. Separate urban and rural background concentration maps are calculated on a grid of 10x10 km resolution and the subsequent final combined concentration map is based on the 1x1 km gridded population density map. The final $PM_{2.5}$ map is presented in this 1x1 km grid resolution. The population exposure table is calculated on basis of this map resolution.

Annex 3 provides details on the regression and kriging parameters applied for deriving the $PM_{2.5}$ annual average map, as well as the uncertainty analysis of the map. Annex 4 discusses briefly the inter-annual changes observed in the concentration maps and the relevant population exposure.

3.1 $PM_{2.5}$ – Annual mean

3.1.1 Concentration map

Map 3.1 presents the final combined map for the 2015 $PM_{2.5}$ annual average as a result of the interpolation and merging of the separate rural and urban map layers. The dark red areas exceed the limit value (LV) of 25 $\mu g \cdot m^{-3}$. Red areas show exceedances of the indicative LV of 20 $\mu g \cdot m^{-3}$ defined as Stage 2.

Supplementary data in the regression used for rural areas consist of EMEP model output, altitude, wind speed, surface solar radiation and population density. The relevant supplementary data for estimating both the pseudo $PM_{2.5}$ station data and the linear regression sub-model with its residual kriging in the rural areas were identified earlier in Denby et al. (2011b). Based on advice of Horálek et al. (2015), EMEP model output is used as supplementary data source for the urban areas. Prior to linear regression and kriging of its residuals, the $PM_{2.5}$ measurement and the modelled pseudo data is logarithmically transformed as that provides better results. After regression, these results are back-transformed.

According to Map 3.1, the areas with the highest $PM_{2.5}$ concentrations seem to be the Krakow - Katowice (PL) – Ostrava (CZ) industrial region, together with the Po Valley in Northern Italy with its high concentrations. Furthermore, the areas around the cities of Warsaw and Lodz in Poland, Sofia in Bulgaria, Tirana in Albania, Belgrade and several other smaller cities in Serbia, Kosovo, FYR of Macedonia and northern Greece also show elevated $PM_{2.5}$ annual average concentrations. Like in the case of PM_{10}, the central and the eastern parts of Europe show higher concentrations than the western and the northern parts.

The *relative mean uncertainty* of the final combined map of $PM_{2.5}$ annual average is 21.9 % for rural areas and 16.6 % for urban areas and determined exclusively on the actual $PM_{2.5}$ measurement data points, i.e. not on the pseudo stations (Annex 3).

Map 3.1 Concentration map of $PM_{2.5}$ annual average, 2015

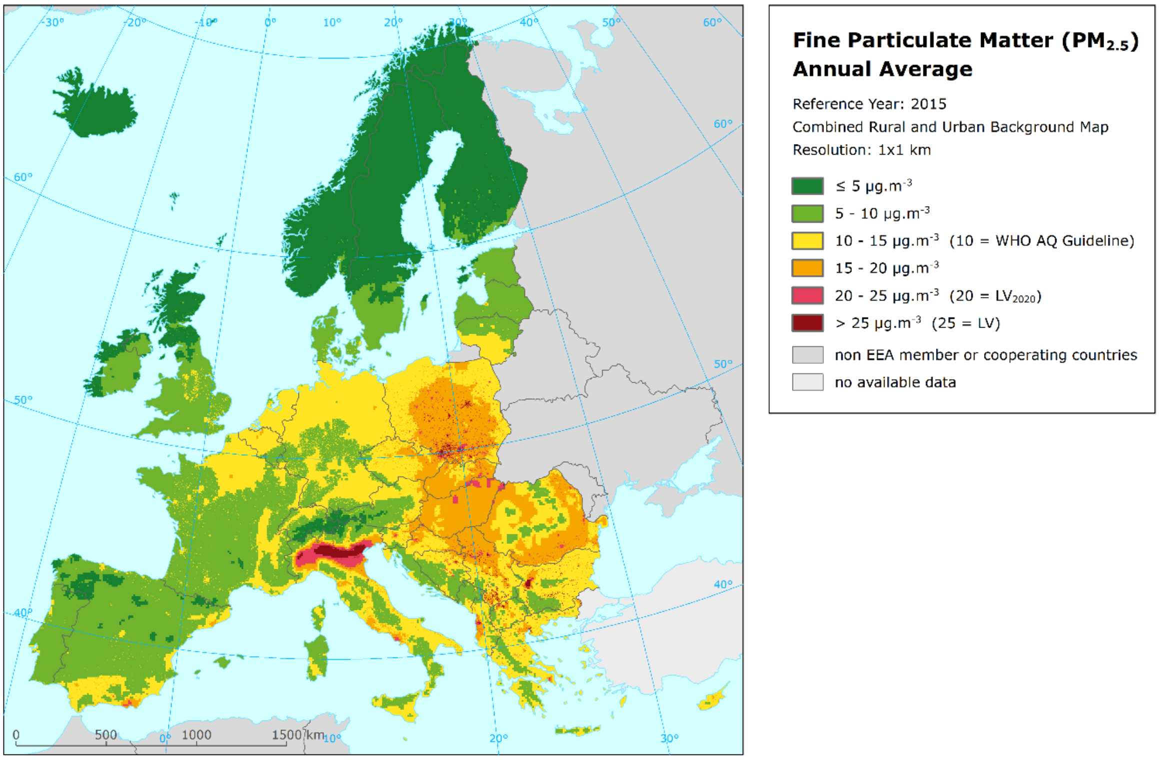

In order to provide more complete information of the air quality across Europe, the final combined map including the measurement data at station points is presented in Map A5.3 of Annex 5.

3.1.2 Population exposure

Table 3.1 gives the population frequency distribution for a limited number of exposure classes calculated on a grid of 1x1 km resolution, as well as the population-weighted concentration for individual countries and for Europe as a whole according to Equation A1.7 of Annex 1. Annex 4 shows details on the nine year evolution of population exposure.

In 2015, almost 81 % of the European population has been exposed to $PM_{2.5}$ annual mean concentrations above the Air Quality Guideline of 10 $\mu g.m^{-3}$ as defined by the World Health Organization (WHO, 2005). The European wide and EU-28 population exposure exceeding the EU limit value (LV) of 25 $\mu g \cdot m^{-3}$ is for both about 6 %. In Bulgaria, FYR of Macedonia, Poland and Serbia (including Kosovo) more than 25 % of the population suffers from exposures above this limit value; in Albania, Bosnia & Herzegovina, Czech Republic, Greece, Italy, Montenegro and Slovakia it is between 1 to 18 %. The indicative Stage 2 limit value LV_{2020} of 20 $\mu g \cdot m^{-3}$ is exceeded for about 14 % (EU-28) and 15 %, (European wide). In Albania, Bosnia & Herzegovina, Bulgaria, Croatia, Greece, Hungary, Italy, FYR of Macedonia, Montenegro, Poland, Romania, Serbia, Slovakia and Slovenia, a quarter or more of the population is exposed to concentrations above the LV_{2020}. As the current mapping methodology tends to underestimate high values (Annex 3), the exceedance percentages and/or the number of countries with population exposed to concentrations above both the current LV and the indicative LV_{2020} will most likely be higher.

Table 3.1 Population exposure and population-weighted concentration, $PM_{2.5}$ annual average 2015

Country		Population	$PM_{2.5}$ annual average, exposed population [%]						Population weighted conc.
			< LV_{2020}				> LV_{2020}		
			< LV					> LV	
		[inhbs . 1000]	< 5 $\mu g.m^{-3}$	5 - 10 $\mu g.m^{-3}$	10 - 15 $\mu g.m^{-3}$	15 - 20 $\mu g.m^{-3}$	20 - 25 $\mu g.m^{-3}$	> 25 $\mu g.m^{-3}$	[$\mu g.m^{-3}$]
Albania	AL	2 892		0.9	11.8	28.3	47.1	12.0	20.5
Andorra	AD	78	0.2	1.6	98.2				13.3
Austria	AT	8 576	0.4	10.1	60.2	29.3			13.3
Belgium	BE	11 237		2.1	88.7	9.2			13.0
Bosnia & Herzegovina	BA	3 825		4.3	21.7	30.0	35.7	8.3	18.9
Bulgaria	BG	7 202		1.0	9.8	9.6	35.6	44.0	24.1
Croatia	HR	4 225		3.1	30.3	32.7	33.9		17.4
Cyprus	CY	1 173		0.2	15.6	84.2			16.9
Czech Republic	CZ	10 538		0.6	20.7	63.1	12.5	3.1	17.0
Denmark	DK	5 660	0.4	51.8	47.8				9.7
Estonia	EE	1 315	1.6	98.2	0.2				6.7
Finland	FI	5 472	31.8	68.2					5.3
France (metropolitan)	FR	64 344	0.0	19.8	70.2	10.0			11.9
Germany	DE	81 198	0.0	3.5	93.7	2.8	0.0		12.3
Greece	GR	10 858		1.1	26.9	30.1	25.3	16.6	19.1
Hungary	HU	9 856			0.4	71.9	27.6	0.0	18.9
Iceland	IS	329	37.1	62.9					5.5
Ireland	IE	4 629	10.6	89.4					6.5
Italy	IT	60 796	0.0	2.7	27.1	36.9	16.0	17.4	18.5
Latvia	LV	1 986		49.3	32.0	18.7			10.6
Liechtenstein	LI	37	0.1	7.9	92.0				11.0
Lithuania	LT	2 921		16.6	83.4				11.7
Luxembourg	LU	563		6.1	93.9				12.0
Macedonia, FYR of	MK	2 069		0.3	2.1	3.1	15.7	78.8	28.7
Malta	MT	429		0.3	99.7				12.8
Monaco	MC	38			100.0				14.4
Montenegro	ME	622		9.4	13.1	50.8	16.8	9.9	18.5
Netherlands	NL	16 901		0.3	99.7				12.3
Norway	NO	5 166	38.4	55.2	6.4				5.9
Poland	PL	38 006		0.0	10.9	29.4	29.4	30.3	21.6
Portugal (excl. Az., Mad.)	PT	9 870	0.3	54.5	45.2				9.8
Romania	RO	19 871		0.4	16.6	52.2	30.3	0.6	18.1
San Marino	SM	33			14.6	85			16.2
Serbia (incl. Kosovo*)	RS	8 919		0.4	4.7	19.8	33.7	41.4	23.9
Slovakia	SK	5 421		0.0	1.1	67.0	30.8	1.0	19.1
Slovenia	SI	2 063		1.3	22.9	46.0	29.9		17.4
Spain (excl. Canarias)	ES	44 323	0.4	20.4	53.7	24.6	0.9		12.7
Sweden	SE	9 747	37.2	60.8	2.0				5.9
Switzerland	CH	8 238	0.9	12.2	84.8	2.2			11.8
United Kingdom (& dep.)	UK	64 875	0.9	57.5	41.5	0.0			9.4
Total		**536 303**	**1.6**	**17.5**	**47.7**	**18.1**	**8.8**	**6.3**	**14.2**
			19.2		**65.7**		**15.1**		
EU-28		**504 055**	**1.3**	**17.8**	**48.9**	**18.4**	**8.1**	**5.5**	**14.0**
			19.1		**67.3**		**13.6**		

Kosovo*	KS	1 805		0.1	5.4	11.6	11.9	71.0	26.4
Serbia (excl. Kosovo*)	RS	7 114		0.5	4.6	21.8	39.0	34.2	23.3

*) under the UN Security Council Resolution 1244/99

Note 1: Turkey is not included in the calculation due to the lack of air quality data.
Note 2: The percentage value "0.0" indicates an exposed population exists, but it is small and estimated less than 0.05 %. Empty cells mean: no population in exposure.

According to EEA CSI004 (EEA, 2017c), about 7 % of the urban population in the EU-28 was exposed to $PM_{2.5}$ concentrations above the limit value in 2015. The difference with the estimated 5.5 % in Table 3.1 is because the EEA accounts for the urban population in the larger agglomerations only. Whereas, Table 3.1 provides estimates for the total population, including the population in rural areas, smaller cities and villages. When it comes to the WHO AQ guideline, the urban population exposed to concentrations above its recommended value (10 $\mu g \cdot m^{-3}$) in 2015 was estimated at 83 %, which is more in line with the total population estimation of 81 % as presented in Table 3.1.

The European-wide population-weighted concentration of the $PM_{2.5}$ daily means is estimated for 2015 at about 14 $\mu g \cdot m^{-3}$ for the EU-28 and Europe as a whole. This is together with 2014 the lowest level of the period 2007 – 2015 (data lacking for 2009; Tables 6.2 and A4.4).

Figure 3.1 shows, for the whole mapped area, the population frequency distribution for exposure classes of 1 $\mu g \cdot m^{-3}$. The highest population frequency is found for classes between 10 and 14 $\mu g \cdot m^{-3}$.

Figure 3.1 Population frequency distribution, $PM_{2.5}$ annual average, 2015

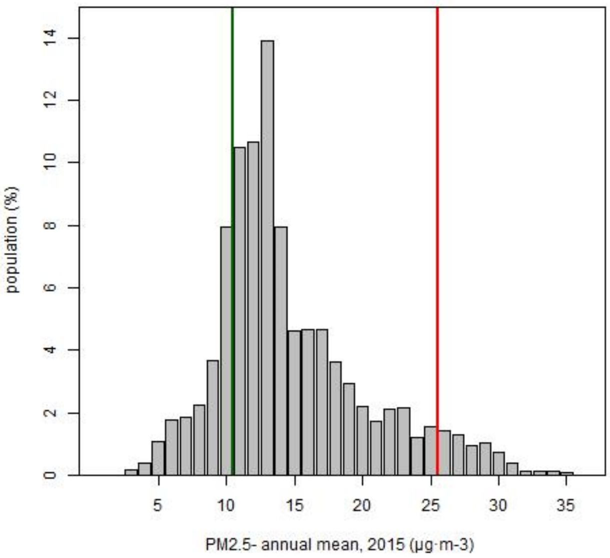

4 Ozone

For ozone, the two health-related indicators *93.2 percentile of maximum daily 8-hour means* (see below) and *SOMO35*, and the two vegetation-related indicators *AOT40 for vegetation* and *AOT40 for forests* are considered. For the definition of the SOMO35 and AOT40 indicators, see following sections and Annex 2.

The separate rural and urban background *health*-related indicator fields are calculated at a resolution of 10x10 km. Subsequently, the final health-related indicator maps are created by combining rural and urban areas based on the 1x1 km gridded population density map. We present these maps on this 1x1 km grid resolution. The population exposure tables are calculated on the basis of these health-related indicator maps.

The *vegetation*-related indicator maps are calculated from observations at rural background stations and are representative for rural areas only (assuming urban areas do not cover vegetation). The maps have a resolution of 2x2 km. This resolution serves the needs of the EEA Core Set Indicator 005 (EEA, 2017d) on ecosystem exposure to ozone.

Annex 3 provides details on the regression and kriging parameters applied for deriving the maps of the ozone indicators, as well as the uncertainty analysis of the maps. Annex 4 discusses briefly the inter-annual changes observed in the concentration maps and the relevant population and vegetation exposure.

4.1 Ozone – 93.2 percentile of maximum daily 8-hour means

The AQ Directive (EU, 2008) describes the ozone target value (TV) as "a maximum daily 8-hour mean of 120 $\mu g \cdot m^{-3}$ not to be exceeded on more than 25 times a calendar year, averaged over three years". On an annual basis, it can be evaluated by the indicator 26th maximum daily 8-hour mean, which is in principle equivalent to the indicator 93.2 percentile of maximum daily 8-hour means. However, for measurement data these two indicators are equivalent only if no data is missing, which is in general not the case. As shown in de Leeuw (2012), the additional uncertainty related to incomplete time series is substantially smaller when using percentile values instead of the x-th highest value. As in the previous ETC/ACM Technical Paper 2016/6 with its 2014 maps, we express this ozone indicator as the 93.2 percentile of maximum daily 8-hour means instead of the formerly used 26th maximum daily 8-hour mean.

4.1.1 Concentration map

Map 4.1 presents the final combined map for 93.2 percentile of the maximum daily 8-hour means as a result of combining the separate rural and urban interpolated maps following the procedures as described in Annex 1 (for a more detailed description, see Horálek et al., 2007, 2010). The supplementary data used are EMEP model output, altitude and surface solar radiation for rural areas and EMEP model output, wind speed and surface solar radiation for urban areas (Annex 3).

In the final combined map the red and dark red areas show values above the TV of 120 $\mu g \cdot m^{-3}$ on more than 25 days in 2015. Note that in the AQ Directive (EU, 2008) the target value is actually defined as 120 $\mu g \cdot m^{-3}$ not to be exceeded on more than 25 days per calendar year *averaged over three years*. Here only 2015 data are presented, and no three-year average is calculated.

The map shows that in 2015 values above 120 $\mu g \cdot m^{-3}$ on more than 25 days occur in large extended areas covering the Iberian Peninsula, the whole southern, central, eastern and south-eastern Europe. In general, these parts of Europe show higher ozone concentrations than the northern parts of Europe, which is caused mainly by higher solar radiation and temperature in these areas. An exception is north-eastern Romania where remarkably low values are observed. Furthermore, in general, higher levels of ozone do also occur more frequently in mountainous areas than in lowlands, resulting in 2015 in elevated levels in the Alpine regions and several other mountainous areas south of 50 degrees latitude. Broadly, the same areas showed in 2014 also higher ozone concentrations, however, not as high and not that much above the TV as in 2015.

The relative mean uncertainty of the 2015 map of the 93.2 percentile of maximum daily 8-h ozone means is about 7.5 % for both rural and urban areas (Annex 3).

In order to provide more complete information of the air quality across Europe, the final combined map including the measurement data at station points is presented in Map A5.4 of Annex 5.

Map 4.1 Concentration map of ozone indicator 93.2 percentile of maximum daily 8-hour means, 2015

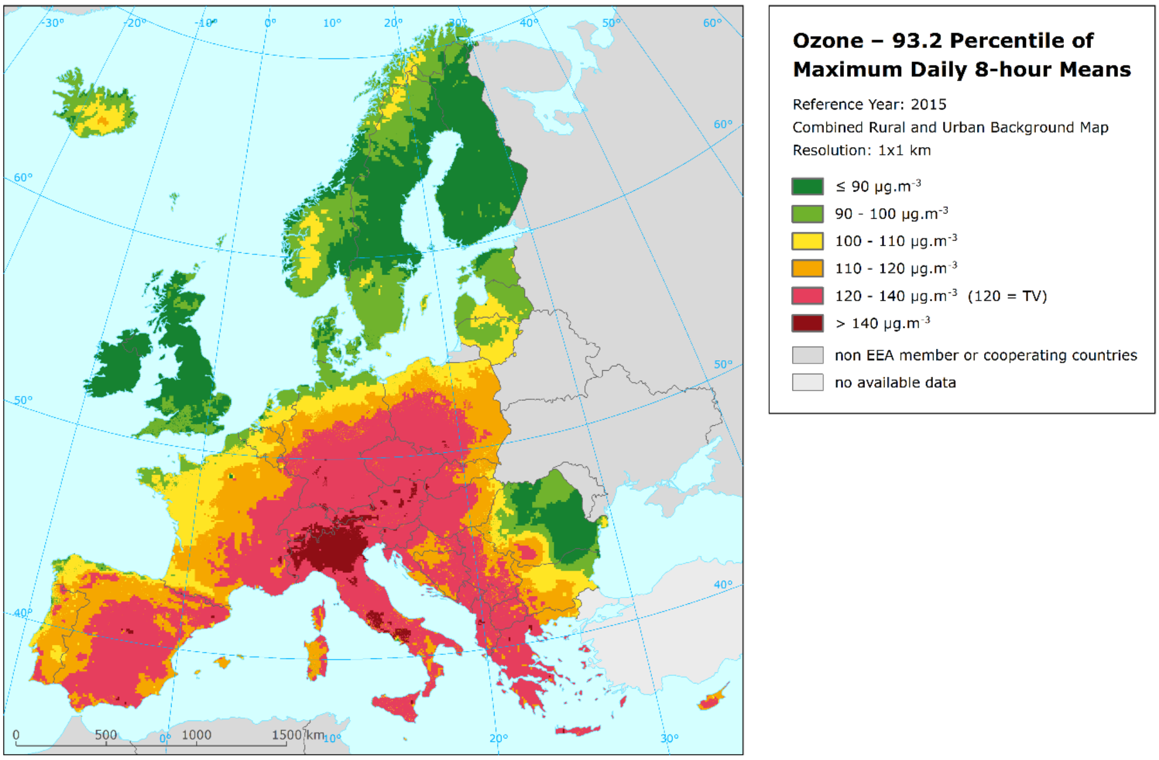

4.1.2 Population exposure

Table 4.1 gives, for 93.2 percentile of maximum daily 8-hour means, the population frequency distribution for a limited number of exposure classes, as well as the population-weighted concentration for individual countries and for Europe as a whole. Annex 4 presents the eleven year evolution of population exposure.

It has been estimated that in 2015 some 34 % of the European population lived in areas where the ozone concentration exceeded the health related target value threshold (TV of 120 $\mu g \cdot m^{-3}$). This is one of the highest levels of the eleven years period 2005 – 2015 (Table 6.3). According to CSI004 (EEA, 2017c), about 30 % of the urban population in the EU-28 was exposed to ozone above the target value threshold in 2015. The difference with the estimated 34 % in Table 6.3 is because the EEA accounts for the urban population in the larger agglomerations only, while Table 6.3 provides estimates for the total population, including the population in rural areas, smaller cities and villages. Note that – contrary to PM – rural ozone concentrations are in general higher than urban ones.

Table 4.1 Population exposure and population-weighted concentrations, ozone indicator 93.2 percentile of maximum daily 8-hour means, 2015

Country		Population	Ozone, 93.2nd percentile of max. daily 8-h means, exposed population						Population-weighted conc.
			< TV				> TV		
		[inhbs . 1000]	< 90 μg.m-3	90 - 100 μg.m-3	100 - 110 μg.m-3	110 - 120 μg.m-3	120 - 140 μg.m-3	> 140 μg.m-3	[μg.m-3]
Albania	AL	2 892			3.2	7.8	87.8	1.1	127.3
Andorra	AD	78				97.7	2.3		114.3
Austria	AT	8 576				4.5	93.7	1.9	131.1
Belgium	BE	11 237	0.2	31.6	45.2	23.0	0.0		104.3
Bosnia & Herzegovina	BA	3 825			0.7	69.2	30.1		118.2
Bulgaria	BG	7 202	6.4	15.2	27.7	50.0	0.7		106.5
Croatia	HR	4 225			0.2	35.8	63.9	0.1	121.4
Cyprus	CY	1 173			48.5	45.5	5.9		110.3
Czech Republic	CZ	10 538				4.0	96.0	0.0	129.2
Denmark	DK	5 660	71.4	27.8	0.8	0.0			89.1
Estonia	EE	1 315	53.4	46.3	0.3				89.3
Finland	FI	5 472	98.3	1.7	0.0				85.3
France (metropolitan)	FR	64 344	9.2	11.7	25.4	29.9	23.8	0.0	110.0
Germany	DE	81 198	1.0	8.3	11.5	32.6	46.5	0.1	118.5
Greece	GR	10 858		0.0	6.3	36.1	57.3	0.3	121.4
Hungary	HU	9 856		0.6	7.6	19.9	71.9		123.9
Iceland	IS	329	95	4.8	0.0				70.1
Ireland	IE	4 629	100						56.1
Italy	IT	60 796	1.1	4.5	7.4	19.8	35.1	32.2	130.9
Latvia	LV	1 986	18.7	34.3	46.2	0.8			98.5
Liechtenstein	LI	37				100			128.2
Lithuania	LT	2 921		44.3	55.7	0.0			100.5
Luxembourg	LU	563			31.6	57.1	11.3		114.1
Macedonia, FYR of	MK	2 069				51.0	49.0		119.6
Malta	MT	429			85.1	12.7	2.0	0.2	107.1
Monaco	MC	38				100			122.9
Montenegro	ME	622				41.6	58.4		120.6
Netherlands	NL	16 901	8.7	32.2	47.4	11.8			101.4
Norway	NO	5 166	84.3	15.1	0.6				83.8
Poland	PL	38 006		5.1	13.9	38.0	43.0	0.0	117.9
Portugal (excl. Az., Mad.)	PT	9 870	4.7	30.5	39.2	24.0	1.6		103.4
Romania	RO	19 871	54.2	27.8	7.9	6.9	3.2		89.8
San Marino	SM	33					100.0		129.3
Serbia (incl. Kosovo*)	RS	8 919		0.5	15.9	47.6	36.0		117.0
Slovakia	SK	5 421		3.2	13.3	30.6	52.6	0.3	120.3
Slovenia	SI	2 063				1.6	98.3	0.1	126.3
Spain (excl. Canarias)	ES	44 323	3.3	9.0	21.2	32.0	34.5	0.0	114.1
Sweden	SE	9 747	54.8	44.0	1.2	0.0			89.7
Switzerland	CH	8 238				1.4	94.3	4.4	131.1
United Kingdom (& dep.)	UK	64 875	91.5	8.4	0.1	0.0			83.2
Total		**536 303**	**19.7**	**10.6**	**13.6**	**22.0**	**30.3**	**3.7**	**110.4**
			30.3		**35.7**		**34.0**		
EU-28		**504 055**	**20.1**	**11.1**	**14.2**	**21.7**	**29.0**	**3.9**	**110.0**
			31.2		**35.9**		**32.9**		
Kosovo*	KS	1 805				68.5	31.5		119.4
Serbia (excl. Kosovo*)	RS	7 114		0.6	19.8	42.4	37.1		116.4

*) under the UN Security Council Resolution 1244/99

Note 1: Turkey is not included in the calculation due to the lack of air quality data.
Note 2: The percentage value "0.0" indicates an exposed population exists, but it is small and estimated less than 0.05 %. Empty cells mean: no population in exposure.

In the following countries about two-third (or even more) of the population suffered exposures above the TV: Albania, Austria, Croatia, Czech Republic, Hungary, Italy, San Marino, Slovenia, and Switzerland. In Bosnia & Herzegovina, France, Germany, Greece, FYR of Macedonia, Montenegro, Poland, Serbia (including Kosovo), Slovakia and Spain between about a quarter and two-third of the population was exposed to levels above the TV. These numbers are considerably higher than in 2014, and have occurred earlier about more than ten years ago. As the current mapping methodology tends to underestimate high values due to interpolation smoothing (Annex 3), the exceedance percentage is most likely even somewhat underestimated; additional exceedances might be expected and in additional countries, like Andorra, Bulgaria, Liechtenstein and Portugal. The reason is that in these countries the estimated percentage population exposed to the concentrations above 110 $\mu g \cdot m^{-3}$ is considerable.

The overall European and EU-28 population-weighted ozone concentrations in terms of the 93.2 percentile of maximum daily 8-hour means were estimated for 2015 as being 110 $\mu g \cdot m^{-3}$, which is one of the highest of the eleven year period 2005 – 2015 and at the same levels as some ten years back in time (Table A4.6).

Figure 4.1 shows, for the whole mapped area, the population frequency distribution for exposure classes of 2 $\mu g \cdot m^{-3}$. The highest population frequency is found for classes between 110 and 130 $\mu g \cdot m^{-3}$.

Figure 4.1 Population frequency distribution, O_3 indicator 93.2 percentile of maximum daily 8-hour means, 2015

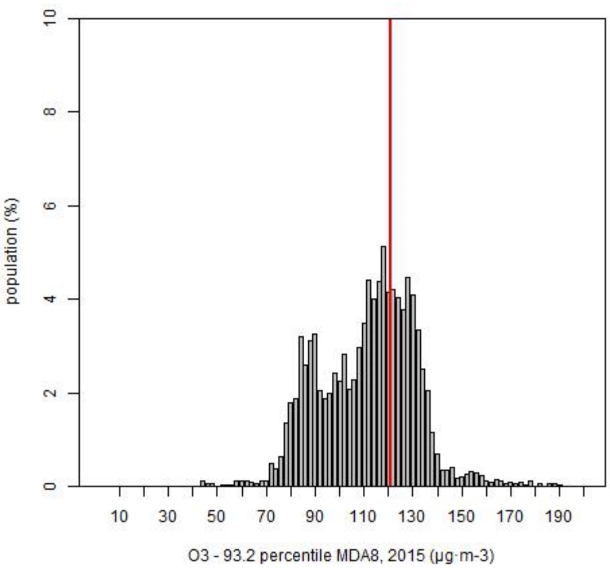

4.2 Ozone – SOMO35

SOMO35 is the annually accumulated ozone maximum daily 8-hourly means in excess of 35 ppb (i.e. 70 $\mu g \cdot m^{-3}$). It is not subject to any of the EU air quality directives and there are no limit or target values defined. Comparing the 93.2 percentile of maximum daily 8-hour means versus the SOMO35 for all background stations shows no simple relationship between the two indicators. However, it seems that the target value of the 93.2 percentile of maximum daily 8-hour means (being 120 $\mu g \cdot m^{-3}$) is related approximately with a SOMO35 value in the range of 6 000 – 8 000 $\mu g \cdot m^{-3} \cdot d$. This comparison motivates a somewhat arbitrarily chosen threshold of 6 000 $\mu g \cdot m^{-3} \cdot d$, in order to facilitate the discussion of the observed distributions of SOMO35 levels in their spatial and temporal context.

This threshold is used in this and previous papers (Horálek et al. 2017b and the references cited therein) when dealing with the population exposure estimates.

4.2.1 Concentration map

Map 4.2 presents the final combined map for SOMO35 as a result of combining the separate rural and urban interpolated maps following the same procedure as for 93.2 percentile of the maximum daily 8-hour means. The mapping details and the uncertainty analysis are presented in Annex 3. In the final combined map the red and dark red areas show values above 8 000 µg·m^{-3}·d, while the orange areas show values above 6 000 µg·m^{-3}·d.

Like in the case of the 93.2 percentile of the maximum daily 8-hour means, Spain, and the southern, central, eastern and south-eastern parts of Europe show higher ozone SOMO35 concentrations than the northern parts. Higher levels of ozone do also occur more frequently in mountainous areas south of 50 degrees latitude than in lowlands. The relative mean uncertainty of the 2015 map of the SOMO35 is about 27 % for rural areas and about 26 % for urban areas (Annex 3).

In order to provide more complete information of the air quality across Europe, the final combined map including the ozone indicator values at station points, based on the measurement data is presented in Map A5.5 of Annex 5.

Map 4.2 Concentration map of ozone indicator SOMO35, 2015

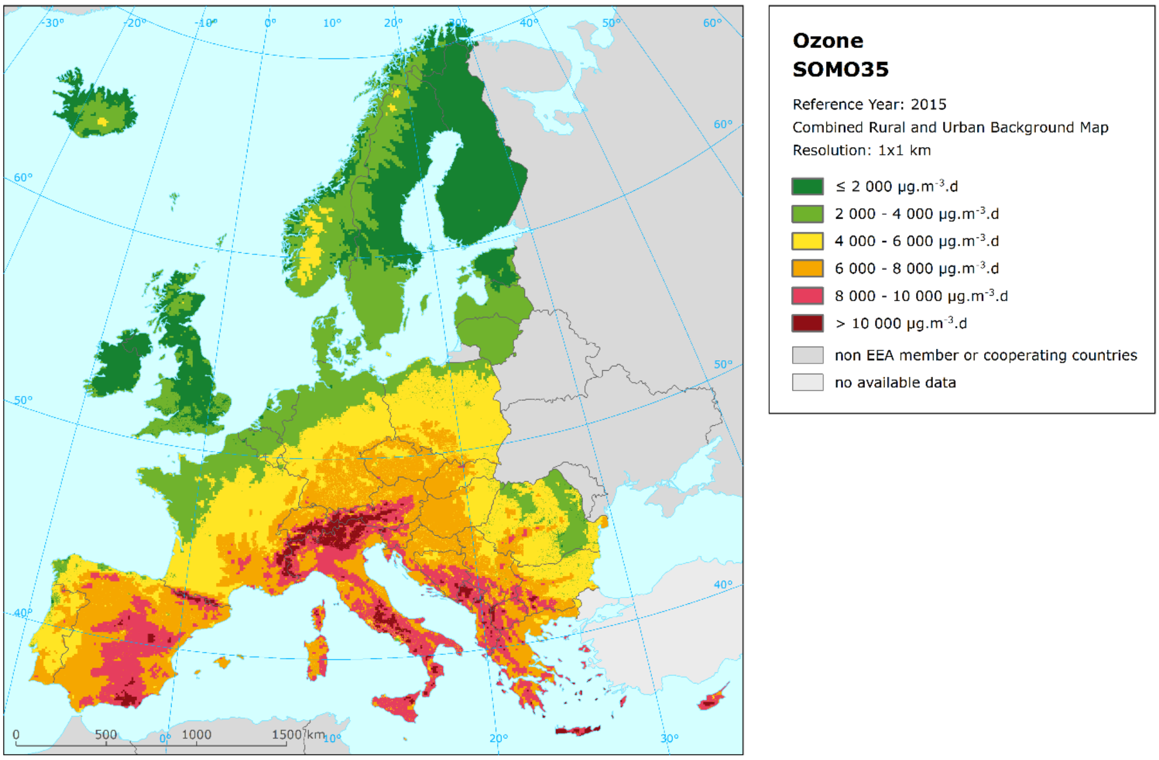

4.2.2 Population exposure

Table 4.2 gives for SOMO35 the population frequency distribution for a limited number of exposure classes, as well as the population-weighted concentration for individual countries and for Europe as a whole. Annex 4 shows details on the eleven-year evolution of population exposure.

Table 4.2 Population exposure and population-weighted concentrations, ozone indicator SOMO35, 2015

Country		Population	Ozone, SOMO35, exposed population [%]						Population-weighted conc.
			< 2000	2000 - 4000	4000 - 6000	6000 - 8000	8000 - 10000	> 10000	
		[inhbs.1000]	$\mu g.m^{-3}.d$	$\mu g.m^{-3}.d$	$\mu g.m^{-3}.d$	$\mu g.m^{-3}.d$	$\mu g.m^{-3}.d$	$\mu g.m^{-3}.d$	[$\mu g.m^{-3}.d$]
Albania	AL	2 892			4.5	82.9	12.3	0.3	7 215
Andorra	AD	78			76.8	21.3	1.3	0.6	6 050
Austria	AT	8 576			49.0	45.8	4.7	0.5	6 169
Belgium	BE	11 237	3.7	94.3	1.9				2 792
Bosnia & Herzegovina	BA	3 825			66.6	28.7	4.7	0.0	6 053
Bulgaria	BG	7 202		39.3	55.0	5.2	0.5	0.0	4 182
Croatia	HR	4 225			53.2	42.8	4.0	0.0	6 239
Cyprus	CY	1 173			37.1	50.4	11.9	0.7	6 390
Czech Republic	CZ	10 538		1.5	75.0	23.5	0.0		5 556
Denmark	DK	5 660	21.5	78.1	0.4				2 200
Estonia	EE	1 315	85.7	14.3	0.0				1 775
Finland	FI	5 472	99.1	0.9					1 358
France (metropolitan)	FR	64 344	1.3	47.9	36.8	13.2	0.8	0.0	4 245
Germany	DE	81 198	0.7	42.8	51.0	5.4	0.0	0.0	4 300
Greece	GR	10 858		0.3	25.5	63.3	10.3	0.7	6 908
Hungary	HU	9 856		5.2	54.5	40.3			5 553
Iceland	IS	329	99.8	0.2					258
Ireland	IE	4 629	95.7	4.3					856
Italy	IT	60 796		4.4	25.4	47.7	20.7	1.9	6 856
Latvia	LV	1 986	21.6	78.3	0.1				2 562
Liechtenstein	LI	37			90.0	9.8	0.1		5 802
Lithuania	LT	2 921		99.9	0.1				2 804
Luxembourg	LU	563		86.9	13.1				3 461
Macedonia, FYR of	MK	2 069			54.6	43.6	1.7	0.1	6 197
Malta	MT	429			74.3	23.6	1.7	0.5	5 791
Monaco	MC	38					100.0		8 015
Montenegro	ME	622			17.8	65.2	15.6	1.5	6 793
Netherlands	NL	16 901	9.6	90.4	0.0				2 678
Norway	NO	5 166	66.0	33.8	0.2				1 764
Poland	PL	38 006		29.1	68.5	2.4	0.0		4 528
Portugal (excl. Az., Mad.)	PT	9 870	9.7	40.6	43.8	5.8	0.1		3 989
Romania	RO	19 871	19.3	62.0	17.9	0.7	0.0		2 952
San Marino	SM	33				98.1	1.9		7 176
Serbia (incl. Kosovo*)	RS	8 919		9.4	71.5	17.0	2.0	0.0	5 449
Slovakia	SK	5 421		6.9	51.0	42.1	0.0		5 456
Slovenia	SI	2 063			39.6	51.8	8.6	0.1	6 649
Spain (excl. Canarias)	ES	44 323	2.7	12.2	30.1	50.0	4.9	0.0	5 820
Sweden	SE	9 747	44.7	55.2	0.1				2 084
Switzerland	CH	8 238			46.4	49.4	3.2	1.0	6 174
United Kingdom (& dep.)	UK	64 875	91.3	8.6	0.1				1 287
Total		**536 303**	**16.5**	**28.8**	**32.5**	**18.5**	**3.4**	**0.3**	**4 312**
			77.8			**22.2**			
EU-28		**504 055**	**16.8**	**30.1**	**31.7**	**17.7**	**3.4**	**0.3**	**4 249**
			78.7			**21.4**			

Kosovo*	KS	1 805			62.5	33.3	4.2	0.1	6 135
Serbia (excl. Kosovo*)	RS	7 114		11.8	73.7	13.0	1.5	0.0	5 282

*) under the UN Security Council Resolution 1244/99

Note 1: Turkey is not included in the calculation due to the lack of air quality data.
Note 2: The percentage value "0.0" indicates an exposed population exists, but is small and estimated less than 0.05 %. Empty cells mean no population in exposure.

It has been estimated that in 2015 about 22 % of the European population lived in areas with SOMO35 values above 6 000 µg·m^{-3}·d (see above on the motivation of this criterion). This is more than in the last two years, but it is also the fifth lowest level in the eleven years period 2005 – 2015 (Table 6.3).

In 2015, the northern and north-western European countries do have little to no people exposed to SOMO35 concentrations above 6 000 µg·m^{-3}·d. Most of the countries in south-western, southern and south-eastern Europe show exposures above or well above 6 000 µg·m^{-3}·d, most notably Albania, Italy, Cyprus, Greece, Montenegro, San Marino, and Slovenia. This can also be observed in Map 4.2.

In 2015, the total European and the EU-28 population-weighted ozone concentrations, in terms of SOMO35, were estimated to be around 4 300 µg·m^{-3}·d, which is the fifth highest in the eleven years period 2005 – 2015 (Table 6.3).

Figure 4.2 shows, for the whole mapped area, the population frequency distribution for exposure classes of 500 µg·m^{-3}.d. A relative flat distribution is seen between 1500 and 5000 µg·m^{-3}.d. Only for exposure classes above 6000 µg·m^{-3}.d a strong decline is seen.

Figure 4.2 Population frequency distribution, ozone indicator SOMO35, 2015

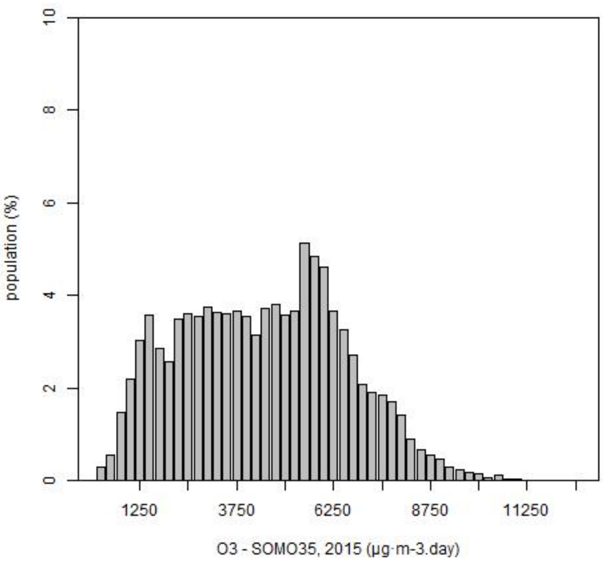

4.3 Ozone – AOT40 vegetation and AOT40 forests

In the Ambient Air Quality Directive (EU, 2008) a target value (TV) and a long-term objective (LTO) for the *vegetation protection* from high ozone concentrations accumulated during the growing season have been defined. TV and LTO are specified using "accumulated ozone exposure over a threshold of 40 parts per billion" (AOT40). This is calculated as a sum of the difference between hourly concentrations greater than 80 µg·m^{-3} (i.e. 40 parts per billion) and 80 µg·m^{-3}, using only observations between 08:00 and 20:00 Central European Time (CET) each day, calculated over three months from 1 May to 31 July. The TV is 18 000 µg.m^{-3}·h (averaged over five years) and the LTO is 6 000 µg.m^{-3}·h.

Note that the term *vegetation* as used in the Air Quality Directive (EU, 2008) is not further defined. Nevertheless, the target value used in the directive is the same as the critical load used in the Mapping Manual (UNECE, 2004) for "agricultural crops", so we have interpreted the term *vegetation* in the AQ directive as primarily agricultural crops. Therefore, the exposure of *agricultural crops* has been evaluated here based on the AOT40 for vegetation as defined in the AQ directive and the agricultural areas, defined as the CORINE Land Cover level-1 class *2 Agricultural areas* (encompassing the level-2 classes *2.1 Arable land, 2.2 Permanent crops, 2.3 Pastures* and *2.4 Heterogeneous agricultural areas)*, see Section 4.3.2. Note that in addition to these agricultural areas there are several other CLC classes that could be considered "vegetation", namely level-2 classes *1.4 Artificial, non-agricultural vegetated areas* (encompassing the level-3 classes *1.4.1 Green urban areas* and *1.4.2 Sport and leisure facilities*), *2.3 Forests* (see below) and *2.4 Scrub and/or herbaceous vegetation associations*.

Next to the AOT40 for vegetation protection, the AQ Directive (EU, 2008) defines also the AOT40 for *forest protection*, which is calculated similarly as the AOT40 for vegetation, but is summed over six months from 1 April to 30 September. For AOT40 for forests there is no TV defined. However, there is a critical level (CL) established by UNECE (2004). This critical level is set at 10 000 $\mu g \cdot m^{-3} \cdot h$.

For the exposure of forests evaluation, the CLC level-2 class *3.1 Forests* has been used.

The ecosystem based accumulative ozone indicators described in this section are specifically prepared for calculation of EEA Core Set Indicator 005 (EEA, 2017d). For the estimation of the vegetation and forested area exposure to accumulated ozone, the maps in this section are created on a grid of 2x2 km resolution. The exposure frequency distribution outcomes are based on the overlay with the 100x100 m grid resolution of the CLC2006 land cover classes.

4.3.1 Concentration maps

The interpolated map of AOT40 for vegetation and of AOT40 for forests are created for rural areas only, as urban areas are considered not to represent agricultural or forested areas. These maps are therefore applicable to rural areas only, and as such they are based on AOT40 data derived from rural background station observations only. These AOT40 monitoring data are combined in the mapping with the supplementary data sources EMEP model output, altitude and surface solar radiation. These supplementary data sources are the same as those selected at the human health related ozone indicators.

Map 4.3 presents the final map of AOT40 for *vegetation* in 2015. Note that in Directive 2008/50/EC the target value is actually defined as 18 000 $\mu g \cdot m^{-3} \cdot h$ *averaged over five years*. Here only 2015 data are presented, and no five-year average is calculated.

The areas in the map with concentrations above the target value (TV) of 18 000 $\mu g \cdot m^{-3} \cdot h$, are marked in red and dark red. The areas below the long term objective (LTO) are marked in green. The high and very high AOT40 levels for vegetation do occur specifically in extended areas of the Iberian Peninsula, the southern, central and south-eastern regions of Europe. The relative mean uncertainty of the 2015 map of the AOT40 for vegetation is about 29 % (Annex 3).

Map 4.4 presents the final map of AOT40 for *forests* in 2015. The areas in the map with concentrations above the critical level (CL) defined by UNECE (2004) are marked in yellow, orange, red and dark red. One can see large European forested areas exceeding this level.

Like for the AOT40 for vegetation indicator, the highest levels of the AOT40 for forests are found in the same south-western, southern, central and south-eastern European regions. The relative mean uncertainty of the 2015 map of the AOT40 for forests is about 29 % (Annex 3).

In order to provide more complete information of the air quality across Europe, the AOT40 maps including the AOT40 values based on the actual rural background measurement data at station points are presented in Maps A5.6 and A5.7 of Annex 5.

Map 4.3 Concentration map of O_3 indicator AOT40 for vegetation, rural map, 2015

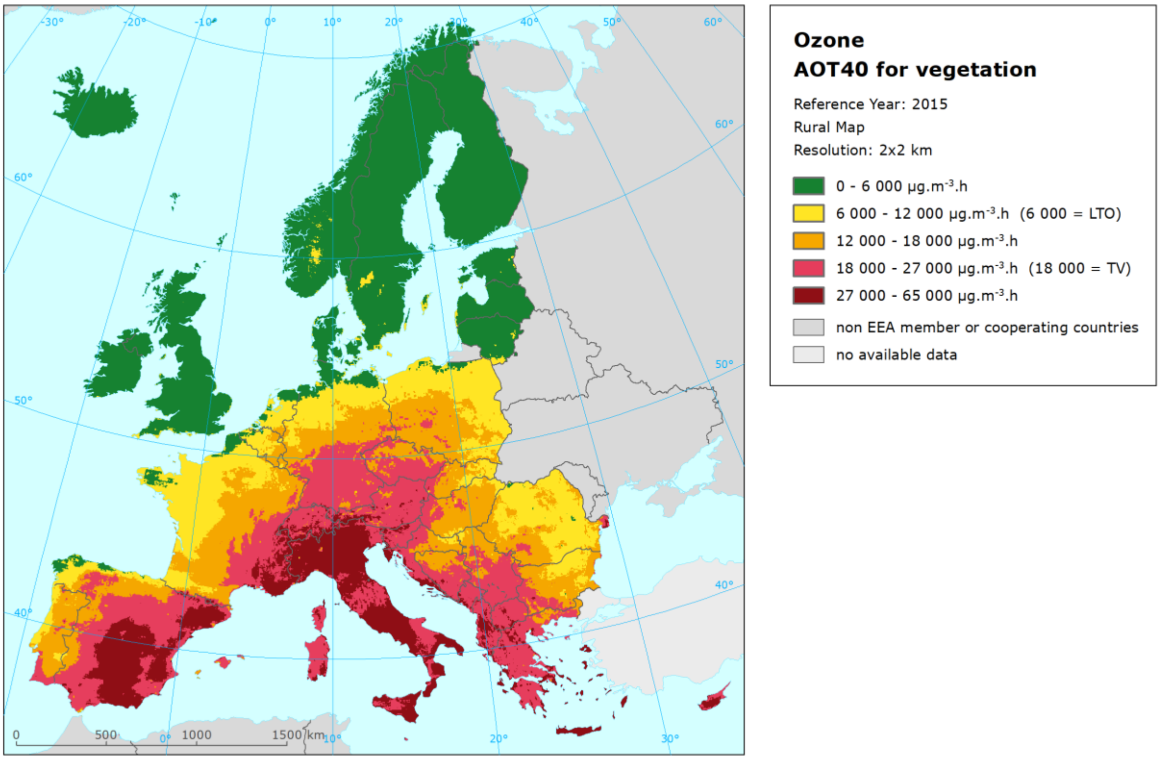

Map 4.4 Concentration map of ozone indicator AOT40 for forests, rural map, 2015

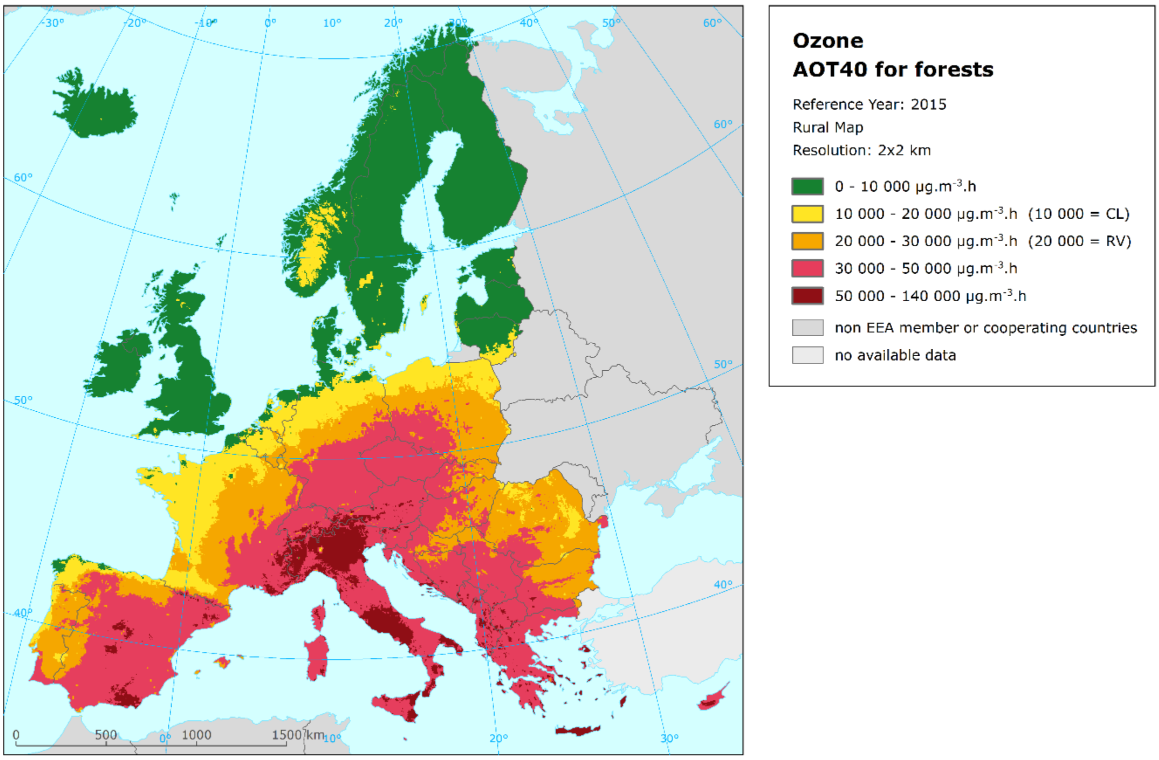

4.3.2 Vegetation exposure

Agricultural crops

The rural map with ozone indicator AOT40 for vegetation has been combined with the land cover CLC2006 map. Following a similar procedure as described in Horálek et al. (2007), the exposure of agricultural areas (as defined above) has been calculated at the country-level.

Table 4.3 gives the absolute and relative agricultural area for each country and for four European regions where the ozone target value (TV) threshold and long-term objective (LTO) for protection of vegetation as defined in the AQ Directive (EU, 2008) are exceeded. The frequency distribution of the agricultural area over some exposure classes per country is presented as well. The table indicates the country grouping with corresponding colours of the region *Northern Europe*: Denmark, Estonia, Finland, Latvia, Lithuania, Norway, and Sweden. *North-western Europe*: Belgium, France north of 45 degrees latitude, Ireland, Iceland, Luxembourg, the Netherlands, and United Kingdom. *Central and Eastern Europe*: Austria, Bulgaria, Czech Republic, Germany, Hungary, Liechtenstein, Poland, Slovakia, Switzerland, and Romania. *Southern Europe*: Albania, Bosnia-Herzegovina, Croatia, Cyprus, France south of 45 degrees latitude, Greece, Italy, F.Y.R. of Macedonia, Malta, Monaco, Montenegro, Portugal, San Marino, Serbia (including Kosovo under the UN Security Council Resolution 1244/99), Slovenia, and Spain.

Table 4.3 illustrates that in 2015, some 31 % of all European agricultural land was exposed to ozone exceeding the target value (TV) of 18 000 $\mu g \cdot m^{-3} \cdot h$. This is one of the highest percentages of the eleven year period 2005 – 2015, and the highest once since 2009, see Table 6.4.

Considering for the long-term objective (LTO) of 6 000 $\mu g \cdot m^{-3} \cdot h$ the area in excess is about 80 %, which is the second lowest for this eleven year period (Table 6.4). Iceland, Ireland, the United Kingdom together with most of Scandinavia and of the Baltic States are the areas with ozone levels not being in excess of the LTO. In most Mediterranean, Alpine and Balkan countries more than half of their agricultural area experienced exposures above the less stringent TV threshold in 2015.

Forests

The rural map with ozone indicator AOT40 for forests was combined with the land cover CLC2006 map. Following a similar procedure as described in Horálek et al. (2007), the exposure of forest areas (as defined above) has been calculated for each country, for the same four European regions as for crops and for Europe as a whole.

Table 4.4 gives the absolute and relative forest area where the Critical Level (CL) as defined in UNECE (2004) and the value 20 000 $\mu g \cdot m^{-3} \cdot h$ (which is equal to the earlier used Reporting Value, RV, as was defined in the repealed ozone directive 2002/3/EC) are exceeded. Next to the forest area in exceedance, the table presents the frequency distribution of the forest area over some exposure classes.

The Critical Level was exceeded in 2015 at about 60 % of all European forested area, which is the lowest exceedance observed for the eleven years period 2005 – 2015 (Table 6.4). As in previous years, most countries continue to have in 2015 considerable forest areas in excess to the CL, with specifically almost all forest area in southern, central, eastern and south-eastern European countries.

In this context, it should be mentioned that the AOT40 indicator probably is not the best proxy for the vegetation damage. E.g., it does not take into account that the Mediterranean vegetation closes its stomata in the warmest and driest season protecting itself from the exposure to ozone. A flux approach – as done e.g. in the EMEP model – taking into account the reduced deposition when stomata are closed would be better. However, there is still a damage to Mediterranean forests – e.g. the Aleppo pine in the southern France seems to be quite sensitive to ozone exposure and suffering damage, UNECE (2016).

Table 4.3 Agricultural area exposure and exceedance, ozone indicator AOT40 for vegetation, 2015

Country	Agricultural Area, 2015					Percentage of agricultural area, 2015 [%]				
	Total area	> LTO (6 000 µg.m^{-3}.h)		> TV (18 000 µg.m^{-3}.h)		< 6 000	6 000 - 12 000	12 000 - 18 000	18 000 - 27 000	> 27 000
	[km^2]	[km^2]	[%]	[km^2]	[%]	µg.m^{-3}.h	µg.m^{-3}.h	µg.m^{-3}.h	µg.m^{-3}.h	µg.m^{-3}.h
Albania	8053	8053	100	8053	100				72.5	27.5
Austria	26897	26897	100	25181	93.6			6.4	92.8	0.8
Belgium	17582	15850	90.1	0		9.9	62.2	28.0		
Bosnia-Herzegovina	17840	17840	100	7282	40.8			59.2	40.1	0.7
Bulgaria	57582	57541	99.9	6127	10.6	0.1	34.9	54.4	10.6	0.0
Croatia	22543	22543	100	11553	51.2		10.6	38.1	40.2	11.0
Cyprus	4324	4324	100	4324	100				60.2	39.8
Czech Republic	45091	45091	100	25473	56.5			43.5	56.5	
Denmark (excl. Faroes)	31792	2454	7.7	0		92.3	7.7	0.1		
Estonia	14382	98	0.7	0		99.3	0.7			
Finland	29002	0		0		100.0				
France (metropolitan)	326663	313686	96.0	45334	13.9	4.0	47.9	34.2	12.0	1.9
Germany	212235	186146	87.7	67760	31.9	12.3	29.4	26.4	31.9	0.0
Greece	50604	50604	100	45709	90.3		0.1	9.6	67.8	22.5
Hungary	61868	61868	100	9145	14.8		10.9	74.4	14.8	
Iceland	2436	0		0		100				
Ireland	46842	105	0.2	0		100	0.2			
Italy	156645	156645	100	156605	100.0		0.0	0.0	31.0	69.0
Latvia	26916	474	1.8	0		98.2	1.7	0.0		
Liechtenstein	39	39	100	39.1	100				95.8	4.2
Lithuania	39197	1049	2.7	0		97.3	2.7			
Luxembourg	1381	1381	100	0			15	85.2		
Macedonia, FYR of	9241	9241	100	9115	98.6			1.4	97.2	1.4
Malta	124	124	100	124	100				49.5	51
Monaco	0	0		0						
Montenegro	2231	2231	100	2226	99.8			0.2	93.8	6.0
Netherlands	24197	17581	72.7	0		27.3	66.1	6.6		
Norway	15671	59	0.4	0		99.6	0.4			
Poland	186974	181653	97.2	2690	1.4	2.8	56.0	39.7	1.4	
Portugal (excl. Az., Mad.)	41587	41582	100.0	4252	10.2	0.0	18.7	71.1	10.2	0.0
Romania	136113	135207	99.3	2395	1.8	0.7	68.4	29.2	1.8	
San Marino	41	41	100	41	100					100
Serbia (incl. Kosovo*)	47414	47414	100	24374	51.4		3.4	45.2	51.4	
Slovakia	23323	23299	99.9	3560	15.3	0.1	33.7	50.9	15.3	0.0
Slovenia	7105	7105	100	7089	99.8			0.2	91.1	8.7
Spain (excl. Canarias)	236873	232416	98.1	184998	78.1	1.9	3.8	16.2	44.8	33.3
Sweden	38606	2531	6.6	0		93.4	6.5	0.0		
Switzerland	11806	11806	100	11656	98.7			1.3	89.2	9.5
United Kingdom (& dep.)	137365	3620	2.6	0		97.4	2.6	0.1		
Total	**2118588**	**1688598**	**79.7**	**665105**	**31.4**	**20.3**	**24.1**	**24.3**	**21.3**	**10.1**
EU-28	**2003326**	**1591641**	**79.4**	**602319**	**30.1**	**20.6**	**25.3**	**24.0**	**19.6**	**10.5**
France over 45N	258998	246021	95.0	24690	9.5	5.0	55.1	30.4	9.3	0.2
France below 45N	67665	67665	100	20644	30.5		20.6	48.9	22.2	8.3
Kosovo*	4405	4405	100	4405	100				100.0	0.0
Serbia (excl. Kosovo*)	43009	43009	100	19969	46.4		3.8	49.8	46.4	0.0
Northern	195567	6664	3.4	0		62.0	37.9	0.0		
North-western	488801	284558	58.2	24690	5.1	37.3	55.6	7.0	0.1	
Central & Eastern	761929	729547	95.8	154026	20.2	0.0	39.9	53.5	6.6	0.0
Southern	672292	667829	99.3	486389	72.3	0.7	14.0	37.1	44.1	4.1

*) under the UN Security Council Resolution 1244/99

Note 1: Countries not included due to the lack of land cover data: Andorra, Turkey.
Note 2: The percentage value "0.0" indicates an exposed agricultural area exists, but is small and estimated less than 0.05 %. Empty cells mean: no agricultural area in exposure.

Table 4.4 Forested area exposure and exceedance, ozone indicator AOT40 for forests, 2015

Country	Forested area, 2015					Percentage of forested area, 2015 [%]				
	Total area	> CL (10 000 μg.m^{-3}.h)		> RV (20 000 μg.m^{-3}.h)		< 10 000	10 000 - 20 000	20 000 - 30 000	30 000 - 50 000	> 50 000
	[km^2]	[km^2]	[%]	[km^2]	[%]	μg.m^{-3}.h	μg.m^{-3}.h	μg.m^{-3}.h	μg.m^{-3}.h	μg.m^{-3}.h
Albania	7672	7672	100	7672	100				76.4	24
Austria	37158	37158	100	37158	100			0.3	95.6	4.1
Belgium	6101	6043	99.1	3767	61.8	0.9	37.3	61.8		
Bosnia-Herzegovina	23421	23421	100	23421	100			8.5	90.8	0.7
Bulgaria	34899	34899	100	34838	99.8		0.2	37.3	62.4	0.1
Croatia	20035	20035	100	20035	100			16.3	77.9	5.8
Cyprus	1527	1527	100	1527	100				45.8	54.2
Czech Republic	26116	26116	100	26116	100			0.1	99.9	
Denmark (excl. Faroes)	3756	676	18.0	3	0.1	82.0	17.9	0.1		
Estonia	20500	194	0.9	0		99.1	0.9			
Finland	194070	4	0.0	0		100.0	0.0			
France (metropolitan)	142330	141820	99.6	114732	80.6	0.4	19.0	43.8	34.1	2.6
Germany	104130	102505	98.4	85776	82.4	1.6	16.1	27.1	55.2	0.1
Greece	25318	25318	100	25318	100			0.4	86.5	13.1
Hungary	17183	17183	100	17094	99.5		0.5	31.8	67.7	
Iceland	421	0		0		100				
Ireland	3701	2	0.0	0		100.0	0.0			
Italy	79310	79309	100.0	79309	100.0	0.0	0.0	0.0	46.3	53.6
Latvia	25914	741	2.9	0	0.0	97.1	2.9	0.0		
Liechtenstein	85	85	100	85	100				98.4	1.6
Lithuania	18922	6652	35.2	17	0.1	64.8	35.1	0.1		
Luxembourg	929	929	100	809	87.1		12.9	87.1		
Macedonia, FYR of	8268	8268	100	8268	100				89.1	11
Malta	2	2	100	2	100				16.2	84
Monaco	0.44	0.44	100	0.44	100				84.1	15.9
Montenegro	5857	5857	100	5857	100				91.6	8
Netherlands	3107	2696	86.7	91	2.9	13.3	83.8	2.9		
Norway	104078	8211	7.9	0		92.1	7.9			
Poland	95506	95498	100.0	69437	72.7	0.0	27.3	48.3	24.4	
Portugal (excl. Az., Mad.)	19676	19673	100.0	16634	84.5	0.0	15.4	67.7	16.8	
Romania	72091	72082	100	67968	94.3	0.0	5.7	73.5	20.7	
San Marino	6	6	100	6	100				4.5	95.5
Serbia (incl. Kosovo)	27156	27156	100	27156	100			1.9	97.7	0.4
Slovakia	20275	20275	100	20230	99.8		0.2	45.2	54.5	
Slovenia	11529	11529	100	11529	100			0.2	93.5	6.4
Spain (excl. Canarias)	110638	107349	97.0	94327	85.3	3.0	11.8	13.7	66.9	4.7
Sweden	242979	2139	0.9	1	0.0	99.1	0.9	0.0		
Switzerland	12387	12387	100	12387	100			1.3	90.4	8.3
United Kingd. (& dep.)	21646	393	1.8	70	0.3	98.2	1.5	0.3		
Total	**1548698**	**925810**	**59.8**	**811572**	**52.4**	**40.2**	**7.4**	**16.6**	**31.7**	**4.1**
EU-28	**1358856**	**832512**	**61.3**	**726719**	**53.5**	**38.7**	**7.8**	**18.7**	**30.4**	**4.4**
France over 45N	88424	87913	99.4	66793	75.5	0.6	23.9	48.4	26.9	0.3
France below 45N	53906	53906	100	47939	88.9		11.1	36.3	46.1	6.5
Kosovo*	4330	4330	100	4330	100				97.8	2.2
Serbia (excl. Kosovo)*	22826	22826	100	22826	100			2.3	97.7	0.0
Northern	610219	18617	25.5	21	0.0	3177.7	99.9	0.1	0.0	0.0
North-western	124329	97975	79.6	71530	57.5	26.9	27.0	48.5	24.2	0.2
Central & Eastern	419829	418187	100	371089	88.4	0.4	11.3	37.1	51.0	0.6
Southern	394321	391030	99.1	369001	93.6	0.8	5.6	13.8	65.0	15.5

*) under the UN Security Council Resolution 1244/99

Note 1: Countries not included due to the lack of land cover data: Andorra, Turkey.
Note 2: The percentage value "0.0" indicates an exposed forested area exists, but is small and estimated less than 0.05 %. Empty cells mean: no forested area in exposure.

5 NO_2 and NO_x

Annual average maps for NO_2 (related to protection of health) and for NO_x (related to protection of vegetation) were produced and presented in the regular mapping report for the first time for year 2014 (Horalek et al., 2017b).

The methodology for creating the concentration maps follows the same principle as for the rest of pollutants: a linear regression model on the basis of European wide station measurement data, followed by kriging of the residuals produced from that regression model (residual kriging).

The map on NO_2 is based on an improved mapping methodology developed in Horálek et al. (2017c). The map layers are created for the rural, urban background and urban traffic areas separately on a grid at 1x1 km resolution. Subsequently, the urban background and urban traffic map layers are merged together using the gridded road data into one urban map layer. This urban map layer is further combined with the rural map layer into the final NO_2 map using a population density grid at 1x1 km resolution. We present this final combined map in this 1x1 km grid resolution.

The map of the vegetation-related indicator NO_x annual average is created on a grid at 2x2 km resolution, based on rural background measurements only, as vegetation is considered not to be extensively present at urban and suburban areas. Hence, this map is applicable to rural areas only. The resolution is chosen equally to the one of the vegetation indicator for ozone.

Annex 3 provides details on the regression and kriging parameters applied for deriving the maps, as well as the uncertainty analysis of the maps.

5.1 NO_2 – Annual mean

5.1.1 Concentration map

The Ambient Air Quality Directive (EU, 2008) sets the Limit Value (LV) for the NO_2 annual average at the level of 40 $\mu g \cdot m^{-3}$. This is the same concentration level as recommended by the World Health Organization for the NO_2 annual average as the Air Quality Guideline (WHO, 2005). The hourly limit value (200 $\mu g \cdot m^{-3}$ not to be exceeded on more than 18 hours per year) has been exceeded in 2015 at less than 1% of all the reporting stations (EEA, 2017b). In view of this low number of exceedances, the short-term LV has not been included in the mapping procedures.

Map 5.1 presents the final combined concentration 1x1 km gridded map for the 2015 NO_2 annual average as the result of interpolation and merging of the separate maps as described in Annex 1.

Supplementary data used in the linear regression are in principle the same as in Horálek et al. (2017d). For rural areas they consist of EMEP model output, altitude, wind speed, population density and land cover; for urban background areas the EMEP model output, altitude, wind speed, population density, and land cover are supplemented with GRIP road data; for traffic areas the EMEP model output, altitude, wind speed and land cover are used (Annex 3).

According to Map 5.1, the areas with the Limit Value (LV) of 40 $\mu g \cdot m^{-3}$ exceeded include the central part of some large cities, particularly Milan, Rome, Paris, Turin, Naples, Barcelona, Madrid, Lyon, London, and Munich. Some other cities show NO_2 levels above 30 $\mu g \cdot m^{-3}$, e.g. in Germany, Italy, the Netherlands, Belgium, United Kingdom, Switzerland. The most of the European area shows NO_2 levels below 20 $\mu g \cdot m^{-3}$, with most of the rural areas below 10 $\mu g \cdot m^{-3}$. Some larger areas above 20 $\mu g \cdot m^{-3}$ can be found in the Po valley, the Benelux, the German Ruhr region, in central and southern England, in the Île de France and around Rome.

It should be noted that the interpolated map is created at 1x1 km only and as such refers to the rural and urban *background* situations only, while the exceedances of the NO_2 limit values occur mostly at local *hotspots* such as dense traffic locations and densely urbanised and industrialised areas. Although the urban traffic map layer is used in the map creation, the traffic locations are smoothed in the 1x1 km resolution.

The relative mean uncertainty of the NO_2 annual average map is 32 % for rural, 22 % for urban background and 25 % for urban traffic areas (Annex 3).

In order to provide more complete information of the air quality across Europe, the final combined map including the measurement data at station points is presented in Map A5.8 of Annex 5.

Map 5.1 Concentration map of NO_2 annual average, 2015

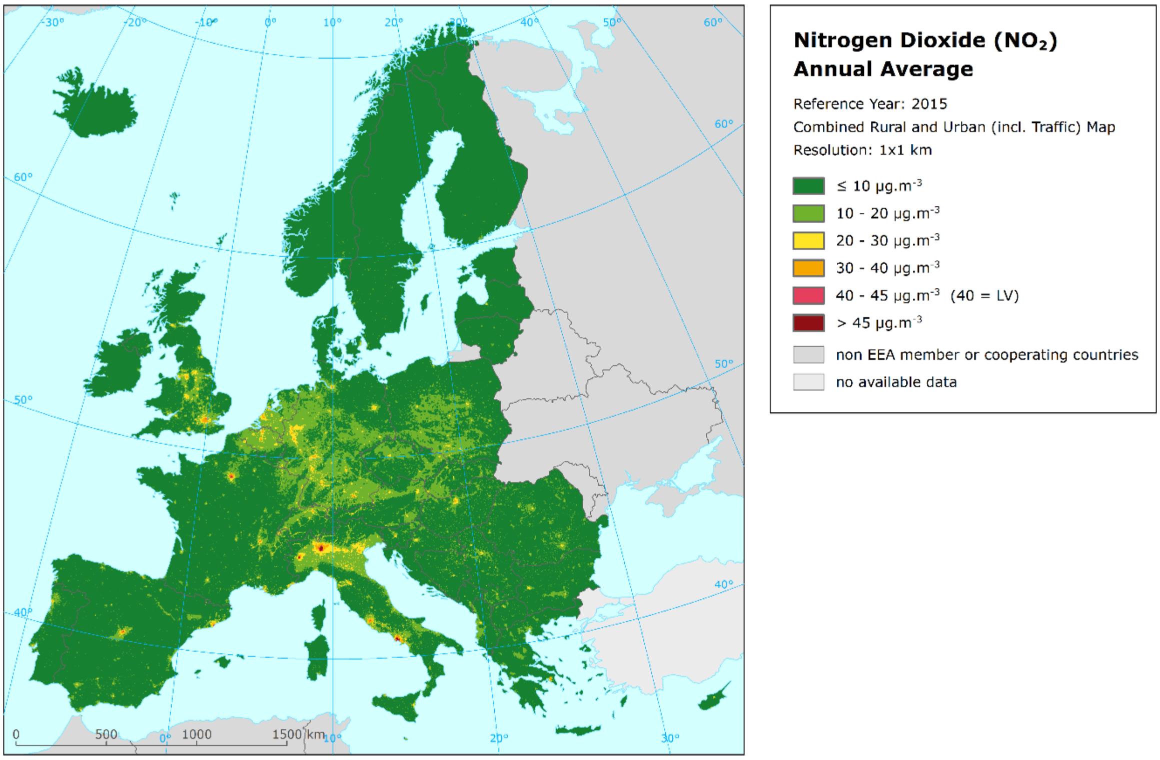

5.1.2 Population exposure

Table 5.1 gives the population frequency distribution for a limited number of exposure classes calculated on a grid of 1x1 km resolution, as well as the population-weighted concentration for individual countries and for Europe as a whole according to Equation A1.7 of Annex 1.

The human exposure to NO_2 has been calculated based on the improved methodology as developed in Horálek et al. (2017c). The population exposure is calculated according to Equation A1.6 of Annex I, i.e. it is calculated separately for urban areas directly influenced by traffic and for the background (both rural and urban) areas, in order to better reflect the population exposed to traffic. Based on this, the different concentration levels in urban background and traffic areas inside the 1x1 km grid cells are taken into account.

Table 5.1 Population exposure and population-weighted concentration, NO_2 annual average, 2015

Country		Population	NO_2 annual average, exposed population [%]						Population weighted conc.
			< LV				> LV		
		[inhbs . 1000]	< 10 $\mu g.m^{-3}$	10 - 20 $\mu g.m^{-3}$	20 - 30 $\mu g.m^{-3}$	30 - 40 $\mu g.m^{-3}$	40 - 45 $\mu g.m^{-3}$	> 45 $\mu g.m^{-3}$	[$\mu g.m^{-3}$]
Albania	AL	2 892	14.0	47.1	35.3	3.6			18.1
Andorra	AD	78	1.0	26.6	72.5				20.5
Austria	AT	8 576	9.2	43.3	40.9	4.8	1.4	0.3	19.8
Belgium	BE	11 237	2.1	52.6	31.8	12.2	1.2	0.1	20.9
Bosnia & Herzegovina	BA	3 825	22.3	49.7	27.3	0.7			16.2
Bulgaria	BG	7 202	17.8	57.3	23.4	1.5			16.1
Croatia	HR	4 225	21.0	43.3	33.8	1.5	0.5		17.3
Cyprus	CY	1 173	34.5	51.1	10.1	4.3			14.1
Czech Republic	CZ	10 538	8.7	70.4	19.0	1.8	0.2		16.6
Denmark	DK	5 660	55.6	35.3	8.1	0.7	0.3	0.0	10.5
Estonia	EE	1 315	61.4	36.3	2.3				8.2
Finland	FI	5 472	61.0	36.4	2.0	0.7			8.8
France (metropolitan)	FR	64 344	28.2	39.9	17.5	9.8	2.3	2.4	17.9
Germany	DE	81 198	5.6	50.4	35.6	5.6	1.1	1.7	20.0
Greece	GR	10 858	27.6	33.6	18.4	17.1	0.8	2.5	18.1
Hungary	HU	9 856	9.2	64.9	15.0	10.1	0.4	0.4	18.0
Iceland	IS	329	31.4	63.3	5.1	0.2			11.9
Ireland	IE	4 629	71.0	25.7	2.9	0.4			7.6
Italy	IT	60 796	5.9	31.1	35.8	16.7	3.0	7.5	24.9
Latvia	LV	1 986	49.8	30.8	17.5	1.4	0.5		12.1
Liechtenstein	LI	37	1.3	33.8	63.6	0.7	0.6		20.5
Lithuania	LT	2 921	40.2	53.0	5.4	1.5			12.2
Luxembourg	LU	563	4.3	51.8	34.6	6.4	3.0		19.9
Macedonia, FYR of	MK	2 069	4.6	63.1	29.9	2.4			18.1
Malta	MT	429	9.4	75.5	10.2	5			16.5
Monaco	MC	38			78	14	7.2		29.7
Montenegro	ME	622	18.5	50.3	29.6	1.6			16.4
Netherlands	NL	16 901	2.0	48.7	41.3	7.5	0.5	0.0	20.5
Norway	NO	5 166	43.4	39.2	14.8	1.8	0.8		12.3
Poland	PL	38 006	18.2	59.5	20.5	1.1	0.4	0.3	15.6
Portugal (excl. Az., Mad.)	PT	9 870	26.9	47.5	19.9	4.3	0.9	0.6	15.7
Romania	RO	19 871	22.6	59.4	16.0	1.4	0.6		14.9
San Marino	SM	33	5.3	90.2	1.8	3			16.2
Serbia (incl. Kosovo*)	RS	8 919	13.1	51.1	34.1	1.5	0.2		17.9
Slovakia	SK	5 421	7.1	72.5	18.6	1.5	0.3		16.9
Slovenia	SI	2 063	23.1	47.8	23.0	5.3	0.9		16.7
Spain (excl. Canarias)	ES	44 323	10.8	41.7	28.0	14.8	3.3	1.3	21.2
Sweden	SE	9 747	45.5	47.6	6.3	0.6			10.8
Switzerland	CH	8 238	3.0	40.3	47.4	7.4	1.3	0.7	21.4
United Kingdom (& dep.)	UK	64 875	11.7	44.4	32.2	9.1	0.7	1.8	19.7
Total		**536 303**	**15.8**	**46.1**	**27.0**	**7.9**	**1.3**	**1.8**	**18.8**
			96.8				**3.2**		
EU-28		**504 055**	**15.8**	**46.1**	**26.7**	**8.2**	**1.4**	**1.9**	**18.9**
			96.7				**3.3**		
Kosovo*	KS	1 805	14.8	65.2	20.0				15.8
Serbia (excl. Kosovo*)	RS	7 114	12.6	47.6	37.6	1.9	0.3		18.4

*) under the UN Security Council Resolution 1244/99

Note 1: Turkey is not included in the calculation due to the lack of air quality data.
Note 2: Empty cells mean: no population in exposure.

Thus – contrary to other pollutants – the population exposure refer not only to the rural and urban *background* areas, but to the urban *traffic* locations as well. However, it should be mentioned that the population density data in 1x1 km only is used. It means that contrary to the concentration levels, the population density is constant inside the 1x1 grid cells. This shortcoming can increase the uncertainty of the population exposure results.

It has been estimated that in 2015 about 3 % of the European population and also the EU-28 population lived in areas with NO_2 annual average concentrations above the EU limit value of 40 µg.m^{-3}. CSI004 (EEA, 2017c) estimates that about 9 % of the population in urban agglomerations in the EU-28 was exposed in 2015 to levels above the EU limit value. The difference with the estimated 3 % in Table 5.1 is mainly because the EEA accounts for the urban population in the agglomerations only. Whereas, Table 5.1 provides estimates, including the population in rural areas, smaller cities and villages.

The European-wide population-weighted concentration of the NO_2 annual average for 2015 is estimated to be about 19 µg·m^{-3}, the same as for the EU-28 only.

Figure 5.1 shows, for the whole mapped area, the population frequency distribution for exposure classes of 1 µg·m^{-3}. The frequency distribution is centred around 17-18 µg·m^{-3}.

Figure 5.1 Population frequency distribution, NO_2 annual average, 2015

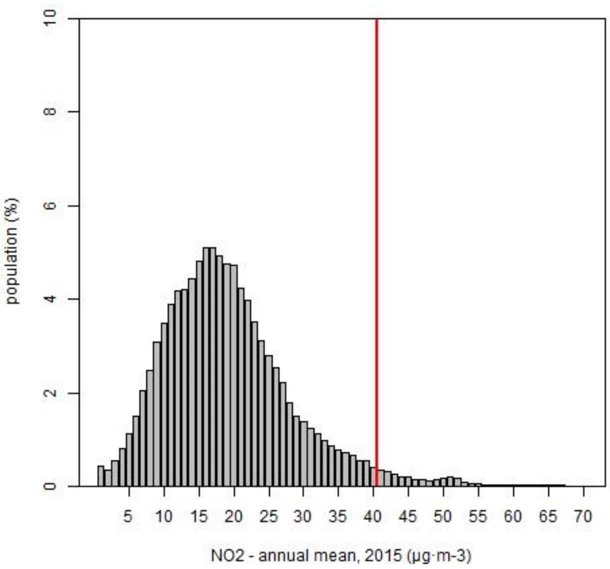

5.2 NO$_x$ – Annual mean

5.2.1 Concentration map

The AQ Directive (EU, 2008) sets a Critical Level (CL) for the protection of vegetation for the NO_x annual mean at 30 µg.m^{-3}. According to this directive, the sampling points targeted at the protection of vegetation and natural ecosystems shall be in general sited more than 20 km away from agglomerations or more than 5 km away from other built-up areas. Thus, only the observations at rural background stations are used for the NO_x mapping and the resulting map is representative for rural areas only.

The number of NO_x measurement stations is limited. The mapping of the NO_x annual average is therefore performed on the basis of an approach presented in Horálek et al. (2007). This approach derives additional *pseudo* NO_x annual mean concentrations from NO_2 annual mean measurement concentrations and increases as such the number and spatial coverage of NO_x 'data points', and applies these data to the NO_x mapping. Section A1.1 of Annex 1 provides some details.

Map 5.2 presents the concentration map of NO_x annual average. It concerns rural areas only, representing an indicator for vegetation exposure to NO_x. The supplementary data used are the same as in Horálek et al. (2014), i.e. EMEP model, altitude and wind speed.

Most of the European area shows NO_x levels below 20 $\mu g \cdot m^{-3}$. However, at the Po valley, the western part of the Netherlands and around some larger European cities (typically being the national capitals) elevated NO_x concentrations above the Critical Level (CL) are observed. Furthermore, around many larger European cities concentrations just below the CL are observed. These concentrations are expected to be the result of large emissions from transport in and around the cities, as well as energy production and industrial facilities taking place at these areas. However, this is relevant only if there is vegetation around those larger cities.

The NO_x annual average rural map has a relative mean uncertainty of 42 %.

The NO_x annual average rural map including the data measured at rural background stations is presented in Map A5.9 of Annex 5. The map illustrates the lack of the NO_x rural stations in the Balkan area.

Map 5.2 Concentration map of NO_x annual average, rural map, 2015

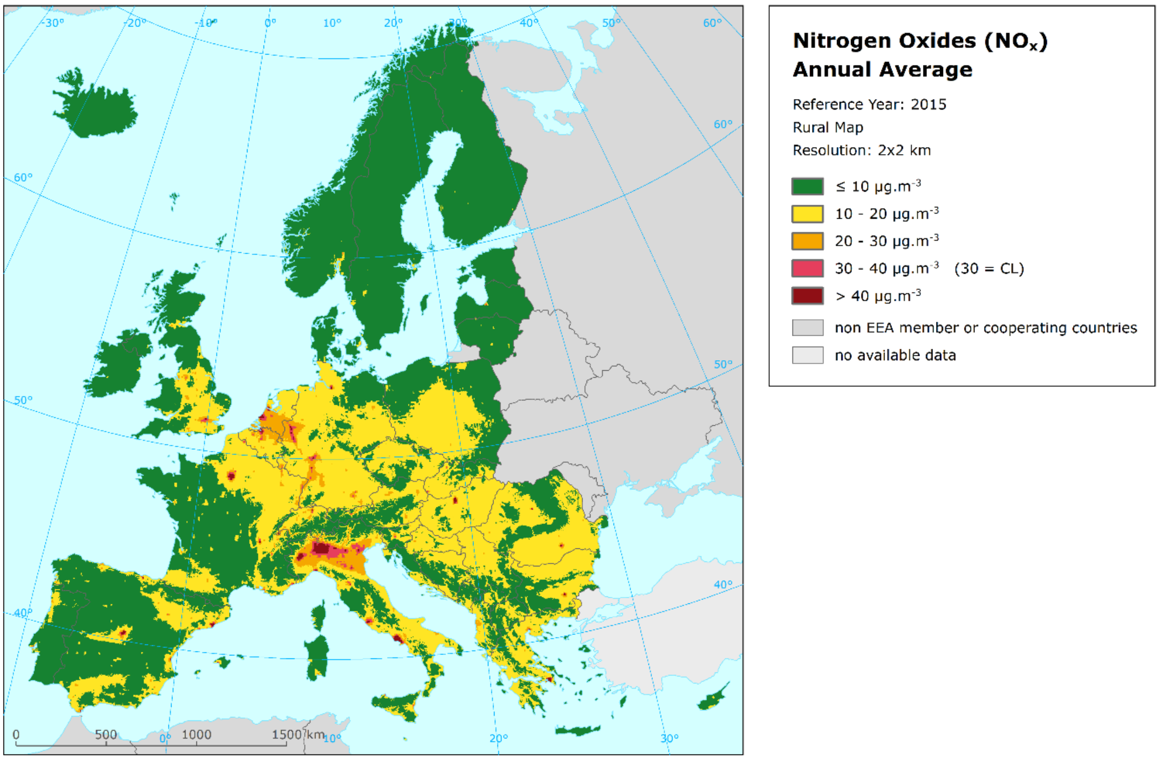

Vegetation exposure is not calculated for NO_x, as the critical level (CL) applies actually to vegetation only, which is by nature mostly allocated in rural areas where there is limited CL exceedance observed. Therefore, the vegetation exposure exceedance would occur in limited vegetation areas only and, as such, is considered not to provide essential information from the European scale perspective. Furthermore, contrary to vegetation exposure to high ozone concentrations in Europe that leads to considerable damage, vegetation exposure to NO_x pollution is of minor importance in terms of actual impacts. On the other hand, NO_x concentrations contribute in part to the total N-deposition, which leads to acidifying and eutrophying effects on vegetation. These effects, especially eutrophication, are still very important in Europe. However, these effects on vegetation cannot be easily expressed by an exposure table.

Concerning the potential exposure estimate of vegetation and natural ecosystems to NO_x there is an additional dilemma: which receptor types should be selected to estimate the exposure and critical level exceedance of vegetation and natural ecosystems? An option would be the use of CLC classes (e.g. like in Horálek et al., 2008); nevertheless this classification is too general. Other option would be the NATURA2000 database. However, that source contains a wide series of receptor types, species and classes. It would need serious additional resources to conclude on the most relevant set of receptors from the NATURA 2000 geographical database.

6 Exposure trend estimates

6.1 Mapping and exposure results

This paper has presented the interpolated maps for 2015 on the PM_{10}, $PM_{2.5}$, ozone and NO_2 *human health* related air pollution indicators. It presents the maps of annual average and the 90.4 percentile of PM_{10} daily mean, annual average for $PM_{2.5}$, the 93.2 percentile of maximum daily 8-hour means and the SOMO35 for ozone, and the annual average for NO_2, together with the tables with the frequency distribution of the estimated population exposures and exceedances per country and as European totals.

Furthermore, interpolated maps on ozone and NO_x *vegetation* related air pollution indicators have been produced. It involves the map of ozone indicators AOT40 for vegetation and AOT40 for forests, including the tables with the frequency distribution of estimated land area exposures and exceedances per country and the European totals. In addition, the map of the annual average for NO_x has been produced, but without exposure estimates.

A mapping approach similar to previous years (Horálek et al., 2017b, 2017c) based primarily on observational data was used. With the interpolated air pollution maps and exposure estimates for the year 2015, an eleven-year (for PM_{10} and ozone) resp. eight-year (for $PM_{2.5}$) and three-year (for NO_2) overview on comparable exposure estimates has been obtained. In this chapter we provide these multi-annual overviews of exposure estimates for each of the indicators of PM_{10}, $PM_{2.5}$ and ozone. The trend analysis is provided in Annex 4.

Maps for the nitrogen related indicators were not produced on a multi-annual basis so far and therefore only three-time series for NO_2 annual average can be given in this chapter.

For the human health indicators, we express the exposure estimates on the one hand as population-weighted concentration and on the other hand as percentage of population exposed to concentrations above the limit/target value. For the vegetation related indicators, the exposure estimates are expressed as agricultural- and forest-weighted concentrations and as the agricultural or forest areas exposed to concentrations above defined thresholds.

It should be noted that the percentage of population resp. agricultural or forest area exposed is a less robust indicator compared to the population resp. agricultural or forest weighted concentration, as a small concentration increase (or decrease) may lead to a major increase (or decrease) of population resp. agricultural or forest area exposed, whereas that is not the case when taking the population- resp. agricultural- or forest-weighted concentration as indicator. Therefore, the trend analysis is done on basis of the population resp. vegetation weighted concentrations only.

When thinking about a trend, we should take into account (i) the meteorologically induced variations, (ii) the uncertainties involved in the interpolation (Annex 3), and (iii) the station densities and their spatial distributions over the European regions. Next to this, we should be aware that different trends in various parts of Europe may occur. However, bearing in mind these limitations we provide here and in Annex 4 a trend analysis for the period 2005 – 2015 on the population- resp. agricultural- and forest-weighted concentrations for individual countries and for Europe as a whole.

Furthermore, the vegetation-weighted concentrations for the AOT40 indicators are included also for the first time.

6.1.1 Human health PM_{10} indicators

Table 6.1 summarises over the eleven year period 2005 – 2015 for both *human health PM_{10} indicators* the average concentration to which the European population is exposed to, expressed as the population-weighted concentration, and the percentage of population exposed to PM_{10} concentrations above the limit values (LV).

For years 2012 and 2013 both the 36th highest value and the 90.4 percentile of daily mean(s) have been calculated. Their results demonstrate an underestimation of almost 1 $\mu g \cdot m^{-3}$ at the 36th highest daily mean. One may conclude that this underestimation has its cause in the fact that when calculating the 36th highest daily mean value there is no correction for the missing values at incomplete time series. Whereas the 90.4 percentile of daily mean(s) adjusts for such missing data.

Table 6.1 Population-weighted concentration and percentage of the European population exposed to concentrations above the PM_{10} limit values (LV) for the protection of health for 2005 to 2015

PM_{10}			2005	2006	2007	2008	2009	2010	2011	2012	2013	2014	2015
Annual average													
Population-weighted concentratio	[µg.m-3]		28.0	28.5	26.2	24.8	24.6	24.3	22.1	22.7	22.2	21.1	21.2
Population exposed > LV (40 µg.m	[%]		13.3	10.3	6.8	5.8	6.0	5.2	2.5	3.4	2.6	2.0	0.6
36th highest daily mean / 90.4 percentile of daily means													
Population-weighted concentratio	[µg.m-3]	36th highest d. m.	46.8	47.8	44.1	41.3	41.2	41.9	39.0	39.7	38.6		
Population-weighted concentratio	[µg.m-3]	90.4 perc. of d. m.								40.6	39.4	37.1	36.9
Population exposed > LV (50 µg.m	[%]	36th highest d. m.	34.3	35.7	26.2	19.4	16.5	20.6	15.8	16.5	16.4		
Population exposed > LV (50 µg.m	[%]	90.4 perc. of d. m.								17.7	17.3	13.3	12.9

In 2015 the population exposed to *annual mean* concentrations of PM_{10} above the limit value of 40 $\mu g \cdot m^{-3}$ is 0.6 % of the total population, which is the lowest percentage of the complete time series and a considerable difference compared to the previous year. Furthermore, it is estimated that European inhabitants living in background (neither hot-spot nor industrial) areas – regardless if these areas are urban or rural – are exposed on average to an annual mean PM_{10} concentration of 21 $\mu g \cdot m^{-3}$, practically the same as in the previous year. This case illustrates well that a clear change in the population exceedance exposure numbers does not lead necessarily to the change in the population-weighted concentrations.

In comparison with the previous nine years, the number of people living in areas with concentrations above the LV is the lowest in the latest two years, 2014 and 2015. The overall picture of the population-weighted concentration of the European totals (i.e. totals of 40 European countries considered) demonstrates a downward trend of -0.7 $\mu g \cdot m^{-3}.year^{-1}$ for the years 2005 – 2015 (Annex 4). This trend is statistically significant and expresses a mean decrease of 0.7 $\mu g \cdot m^{-3}$ per year.

In 2015 almost 13 % of the European population lived in areas where the PM_{10} daily limit value (calculated using the *90.4 percentile*) was exceeded, being slightly less than in the previous year. The overall European population-weighted concentration of the 90.4 percentile of the PM_{10} daily means (formerly the 36th highest daily mean) for the background areas is estimated to be about 37 $\mu g \cdot m^{-3}$ in 2015, which is the lowest of the eleven years considered, but close to its previous year. This is the case even though the underestimated data have been used in the 2005 – 2011 calculations. The population-weighted concentration of the European total (i.e. total of 40 European countries considered) in Annex 4 demonstrate a statistically significant downward trend of -1.0 $\mu g \cdot m^{-3}$ per year for the years 2005 – 2015.

6.1.2 Human health $PM_{2.5}$ indicator

Table 6.2 summarises for *human health $PM_{2.5}$ indicator* (annual average) the population-weighted concentration and the percentage of European population exposed to $PM_{2.5}$ concentrations above the EU target value (LV) for the years 2007 to 2015 (without 2009, for which neither a map nor a population exposure was prepared).

Table 6.2 Population-weighted concentration and percentage of the European population exposed to concentrations above the $PM_{2.5}$ limit value (LV) for the protection of health for 2007 to 2015

$PM_{2.5}$		2007	2008	2009	2010	2011	2012	2013	2014	2015
Annual average										
Population-weighted concentration	[µg.m^{-3}]	16.3	16.3	not mapped	16.8	15.9	15.6	15.3	14.1	14.2
Population exposed > LV (25 µg.m^{-3})	[%]	7.8	7.6		8.3	6.2	9.0	5.8	4.2	6.3

The percentage of population exposed in 2015 to annual mean concentrations of $PM_{2.5}$ above the limit value (LV) of 25 µg·m^{-3} is about 6 %, which is slightly below the average of the limited time series, but higher than in the previous two years. Furthermore, it is estimated that European inhabitants living in background (neither hot-spot, nor industrial) areas – regardless if these areas are urban or rural – are exposed on average to an annual mean $PM_{2.5}$ concentration of about 14 µg·m^{-3}, being together with 2014 the lowest in the time series.

Annex 4 provides the trend analysis of the population-weighted concentrations across the period 2007 – 2015 for individual countries and for Europe as a whole. At European scale a slightly downward trend can be observed, estimated to be -0.3 µg·m^{-3} per year.

6.1.3 Human health ozone indicators

Table 6.3 summarises for both *human health ozone indicators* the exposure levels of the European inhabitants in terms of population-weighted concentrations. Furthermore, it presents the percentage of European population exposed to concentrations above the target value (TV) and above a level of 6 000 µg·m^{-3}·d for the SOMO35 for the years 2005 to 2015.

Table 6.3 Population-weighted concentration and percentage of the European population exposed to concentrations above the target value (TV) threshold for the protection of health and a SOMO35 threshold of 6 000 µg·m^{-3}·d for 2005 to 2015

Ozone			2005	2006	2007	2008	2009	2010	2011	2012	2013	2014	2015
26th highest daily max. 8-h mean / 93.2 percentile of daily max. 8-h means													
Popul.-weighted concentr.	[µg.m^{-3}]	26th highest d. max8h	112.1	118.2	110.7	109.8	108.1	106.8	108.9	107.9	108.3		
Popul.-weighted concentr.	[µg.m^{-3}]	93.2 perc. of d. max8h								108.5	108.9	102.9	110.4
Popul. exposed > TV (120 µg.m^{-3})	[%]	26th highest d. max8h	31.6	51.4	27.1	15.0	16.0	16.3	16.5	20.7	15.0		
Popul. exposed > TV (120 µg.m^{-3})	[%]	93.2 perc. of d. max8h								21.9	15.9	5.6	34.0
SOMO35													
Popul.-weighted concentration		[µg.m^{-3}.d]	4706	5167	4411	4275	4275	3917	4414	4279	4088	3500	4312
Popul. exposed > 6000 µg.m^{-3}.d		[%]	27.0	29.5	28.1	19.6	24.6	16.6	23.6	24.5	18.8	9.4	22.2

The table presents the results obtained with the 1x1 km merging resolution as tested on the 2006 data in Horálek et al (2010), then recomputed for 2005 and 2007, and finally implemented fully on the 2008 data and onwards. For 2012 and 2013, both the 26th highest value and the 93.2nd percentile of maximum daily 8-hour mean(s) have been calculated. It demonstrates an underestimation of about 0.6

$\mu g \cdot m^{-3}$ at the 26th maximum daily 8-hour mean, which is caused by the fact that when calculating this indicator there is no correction for the missing values in the incomplete measurement time series.

Using the *93.2 percentile of ozone maximum daily 8-hour means* it is estimated that 34 % of the population lived in 2015 in areas where concentrations were above the ozone target value (TV) of 120 $\mu g \cdot m^{-3}$, which is about the highest number, with the exception of 2006, of the eleven years period. The overall European population-weighted ozone concentration in terms of the 93.2 percentile maximum daily 8-hour means in the background areas is estimated at about 110 $\mu g \cdot m^{-3}$, which is also one of the highest values of the whole eleven years period (please be aware that for 2005–2011 the 26th highest value of the maximum daily eight-hour mean was considered instead).

Examining the time series 2005 – 2015, it can be concluded that 2006, but also 2005 and 2015 are exceptional years with high ozone concentrations, leading to increased exposure levels compared to the other eight years.

Annex 4 presents some details on the trend analysis of the population-weighted concentrations for the 93.2 percentile of the maximum daily 8-hour means across the period 2005 – 2015 for individual countries and for Europe as a whole. The population-weighted concentration of the European totals (i.e. totals of 40 European countries considered) demonstrates a statistically significant downward trend of -0.5 $\mu g \cdot m^{-3}$ per year

A similar tendency is observed for the *SOMO35*. In 2006 – 2007 almost one-third of the population lived in areas where a level of 6 000 $\mu g \cdot m^{-3} \cdot d$[2] was exceeded, with the highest level in 2006. In the period of 2008 – 2015 it fluctuates from about 17 % to 25 % of the population, except 2014 with about 9 %. The population-weighted SOMO35 concentrations show a quite similar kind of pattern over time. Trend analysis in Annex 4 on the population-weighted concentration of the European totals shows a slightly downward trend of about -95 $\mu g \cdot m^{-3} \cdot d$, for the period 2005 – 2015, which is statistically significant and expresses a mean decrease of about 95 $\mu g \cdot m^{-3} \cdot d$ per year.

6.1.4 Vegetation and forest ozone indicators

Exposure indicators describing the *agricultural and forest areas exposed to accumulated ozone* concentrations above defined thresholds are summarised in Table 6.4. Those thresholds are the target value (TV) of 18 000 $\mu g \cdot m^{-3} \cdot h$ and the long-term objective (LTO) of 6 000 $\mu g \cdot m^{-3} \cdot h$ for the AOT40 for vegetation, and the former Reporting Value (RV) of 20 000 $\mu g \cdot m^{-3} \cdot h$ and the Critical Level (CL) of 10 000 $\mu g \cdot m^{-3} \cdot h$ for the AOT40 for forests.

[2] Note that the 6 000 $\mu g \cdot m^{-3} \cdot d$ does not represent a health-related legally binding 'threshold'. In this and previous papers it concerns a somewhat arbitrarily chosen threshold to facilitate the discussion of the observed distributions of SOMO35 levels in their spatial and temporal context. For motivation of this choice, see Section 4.2.

Table 6.4 Percentages of the European agricultural and forest area exposed to ozone concentrations above the target value (TV) and the long-term objective (LTO) for AOT40 for vegetation, and above Critical Level (CL) and Reporting Value (RV) for AOT40 for forests for 2005 to 2015

Ozone		2005	2006	2007	2008	2009	2010	2011	2012	2013	2014	2015
AOT40 for vegetation												
Agricultural area % > TV (18 000 µg.m^{-3}.h)	[%]	48.5	69.1	35.7	37.8	26.0	21.3	19.2	30.0	22.1	17.8	31.4
Agricultural area % > LTO (6 000 µg.m^{-3}.h)	[%]	88.8	97.6	77.5	95.5	81.0	85.4	87.9	86.4	81.0	85.5	79.7
Agricultural-weighted concentration (µg.m-3.h)		17481	22344	14597	15214	13157	13310	13255	14041	12838	12427	14223
AOT40 for forests												
Forest area exposed > RV (20 000 µg.m^{-3}.h)	[%]	59.1	69.4	48.4	50.2	49.2	49.3	53.0	47.2	44.1	37.7	52.4
Forest area exposed > CL (10 000 µg.m^{-3}.h)	[%]	76.4	99.8	62.1	79.6	67.4	63.4	68.6	65.0	67.2	68.2	59.8
Forest-weighted concentration (µg.m-3.h)		25900	31154	23744	21951	23532	19625	21892	21580	21753	17124	21150

In 2015, some 31 % of all agricultural land (crops) was exposed to accumulated ozone concentrations (AOT40 for vegetation) exceeding the target value (TV), which is one of the highest percentages of the eleven years period and the highest since 2009. Almost 80 % of all agricultural land was exposed to levels in excess of the long-term objective (LTO), which is the second lowest of all eleven years. In this paper for the first time also the agricultural area weighted concentration is included as exposure indicator. For 2015 its value of 14 223 µg.m^{-3}·h appears to be within the average range of the eleven year period.

For the ozone indicator AOT40 for *forests* the level of 20 000 µg·m^{-3}·h (earlier used Reporting Value, RV) was exceeded in about 52 % of the European forest area in 2015, which is one of the highest of the whole time series. The forest area exceeding the Critical Level (CL) was in 2015 about 60 %, which is the lowest percentage of the eleven years period. The forest area weighted concentration for 2015 is 21 150 µg.m^{-3}·h and appears to be in the mid-range of values for the eleven years period.

The temporal pattern of the AOT40 for forests exceedances shows some similarity with those of the AOT40 for vegetation, despite their different definitions and receptors and their natural difference in area type characteristics and occurrence. Their annual variability is, however, heavily dependent on meteorological variability.

6.1.5 Human health NO_2 indicators

Table 6.5 summarises for the *human health NO_2 indicator* the exposure levels of the European inhabitants in terms of population-weighted concentrations. Furthermore, it presents the percentage of European population exposed to concentrations above the limit value (LV) of 40 µg·m^{-3} for the years 2013 to 2015.

Table 6.5 Population-weighted concentration and percentage of the European population exposed to concentrations above the NO_2 limit value (LV) of 40 µg·m^{-3} for the protection of health for 2013 to 2015

NO_2		2013	2014	2015
Annual average				
Population-weighted concentration	[µg.m^{-3}]	19.4	18.6	18.8
Population exposed > LV (40 µg.m^{-3})	[%]	3.2	2.8	3.2

In 2015 the population exposed to NO_2 annual mean concentrations above the limit value of 40 µg·m^{-3} is 3.2 % of the total population, which is the same as in 2013 and slightly more than in 2014. Furthermore, it is estimated that European inhabitants are exposed on average to an annual mean NO_2 concentration of 19 µg·m^{-3}, about the same as in two previous years.

References

CHMI (2017). Air Pollution and Atmospheric Deposition in Data, the Czech Republic. http://portal.chmi.cz/files/portal/docs/uoco/isko/tab_roc/tab_roc_en.html

Cressie N (1993). Statistics for spatial data. Wiley series, New York.

Danielson JJ, Gesch DB (2011). Global multi-resolution terrain elevation data 2010 (GMTED2010): U.S. Geological Survey Open-File Report 2011–1073. https://lta.cr.usgs.gov/GMTED2010

De Leeuw F (2012). AirBase: a valuable tool in air quality assessments at a European and local level. ETC/ACM Technical Paper 2012/4. http://acm.eionet.europa.eu/reports/ETCACM_TP_2012_4_AirBase_AQassessment

Denby B, Schaap M, Segers A, Builtjes P, Horálek J (2008). Comparison of two data assimilation methods for assessing PM_{10} exceedances on the European scale. Atmospheric Environment 42, 7122–7134.

Denby B, Gola G, De Leeuw F, De Smet P, Horálek J (2011a). Calculation of pseudo $PM_{2.5}$ annual mean concentrations in Europe based on annual mean PM10 concentrations and other supplementary data. ETC/ACC Technical Paper 2010/9. http://acm.eionet.europa.eu/reports/ETCACC_TP_2010_9_pseudo_PM2.5_stations

Denby B, Horálek J, de Smet P, de Leeuw F (2011b). Mapping annual mean $PM_{2.5}$ concentrations in Europe: application of pseudo $PM_{2.5}$ station data. ETC/ACM Technical Paper 2011/5. http://acm.eionet.europa.eu/reports/ETCACM_TP_2011_5_spatialPM2.5mapping

De Smet P, Horálek J, Coňková M, Kurfürst P, de Leeuw F, Denby B (2009). European air quality maps of ozone and PM_{10} for 2006 and their uncertainty analysis. ETC/ACC Technical Paper 2008/8. http://acm.eionet.europa.eu/reports/ETCACC_TP_2008_8_spatAQmaps_2006

De Smet P, Horálek J, Coňková M, Kurfürst P, de Leeuw F, Denby B (2010). European air quality maps of ozone and PM_{10} for 2007 and their uncertainty analysis. ETC/ACC Technical Paper 2009/9. http://acm.eionet.europa.eu/reports/ETCACC_TP_2009_9_spatAQmaps_2007

De Smet P, Horálek J, Coňková M, Kurfürst P, de Leeuw F, Denby B (2011). European air quality maps of ozone and PM_{10} for 2008 and their uncertainty analysis. ETC/ACC Technical Paper 2010/10. http://acm.eionet.europa.eu/reports/ETCACC_TP_2010_10_spatAQmaps_2008

ECMWF: Meteorological Archival and Retrieval System (MARS). http://www.ecmwf.int/

EEA (2008). ORNL Landscan 2008 Global Population Data conversion into EEA ETRS89-LAEA5210 1km grid (eea_r_3035_1_km_landscan-eurmed_2008, by Hermann Peifer of EEA).

EEA (2011). Guide for EEA map layout. EEA operational guidelines. August 2011, version 4. http://www.eionet.europa.eu/gis/docs/GISguide_v4_EEA_Layout_for_map_production.pdf

EEA (2016). Corine land cover 2006 (CLC2006) raster data. 100x100m gridded version 18 (09/2016) https://www.eea.europa.eu/data-and-maps/data/clc-2006-raster-4

EEA (2017a). Air Quality e-Reporting. Air quality database. http://www.eea.europa.eu/data-and-maps/data/aqereporting-2

EEA (2017b). Air quality in Europe – 2017 Report. EEA Report 13/2017. https://www.eea.europa.eu//publications/air-quality-in-europe-2017

EEA (2017c). Exceedance of air quality limit values in urban areas. CSI004 indicator assessment. https://www.eea.europa.eu/data-and-maps/indicators/exceedance-of-air-quality-limit-3/assessment-3

EEA (2017d). Exposure of ecosystems to acidification, eutrophication and ozone. https://www.eea.europa.eu/data-and-maps/indicators/exposure-of-ecosystems-to-acidification-14/assessment

EU (2008). Directive 2008/50/EC of the European Parliament and of the Council of 21 May 2008 on ambient air quality and cleaner air for Europe. OJ L 152, 11.06.2008, 1-44. http://eur-lex.europa.eu/LexUriServ/LexUriServ.do?uri=OJ:L:2008:152:0001:0044:EN:PDF

Eurostat (2014). GEOSTAT 2011 grid dataset. Population distribution dataset. http://ec.europa.eu/eurostat/web/gisco/geodata/reference-data/population-distribution-demography

Eurostat (2017). Total population for European states for 2015. http://epp.eurostat.ec.europa.eu/tgm/table.do?tab=table&language=en&pcode=tps00001&tableSelection=1&footnotes=yes&labeling=labels&plugin=1

EMEP (2017). Transboundary particular matter, photo-oxidants, acidifying and eutrophying components. EMEP Report 1/2017. http://emep.int/publ/reports/2017/EMEP_Status_Report_1_2017.pdf

Gilbert, RO (1987). Statistical Methods for Environmental Pollution Monitoring. Van Nostrand Reinhold, New York.

Guerreiro C, Horálek J, de Leeuw F, Couvidat F (2015). Mapping ambient concentrations of benzo(a)pyrene in Europe. ETC/ACM Technical paper 2014/6. http://acm.eionet.europa.eu/reports/ETCACM_TP_2014_6_BaP_HIA

Horálek J, Kurfürst P, Denby B, de Smet P, de Leeuw F, Brabec M, Fiala J (2005). Interpolation and assimilation methods for European scale air quality assessment and mapping. Part II: Development and testing new methodologies. ETC/ACC Technical paper 2005/8. http://acm.eionet.europa.eu/docs/ETCACC_TechnPaper_2005_8_SpatAQ_Part_II.pdf

Horálek J, Denby B, de Smet P, de Leeuw F, Kurfürst P, Swart R, van Noije T (2007). Spatial mapping of air quality for European scale assessment. ETC/ACC Technical paper 2006/6. http://acm.eionet.europa.eu/reports/ETCACC_TechnPaper_2006_6_Spat_AQ

Horálek J, de Smet P, de Leeuw F, Denby B, Kurfürst P, Swart R (2008). European air quality maps for 2005 including uncertainty analysis. ETC/ACC Technical paper 2007/7. http://acm.eionet.europa.eu/reports/ETCACC_TP_2007_7_spatAQmaps_ann_interpol

Horálek J, de Smet P, de Leeuw F, Coňková M, Denby B, Kurfürst P (2010). Methodological improvements on interpolating European air quality maps. ETC/ACC Technical Paper 2009/16. http://acm.eionet.europa.eu/reports/ETCACC_TP_2009_16_Improv_SpatAQmapping

Horálek J, Kurfürst P, de Smet P (2014). Additional 2011 European air quality maps. ETC/ACM Technical Paper 2014/5. http://acm.eionet.europa.eu/reports/ETCACM_TP_2014_5_add_2011_aqmaps

Horálek J, de Smet P, Kurfürst P, de Leeuw F, Benešová N (2015). European air quality maps of PM and ozone for 2012 and their uncertainty. ETC/ACM Technical Paper 2014/4. http://acm.eionet.europa.eu/reports/ETCACM_TP_2014_4_spatAQmaps_2012

Horálek J, Benešová N, de Smet P (2016a). Application of FAIRMODE Delta tool to evaluate interpolated European air quality maps for 2012. ETC/ACM Technical Paper 2015/2. http://acm.eionet.europa.eu/reports/ETCACM_TP_2015_2_Delta_Evaluation_AQMaps2012

Horálek J, de Smet P, Kurfürst P, de Leeuw F, Benešová N (2016b). European air quality maps of PM and ozone for 2013 and their uncertainty. ETC/ACM Technical Paper 2015/5. http://acm.eionet.europa.eu/reports/ETCACM_TP_2015_5_spatAQmaps_2013

Horálek J, Guerreiro C., de Leeuw, de Smet (2017a). Potential improvements on benzo(a)pyrene (BaP) mapping. ETC/ACM Technical Paper 2016/3. http://acm.eionet.europa.eu/reports/ETCACM_TP_2016_3_BaP_improved_mapping

Horálek J, de Smet P, de Leeuw F, Kurfürst P, Benešová N (2017b). European air quality maps for 2014. ETC/ACM Technical Paper 2016/6. http://acm.eionet.europa.eu/reports/ETCACM_TP_2016_6_AQMaps2014

Horálek J, de Smet P, Schneider P, Kurfürst P, de Leeuw F (2017c). Inclusion of land cover and traffic data in NO_2 mapping methodology. ETC/ACM Technical Paper 2016/12. http://acm.eionet.europa.eu/reports/ETCACM_TP_2016_12_LC_and_traffic_data_in_NO2_mapping

Horálek J, de Smet P, de Leeuw F, Kurfürst P, de Leeuw F (2017d). European NO_2 air quality map for 2014. Improved mapping methodology using land cover and traffic data. ETC/ACM Technical Paper 2017/6. http://acm.eionet.europa.eu/reports/ETCACM_TP_2017_6_improved2014NO2_AQMap

IPCC (2010). Guidance note for lead authors of the IPCC Fifth Assessment Report on consistent treatment of uncertainties. Jasper Ridge, USA. http://www.ipcc.ch/pdf/supporting-material/uncertainty-guidance-note.pdf

JRC (2009). Population density disaggregated with Corine land cover 2000. 100x100 m grid resolution, EEA version popu01clcv5.tif of 24 Sep 2009. http://www.eea.europa.eu/data-and-maps/data/population-density-disaggregated-with-corine-land-cover-2000-2

Mareckova K, Pinterits M, Ullrich B, Wankmüller R, Mandl N (2017). Inventory Review 2017. Review of emission data reported under the LRTAP Convention and NEC Directive. Stage 1 and 2 review & Status of gridded and LPS data. EEA/CEIP Technical Report 2/2017. http://www.ceip.at/fileadmin/inhalte/emep/pdf/2017/InventoryReport_2017_v3.pdf

NILU (2017). EBAS, database of atmospheric chemical composition and physical properties (NILU, Norway). http://ebas.nilu.no/

NMI (2017). EMEP/MSC-W modelled air concentrations and depositions. Yearly NetCDF file for 2015 (2017_Reporting), EMEP01deg. http://www.emep.int/mscw/mscw_ydata.html

ORNL (2008). ORNL LandScan high resolution global population data set. http://www.ornl.gov/sci/landscan/landscan_documentation.shtml

Simpson D, Benedictow A, Berge H, Bergström R, Emberson LD, Fagerli H, Hayman GD, Gauss M, Jonson JE, Jenkin ME, Nyíri A, Richter C, Semeena VS, Tsyro S, Tuovinen J-P, Valdebenito A, Wind P (2012). The EMEP MSC-W chemical transport model – technical description. Atmospheric Chemistry and Physics, 12, 7825–7865, doi:10.5194/acp-12-7825-2012. http://www.atmos-chem-phys.net/12/7825/2012/acp-12-7825-2012.html

UNECE (2004). Manual on methodologies and criteria for modelling and mapping critical loads and levels and air pollution effects, risks and trends. UNECE Convention on Long-range Transboundary Air Pollution. http://www.icpmapping.org/Mapping_Manual

UNECE (2016). Forest condition in Europe. 2016 report of ICP Forests. UNECE Convention on Long-range Transboundary Air Pollution.
http://www.wsl.ch/info/mitarbeitende/schaub/ICPF_TR_2016.pdf

WHO (2005). WHO Air quality guidelines for particulate matters, ozone, nitrogen dioxide and sulphur dioxide. Global update 2005.
http://www.who.int/phe/health_topics/outdoorair/outdoorair_aqg/en/index.html

Annex 1 Methodology

A1.1 Mapping method

Previous technical papers prepared by Horálek et al. (2005, 2007, 2008, 2010, 2014, 2017c), De Smet et al. (2011), Denby et al. (2011a, 2011b) discuss methodological developments and details on spatial interpolations and their uncertainties. No changes took place in the mapping methodology of PM_{10}, $PM_{2.5}$, ozone and NO_x indicators compared to the preceding reports (Horálek et al., 2017b and references cited therein). For NO_2, the mapping methodology variant developed in Horálek et al. (2017c) and applied in Horálek et al. (2017d) is used. This annex summarizes the currently applied method for all these indicators. The mapping method has been evaluated with the FAIRMODE Delta tool in Horálek et al. (2016a). The method can be described as the regression – interpolation – merging mapping.

Pseudo $PM_{2.5}$ and NO_x station data estimation

To supplement $PM_{2.5}$ measurement data, in the mapping procedure we also use data from so-called *pseudo $PM_{2.5}$ stations*. These data are the estimates of $PM_{2.5}$ concentrations at the locations of PM_{10} stations with no $PM_{2.5}$ measurement. These estimates are based on PM_{10} measurement data and different supplementary data, using linear regression:

$$\hat{Z}_{PM2.5}(s) = c + b.Z_{PM10}(s) + a_1.X_1(s) + \ldots + a_n.X_n(s) \qquad \text{(A1.1)}$$

where $\hat{Z}_{PM2.5}(s)$ is the estimated value of $PM_{2.5}$ at the station s,
$Z_{PM10}(s)$ is the measurement value of PM_{10} at the station s,
$X_1(s), \ldots, X_n(s)$ are the values of other supplementary variables at the station s,
$c, b, a_1, \ldots, a_n$ are the parameters of the linear regression model calculated based on the data at the points of measuring stations with both $PM_{2.5}$ and PM_{10} measurements,
n is the number of other supplementary variables used in the linear regression model (apart from PM_{10}).

When applying this estimation method, all background stations (either classified as rural, urban or suburban) are handled together. For details, see Denby et al. (2011b).

To supplement NO_x measurement data, we estimate NO_x values at the locations of NO_2 stations with no NO_x data. The estimates are calculated similarly as in Horálek et al. (2007), using quadratic regression:

$$\hat{Z}_{NOx}(s) = a.Z_{NO2}(s)^2 + b.Z_{NO2}(s) + c \qquad \text{(A1.2)}$$

where $\hat{Z}_{NOx}(s)$ is the estimated value of NO_x at the station s,
$Z_{NO2}(s)$ is the measurement value of NO_2 at the station s,
a, b, c are the parameters of the quadratic regression calculated based on the data at the points of measuring stations with both NO_x and NO_2 measurements.

Interpolation

The mapping method used is a linear regression model followed by kriging of the residuals produced from that model (residual kriging). Interpolation is therefore carried out according to the relation:

$$\hat{Z}(s_0) = c + a_1.X_1(s_0) + a_2.X_2(s_0) + \ldots + a_n.X_n(s_0) + \eta(s_0) \qquad \text{(A1.3)}$$

where $\hat{Z}(s_0)$ is the estimated value of the air pollution indicator at the point s_o,

$X_1(s_0), X_2(s_0), \ldots, X_n(s_0)$ are the n number of individual supplementary variables at the point s_o

$c, a_1, a_2, \ldots, a_n$ are the $n+1$ parameters of the linear regression model calculated based on the data at the points of measurement,

$\eta(s_0)$ is the spatial interpolation of the residuals of the linear regression model at the point s_o calculated based on the residuals at the points of measurement.

For different pollutants and area types (rural, urban background, and in the case of NO_2 also urban traffic), different supplementary data are used, depending on their improvement to the fit of the regression. Ordinary kriging is used to interpolate the residuals:

$$\hat{R}(s_0) = \sum_{i=1}^{N} \lambda_i R(s_i), \ \sum_{i=1}^{N} \lambda_i = 1, \tag{A1.4}$$

where $R(s_i)$ are the residuals in the points of the measuring stations s_i,

$\lambda_1, \ldots, \lambda_N$ are the weights estimated based on variogram,

N is the number of the stations used in the interpolation.

The variogram (as a measure of a spatial correlation) is estimated using a spherical function (with parameters *nugget, sill, range*). For details, see Horálek et al. (2007), Section 2.3.5 and Cressie (1993).

For $PM_{2.5}$ and NO_x, both measurement data and the estimated data from the pseudo stations are used.

For the PM_{10} and $PM_{2.5}$ indicators we apply, prior to linear regression and interpolation, a logarithmic transformation to measurement and EMEP model concentrations. In the case of $PM_{2.5}$ rural map layer creation, population density is also log-transformed. After interpolation, we apply a back-transformation. For details, see De Smet et al. (2011) and Denby et al. (2008). In the case of urban background $PM_{2.5}$ map, we do not use any supplementary data – we apply just lognormal kriging.

For the vegetation related indicators (AOT40 for vegetation and forests and NO_x) we only construct rural maps based on rural background stations, based on the assumption that no vegetation is located in urban areas. For the health related indicators, we construct the rural and urban background map layers (and for NO_2 also urban traffic map layer) separately and then we merge them.

Merging of rural and urban background (and urban traffic) map layers

Health related indicator map layers for PM_{10}, $PM_{2.5}$ and ozone are constructed (using linear regression with kriging of its residuals) for the rural and urban background areas separately on a grid at 10x10 km resolution. The rural map is based on rural background stations and the urban background map on urban and suburban background stations. Subsequent to this, the rural and urban background maps are merged into one combined air quality indicator map using a European-wide population density grid at 1x1 km resolution. For the 1x1 km grid cells with a population density less than a defined value of α_1, we select the rural map value and for grid cells with a population density greater than a defined value α_2, we select the urban background map value. For areas with population density within the interval (α_1, α_2) a weighting function of α_1 and α_2 is applied (for details and the setting of the parameters α_1 and α_2, see Horálek et al., 2005, 2007, 2010). This applies to the grid cells where the estimated rural value is lower (PM_{10} and $PM_{2.5}$) or higher (ozone), than the estimated urban background map value. In the exceptional cases when this criterion does not hold, we apply a joint urban/rural map layer (created using all background stations regardless their type), as far as its value lies in between the rural and urban background map value. For details, see De Smet et al. (2011).

Summarising, the separate rural, urban and joint urban/rural map layers are constructed at a resolution of 10x10 km; their merging however takes place on the basis of the 1x1 km resolution population density grid, resulting in a final combined pollutant indicator map on this 1x1 km resolution grid. This map is used both for the population exposure estimates and for presentational purposes.

In the case of NO_2, separate map layers are created for rural, urban background and urban traffic areas on a grid at 1x1 km resolution. The rural background map layer is based on the rural background stations, the urban background map layer on the urban and the suburban background stations, and the urban traffic map layer on the urban and the suburban traffic stations. For different map layers (rural, urban background, urban traffic) different supplementary data are used, depending on their improvement to the fit of the regression. The three map layers are merged into one final map using a weighting procedure

$$\hat{Z}_F(s_0) = \left(1 - w_U(s_0)\right) \cdot \hat{Z}_R(s_0) + w_U(s_0)\left(1 - w_T(s_0)\right) \cdot \hat{Z}_{UB}(s_0) + w_U(s_0) w_T(s_0) \cdot \hat{Z}_T(s_0) \qquad \text{(A1.5)}$$

where $\hat{Z}_F(s_0)$ is the resulting estimated concentration in a grid cell s_o for the final map,

$\hat{Z}_{UB}(s_0)$ is the estimated concentration in a grid cell s_o for the urban background map layer,

$\hat{Z}_R(s_0)$ is the estimated concentration in a grid cell s_o for the rural background map layer,

$\hat{Z}_T(s_0)$ is the estimated concentration in a grid cell s_o for the urban traffic map layer,

$w_U(s_0)$ is the weight representing the ratio of the urban character of the a grid cell s_o,

$w_T(s_0)$ is the weight representing the ratio of areas exposed to traffic air quality in a grid cell s_o.

The weight $w_U(s_0)$ is based on the population density grid, while $w_T(s_0)$ is based on the buffers around the roads. For further details, see Horálek et al. (2017b and references therein).

In all calculations and map presentations the EEA standard projection ETRS89-LAEA5210 (also known as ETRS89 / LAEA Europe, see www.epsg-registry.org) is used. The interpolation and mapping domain consists of the areas of all EEA member and cooperating countries, as far as they fall into the EEA map extent *Map_1c* (EEA, 2011). The mapping area covers the whole Europe apart from Belarus, Moldova, Ukraine and the European parts of Russia and Kazakhstan.

A1.2 Calculation of population and vegetation exposure

Population and vegetation exposure estimates are based on the interpolated concentration maps, population density data and land cover data.

Population exposure

Population exposure for individual countries and for Europe as a whole is calculated for PM_{10}, $PM_{2.5}$ and ozone from the air quality maps and population density data, both at 1x1 km resolution. For each concentration class, the total population per country as well as the European-wide total is determined.

For NO_2, the population exposure is calculated separately for the areas where the air quality is considered to be directly influenced by traffic and for the background (both rural and urban) areas. For each concentration class '*j*', the percentage population per country as well as the European-wide total is determined according to:

$$P_j = \frac{\sum_{i=1}^{N} I_{Bij}\left(1 - w_U(i) w_T(i)\right) p_i + \sum_{i=1}^{N} I_{Tij} w_U(i) w_T(i) p_i}{\sum_{i=1}^{N} p_i} \cdot 100 \qquad \text{(A1.6)}$$

where P_j is the percentage population living in areas of the *j*-th concentration class in either the country or in Europe as a whole,

p_i is the population in the i-th grid cell,

I_{Bij} is the Boolean 0-1 indicator showing whether the background air quality concentration (estimated by the combined rural/urban background map layer) in the i-th grid cell is within the j-th concentration class (I_{Bij} = 1), or not (I_{Bij} = 0),

I_{Tij} is the Boolean 0-1 indicator showing whether the traffic air quality concentration in the i-th grid cell is within the j-th concentration class (I_{Tij} = 1), or not (I_{Tij} = 0),

N is the number of grid cells in the country or in Europe as a whole.

In addition, we express per-country and European-wide exposure as the population-weighted concentration, i.e. the average concentration weighted according to the population in a 1x1 km grid cell:

$$\hat{c} = \frac{\sum_{i=1}^{N} c_i p_i}{\sum_{i=1}^{N} p_i} \tag{A1.7}$$

where $\hat{c}$ is the population-weighted average concentration in the country or in the whole of Europe,

p_i is the population in the i^{th} grid cell,

c_i is the concentration in the i^{th} grid cell,

N is the number of grid cells in the country or in Europe as a whole.

Estimation of trends

For detecting and estimating the trends in time series of annual values of population exposure, the nonparametric Mann-Kendall's test for testing the presence of the monotonic increasing or decreasing trend is used. Next to that, the nonparametric Sen's method for estimating the slope of a linear trend is executed. For details, see Gilbert (1987). The significance of the Mann-Kendal test is shown by the usual way, i.e. + for 0.1, * for 0.05, ** for 0.01, and *** for 0.001.

Vegetation (and forest) exposure

Vegetation (and forest) exposure for individual countries and for Europe as a whole is calculated based on the air quality maps and land cover data, both in 2x2 km grid resolution. For each concentration class, the total vegetation (and forest) area per country as well as European-wide is determined.

Next to this, we express per-country and European-wide exposure as the vegetation (forest)-weighted concentration, i.e. the average concentration weighted according to the vegetation (and forest) in a 1x1 km grid cell, similarly like in Eq. A1.7.

A1.3 Methods for uncertainty analysis

The uncertainty estimation of the European map is based on cross-validation. The cross-validation method computes the quality of the spatial interpolation for each measurement point from all available information except from the point in question, i.e. it withholds one data point and then makes a prediction at the spatial location of that point. This procedure is repeated for all measurement points in the available set. The predicted and measurement values at these points are plotted in the form of a scatter plot. With help of statistical indicators the quality of the predictions is demonstrated objectively. The advantage of the nature of this cross-validation technique is that it enables evaluation of the quality of the predicted values at locations without measurements, as long as they are within the area covered by the measurements.

In addition, we make a simple comparison between the point measurements and interpolated values of the 10x10 km grid for the separate rural and urban maps and the 1x1 km grid for the final combined maps, for the health-related indicators, resp. the 2x2 km grid in the case of AOT40 and NO_x. Note that the grid cell value is the averaged result of the interpolation in this grid cell area. The interpolated value within a grid cell will only approximate the predicted value(s) at the station(s) lying within that cell.

Another method to estimate uncertainties is based on geostatistical theory: together with the prediction, the prediction standard error is computed at all the grid cells, which represents in fact the interpolation uncertainty map (see Cressie, 1993 for a detailed discussion). Based on the concentration and the uncertainty map, the exceedance probability map is created.

Cross-validation

The results of cross-validation are described by the statistical indicators and scatter plots. The main indicator used is root mean squared error (RMSE) and additional is bias (mean prediction error, MPE):

$$RMSE = \sqrt{\frac{1}{N}\sum_{i=1}^{N}(\hat{Z}(s_i) - Z(s_i))^2} \quad \text{(A1.8)}$$

$$bias(MPE) = \frac{1}{N}\sum_{i=1}^{N}(\hat{Z}(s_i) - Z(s_i)) \quad \text{(A1.9)}$$

where $Z(s_i)$ is the air quality indicator value derived from the measured concentration at the i^{th} point, $i = 1, ..., N$,

$\hat{Z}(s_i)$ is the air quality estimated indicator value at the i^{th} point using other information, without the indicator value derived from the measured concentration at the i^{th} point,

N is the number of the measuring points.

Next to the RMSE expressed in the absolute units, one could express this uncertainty in relative terms by relating the RMSE to the mean of the air pollution indicator value for all stations:

$$RRMSE = \frac{RMSE}{Z}.100 \quad \text{(A1.10)}$$

where $RRMSE$ is the relative RMSE, expressed in percent,

$\overline{Z}$ is the arithmetic average of the indicator values $Z(s_1), ..., Z(s_N)$, as derived from measurement concentrations at the station points $i = 1, ... , N$.

Other indicators are R^2 and the regression equation parameters *slope* and *intercept*, following from the scatter plot between the predicted (using cross-validation) and the observed concentrations.

RMSE should be as small as possible, bias (MPE) should be as close to zero as possible, R^2 should be as close to *1* as possible, slope *a* should be as close to *1* as possible, and intercept *c* should be as close to zero as possible (in the regression equation $y = a.x + c$).

In the cross-validation of $PM_{2.5}$ and NO_x, only stations with $PM_{2.5}$ resp. NO_x measurement data are used (not the pseudo $PM_{2.5}$ resp. NO_x stations).

Comparison of the point measurement and interpolated grid values

The comparison of point measurement and predicted grid values is described by the linear regression equation and its parameters and statistical values. The comparison is executed separately for rural and urban background maps and for the final combined map. In the case of $PM_{2.5}$ and NO_x, only the stations with actual $PM_{2.5}$ resp. NO_x measurement data are used (not the pseudo $PM_{2.5}$ resp. NO_x stations).

The point observation – point cross-validation prediction analysis (Annex 3) describes interpolation performance at point locations when there is no observation (as it follows the leave-one-out approach). In this case, the smoothing effect of the interpolation is most prevalent.

The point observation – grid prediction approach indicates performance of the value for the 10x10 km (resp. 2x2 km or 1x1 km) grid cell with respect to the observations that are located within that cell. As such, some variability is due to smoothing but it also includes smoothing due to spatial averaging into the 10x10 km (2x2 km) grid cells. As such, the point-grid validation approach tells us how well our interpolated and aggregated grid values approximate the measurements at the actual station (point) locations. Whereas the point-point approach tells us how well our interpolated values estimate the indicator at a point where there is no actual measurement at that location, under the constrained that the point lies within the area covered by measurements.

Exceedance probability mapping

The maps with the probability of exceedance (PoE) of a specific threshold value (e.g. limit or target value) are constructed using the concentration and uncertainty maps:

$$PoE(x) = 1 - \Phi\left(\frac{LV - C_c(x)}{\sigma_c(x)}\right) \qquad \text{(A1.11)}$$

where $PoE(x)$ is the probability of limit/target value (*LV/TV*) exceedance in the grid cell x,
$\Phi(\,)$ is the cumulative distribution function of the normal distribution,
LV is the limit or target value of the relevant indicator,
$C_c(x)$ is the interpolated concentration in the grid cell x,
$\sigma_c(x)$ is the standard error of the estimation in the grid cell x.

The standard error of the probability map of the combined (rural and urban background) map is calculated from the standard errors of the separate rural and urban background maps; see Horálek et al. (2008), Section 2.3 and De Smet et al. (2011), Chapter 2. The maps with the probability of threshold value exceedance (PoE) are constructed in 1 x 1 km grid resolution.

In the probability of exceedance maps in this paper, the areas with 33–50 % and 50–66 % probability of LV exceedance are marked in yellow and orange respectively. The yellow colour indicates the areas with the estimated concentrations below limit value, but for which there exists a *modest* probability of exceeding the limit. The orange coloured areas have estimated concentrations above the limit value, but with a *moderate* chance of non-exceedance caused by its accompanying uncertainty. On the contrary, the areas with 66–90 % and 90–100 % are marked with red colour in two shades, indicating large or high probability of LV exceedance. Similarly, the areas with 0–10 % and 10–33 % are marked with green in two shades, indicating little or low probability of LV exceedance. Table A1.1 summarises the classes and terminology for probability (i.e. likelihood) that are distinguished in this paper.

Table A1.1 Probability mapping classes and terminology use in this paper

Map class colour	Percentage probability of threshold exceedance	Degree of probability (or likelihood) of exceedance	Likelihood of exceedance	
Green	0 – 10	Little	Very unlikely	More unlikely than likely
Light green	10 – 33	Low	Unlikely	
Yellow	33 – 50	Modest	About as likely as not	
Orange	50 – 66	Moderate		More likely than not
Light red	66 – 90	Large	Likely	
Dar red	90 – 100	High	Very likely	

The probability classes are used based on the classification used in IPCC (2010). Its basic likelihood scale of "very likely", "likely", "about as likely as not", "unlikely" and "very unlikely" is combined with an additional option of "more likely than not".

Annex 2 Input data

The types of input data in this paper are not different from that of Horálek et al. (2017b). The air quality and meteorological data has been updated. No further changes in selecting and processing of the input data have been implemented. For readability of this paper, we reproduce here the list of the input data. The key data is the air quality measurements at the monitoring stations extracted from Air Quality e-Reporting database, including geographical coordinates (*latitude*, *longitude*). The supplementary data cover the whole mapping domain and are converted into the EEA reference projection ETRS89-LAEA5210 on a 10 x 10 km grid resolution (for health related indicators apart from NO_2) resp. a 1x1 km grid resolution (for NO_2). The data for the AOT40 maps of vegetation related indicators (particularly AOT40) were converted – like in the previous reports (Horálek et al., 2017b and references cited therein) – into a 2 x 2 km resolution to allow accurate land cover exposure estimates to be prepared for use in Core Set Indicator 005 of the EEA.

A2.1 Air quality monitoring data

Air quality station monitoring data for the relevant year are extracted from the official EEA Air Quality e-Reporting database, made public on 27 April 2017, EEA (2017a). This data set is supplemented with several EMEP stations from the database EBAS (NILU, 2017) not reported to the Air Quality e-Reporting database. Specifically, 10 additional stations for PM_{10}, 10 for $PM_{2.5}$, 17 for NO_2 and 7 for NO_x from the EBAS database are added. With one exception, all these stations are classified as rural background. Next to this, several additional stations presented in CHMI (2017) and not included in EEA (2017a) are added. Specifically, these are 31 stations (20 rural background and 11 urban and suburban background) for PM_{10} and 9 stations (6 rural background and 3 urban and suburban background) for $PM_{2.5}$. Only data from stations classified as *background* (for the three types of area, *rural*, *suburban* and *urban*) are used for most of the pollutants. *Industrial* and *traffic* station types are not considered; they represent local scale concentration levels not applicable at the mapping resolution employed. For NO_2, next to the background stations, also the stations classified as *traffic* (for the types of area *suburban* and *urban*) are used, in agreement with Horálek et al. (2017c). Rural traffic stations are not considered due to their small number (i.e. 13).

The following pollutants and aggregations are considered:

PM_{10} – annual average [$\mu g \cdot m^{-3}$], year 2015
– 90.4 percentile of the daily average values [$\mu g \cdot m^{-3}$], year 2015

$PM_{2.5}$ – annual average [$\mu g \cdot m^{-3}$], year 2015

Ozone – 93.2 percentile of the maximum daily 8-hour average values [$\mu g \cdot m^{-3}$], year 2015
– SOMO35 [$\mu g \cdot m^{-3} \cdot day$], year 2015
– AOT40 for vegetation [$\mu g \cdot m^{-3} \cdot hour$], year 2015
– AOT40 for forests [$\mu g \cdot m^{-3} \cdot hour$], year 2015

NO_2 – annual average [$\mu g \cdot m^{-3}$], year 2015

NO_x – annual average [$\mu g \cdot m^{-3}$], year 2015

NO – annual average [$\mu g \cdot m^{-3}$], year 2015 (for the purposes of NO_x mapping only)

The exact values of percentiles are actually 90.41 in the case of PM_{10} daily means and 93.15 in the case of ozone maximum daily 8-hour means.

For a considerable number of stations NO_x is measured, but it is not reported as such but separately as NO and NO_2. For these stations reporting NO and NO_2 separately, the NO_x concentrations were derived according to the equation

$$NO_x = NO_2 + \frac{46}{30} \cdot NO \qquad \text{(A2.1)}$$

where all components are expressed in $\mu g \cdot m^{-3}$, with a molecular mass for NO of 30 and for NO_2 of 46 $g.mol^{-1}$.

SOMO35 is the annual sum of the differences between maximum daily 8-hour concentrations above 70 $\mu g \cdot m^{-3}$ (i.e. 35 ppb) and 70 $\mu g \cdot m^{-3}$. AOT40 is the sum of the differences between hourly concentrations greater than 80 $\mu g \cdot m^{-3}$ (i.e. 40 ppb) and 80 $\mu g \cdot m^{-3}$, using only observations between 08:00 and 20:00 CET, calculated over the three months from May to July for AOT40 for vegetation and over the six months from April to September for AOT40 for forests.

Only the stations with annual data coverage of at least 75 percent are used. In the case of SOMO35 and AOT40 indicators, a correction for the missing data is applied according to the equation

$$I_{corr} = I \cdot \frac{N_{\max}}{N} \qquad \text{(A2.2)}$$

where I_{corr} is the corrected indicator (SOMO35, AOT40 for vegetation or AOT40 for forests),
I is the value of the given indicator without any correction,
N is the number of the available daily resp. hourly data in a year for the given station,
N_{max} is the maximum possible number of the days or hours applicable for the given indicator.

For the x^{th} highest values (i.e. for the PM_{10} indicator 36^{th} highest daily mean and for the ozone indicator 26^{th} highest maximum daily 8-hour running mean) used in the previous reports (Horálek et al., 2016b and references cited therein), no correction for missing data was applied. The most straightforward way to solve the missing data issue in these cases is to use percentiles instead of the x^{th} highest values. As of ETC/ACM Technical Paper 2016/6 with its 2014 maps, the 90.4 percentile of PM_{10} daily means and the 93.2 percentile of ozone maximum daily 8-hour means is used.

For the indicators relevant to human health (i.e. for all PM_{10} and $PM_{2.5}$ indicators, ozone indicators 93.2 percentile of maximum daily 8-hour means and SOMO35, and NO_2 annual average), data from *rural*, *urban* and *suburban background* stations are considered. (Throughout the paper, the urban and suburban stations are handled together.) For NO_2, also *urban* and *suburban traffic* stations are considered. For the indicators relevant to vegetation damage (i.e. for both ozone AOT40 parameters and NO_x annual average), only *rural background* stations are considered. In case of existing data (with sufficient annual time coverage) from two or more different measurement devices in the same station location, the average of these data is used.

We excluded the stations from French overseas areas (departments), Svalbard, Azores, Madeira and Canary Islands. These areas outside the EEA map extent *Map_1c* (EEA, 2011) were excluded from the interpolation and mapping domain.

Table A2.1 shows the number of the measurement stations selected for the individual pollutants and their respective indicators.

Table A2.1 Number of stations selected for each pollutant indicator and area type

Station type	PM_{10}		$PM_{2.5}$	ozone				NO_2	NO_x
	Ann. avg.	90.4 perc. of d. means	Annual average	93.2 perc. of max. d. 8h	SOMO35	AOT40 for veg.	AOT40 for forests	Ann. avg.	Ann. avg.
Rural background	348	348	167	488	488	494	475	425	319
Urban/suburban backgr.	1102	1102	543	1009	1009			1180	
Urban/suburban traffic								726	

Compared to 2014, the number of rural background stations selected for 2015 is about the same for PM_{10}, while it decreased by approximately 5 % for $PM_{2.5}$, by 1 – 5 % for ozone and by about 1 % for NO_x, and increased by about 5 % for NO_2. The number of the urban/suburban background stations increased by approximately 3 % for PM_{10}, by approximately 7 % for $PM_{2.5}$, and by about 5 % for NO_2, while it decreased by about 1 % for ozone. The number of the NO_2 urban/suburban traffic stations increased by approximately 3 %.

For the $PM_{2.5}$ mapping, 209 additional rural background and 666 additional urban/suburban background PM_{10} stations (at locations without $PM_{2.5}$ measurement) were also used for the purpose of calculating the pseudo $PM_{2.5}$ station data.

In the case of NO_x, for 286 stations NO_x data is reported, while for 33 stations NO_x values are calculated from reported NO_2 and NO data using Eq. A2.1. Next to this, for the NO_x mapping 108 additional rural background NO_2 stations (at locations without NO_x measurement) were also used for the purpose of calculating the pseudo NO_x station data.

Due to the lack of reporting stations in Turkey, no proper interpolation results could be presented for this country for any of the indicators. Therefore, we excluded Turkey from the production process of the maps and exposure tables of this paper.

A2.2 EMEP MSC-W model output

The chemical dispersion model used in this paper is the EMEP MSC-W (formerly called Unified EMEP) model (version rv4.15), which is an Eulerian model. Simpson et al. (2012) and https://wiki.met.no/emep/page1/emepmscw_opensource (web site of Norwegian Meteorological Institute) describe the model in more detail. Emissions for the relevant year 2015 (Mareckova et al., 2017) are used and the model is driven by ECMWF meteorology for the relevant year 2015. EMEP (2017) provides details on the EMEP modelling for 2015. The resolution of the model is 0.1°x0.1°, i.e. circa 10x10 km. Information from this model was converted to the standard EEA 10x10 km grid resolution (for health related indicators apart from NO_2), resp. into the 2x2 km grid resolution (for vegetation related indicators) or 1x1 km grid resolution (for NO_2) for the interpolation process.

We downloaded the EMEP data from NMI (2017) in the form of annual means. Next to this, we received the EMEP data in the form of daily means for PM_{10} and $PM_{2.5}$ and hourly means for ozone, and we aggregated these primary data to the same set of parameters as we have for the air quality observations:

PM_{10} – annual average [$\mu g \cdot m^{-3}$], year 2015
– 90.4 percentile of the daily average value [$\mu g \cdot m^{-3}$], year 2015 (aggregated from daily means)

$PM_{2.5}$ – annual average [$\mu g \cdot m^{-3}$], year 2015

Ozone – 93.2 percentile of the highest maximum daily 8-hour average value [$\mu g \cdot m^{-3}$], year 2015 (aggregated from hourly means)
– SOMO35 [$\mu g \cdot m^{-3} \cdot day$], year 2015 (aggregated from hourly means)
– AOT40 for vegetation [$\mu g \cdot m^{-3} \cdot hour$], year 2015 (aggregated from hourly means)

– AOT40 for forests [$\mu g \cdot m^{-3} \cdot hour$], year 2015 (aggregated from hourly means)

NO_2 – annual average [$\mu g \cdot m^3$], year 2015

NO_x – annual average [$\mu g \cdot m^3$], year 2015

Due to the complete temporal data coverage available at the modelled data, the PM_{10} indicator 90.4 percentile of daily means is identical with the 36th highest daily mean and the ozone indicator 93.2 percentile of maximum daily 8-hour means is identical with the 26th highest maximum daily 8-hour mean.

In the original format of the model results, a point represents the centre of a grid cell (in 50x50 km resolution). The data are imported into *ArcGIS* as a point shapefile and converted into ETRS89-LAEA5210 projection, subsequently converted into a 100x100 m resolution raster grid and spatially aggregated into the reference EEA 10x10 km grid (for health related indicators), resp. into the 2x2 km grid (for vegetation related indicators).

A2.3 Other supplementary data

Altitude

We use the altitude data field (in meters) of *Global Multi-resolution Terrain Elevation Data 2010 (GMTED2010)*, with an original grid resolution of 15x15 arcseconds (some 463x463 m at 60N). Source: U.S. Geological Survey Earth Resources Observation and Science, see Danielson et al. (2011). We converted the field into the ETRS 1989 LAEA projection. (The resolution after projection was in 449.2x449.2 m). In the following step, we resampled the raster dataset to 100x100 m resolution and shifted it to the extent of EEA reference grid. As a final step, the dataset was spatially aggregated into 1x1 km, 2x2 km and 10x10 km resolutions.

Meteorological parameters

Actual meteorological surface layer parameters were extracted from the *Meteorological Archival and Retrieval System (MARS)* of the *ECMWF (European Centre for Medium-range Weather Forecasts)*. Currently we use the following ECMWF variables (details specified in Horálek et al. 2007, Section 4.5) on a 0.25x0.25 degrees (about 28x28 km at 60N) resolution as supplementary data in the regressions:

Wind speed	– annual average [$m.s^{-1}$], year 2015 (aggregated from 6-hour means)
Surface solar radiation	– annual average of daily sum [$MWs.m^{-2}$], year 2015 (aggregated from daily sums)

The 6-hour mean wind speed used in the aggregation is derived from the 10 meter height wind speed in U (*10U*) and V (*10V*) directions (where U and V are perpendicular vectors in horizontal directions) with magnitude $\sqrt{(10U)^2 + (10V)^2}$.

The data are imported into *ArcGIS* as a point shapefile. Each point represents the centre of a grid cell. The shapefile is converted into ETRS89-LAEA5210 projection, converted into a 100x100 m resolution raster grid and spatially aggregated into the reference EEA 1x1 km grid, 10x10 km grid, resp. into the 2x2 km grid.

Population density and population totals

Population density (in $inhbs.km^{-2}$, census 2011) is based on *Geostat 2011* grid dataset, Eurostat (2014). The dataset is in 1x1 km resolution, in the EEA reference grid.

For regions not included in the Geostat 2011, alternative sources were used. Primarily, *JRC (Joint Research Centre)* population data in resolution 100x100 m were used (JRC, 2009). The JRC 100x100 m population density data is spatially aggregated into the reference 1x1 km EEA grid. For regions that are neither included in the Geostat 2011 nor in the JRC database, we used population density data from *ORNL LandScan Global Population Dataset* (ORNL, 2008). This dataset is in 30x30 arcsec resolution; its values are based on the annual mid-year national population estimates for 2008 from the Geographic Studies Branch, US Bureau of Census, http://www.census.gov. The ORNL data is re-projected and converted from its original WGS1984 30x30 arcsecs grids into EEA's reference projection ETRS89-LAEA5210 at 1x1 km resolution by EEA (eea_r_3035_1_m_landscan-eurmed_2008, EEA, 2008).

The areas lacking Geostat 2011 data, and supplemented with JRC or ORNL data were: Gibraltar (JRC); Faroe Islands, British crown dependencies (Jersey, Guernsey and Man) and northern Cyprus (ORNL). As such, the Geostat 2011 1x1 km data and these supplements cover the entire mapping area.

To verify the consistency of merging Geostat 2011 with JRC and ORNL data, we compared the Geostat 2011 data and the JRC supplemented with ORNL data on the basis of the national population totals of the individual countries (see Horálek et al., 2015 for details). Additionally, we verified the national population totals for the Geostat 2011 gridded data with the Eurostat national population data for 2014 (Eurostat, 2016). Figure A2.1 presents both comparisons. From these verifications, one can conclude a high correlation of the national population totals of each data source. Slight underestimation of the supplemented JRC and ORNL data in comparison with the Geostat 2011 data can be seen, which is caused by the fact that the Geostat 2011 data is more up-to-date than both the JRC and the ORNL data source. Geostat 2011 and Eurostat 2014 data correlate even better and leads to a similar conclusion. Based on this, we used in the further calculations on national population totals the actual Eurostat data for 2014 (Eurostat, 2016), as described further.

Population density data can be used to classify the spatial distribution of each type of area (rural, urban or mixed population density) in Europe. We use this information to select and weight the air quality values, grid cell by grid cell and merge them into a final combined map (Annex 1). Furthermore, we use it to estimate population health exposure and exceedance numbers per country and for Europe as a whole, including involved uncertainties. These activities take place on the 1x1 km resolution grid in accordance with the recommendations of Horálek et al. (2010). The supplemented Geostat data (as described above) are used in all the calculations.

Figure A2.1 Correlation of national population totals for Geostat 2011 with JRC supplemented with ORNL, and with Eurostat 2015

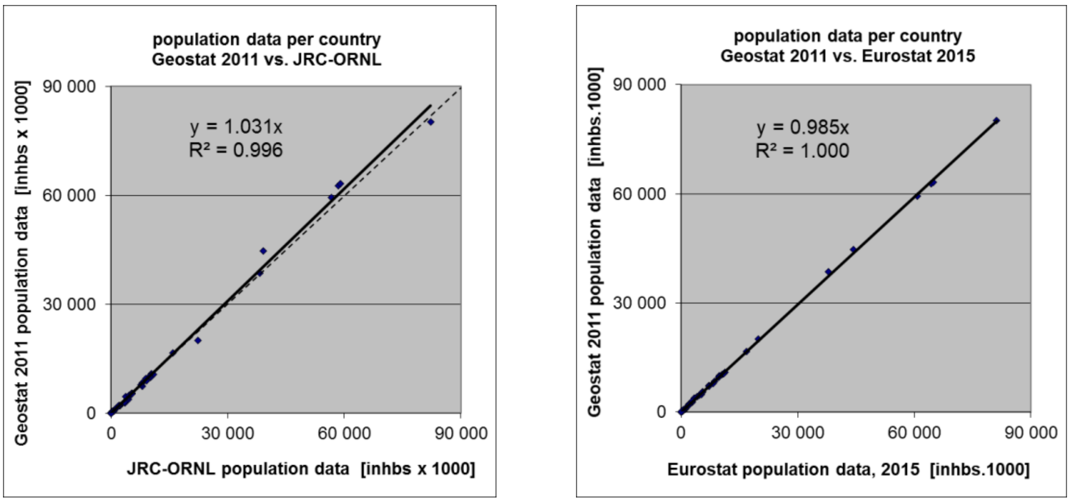

National population totals presented in the exposure tables of this paper are based on Eurostat national population data for 2015 (Eurostat, 2017). For France, Portugal and Spain, the population totals of areas outside the mapping area (i.e. Azores, Canarias, Madeira, French oversea departments) are subtracted. For Andorra, Monaco, and northern part of Cyprus which do not have 2015 data in the Eurostat database, the population total is based on alternative data[3].

Land cover

CORINE Land Cover 2006 – grid 100 x 100 m, Version 18.5 (09/2016) is used (EEA, 2016). The country missing in this database is Andorra, the area missing in this database is the Faroe Islands. Due to the lack of land cover data for Andorra, we excluded this country from the process of exposure estimates related to the vegetation based AOT40 ozone indicators.

In agreement with Horálek et al. (2017b), the 44 CLC classes have been re-grouped into the 8 more general classes. In this paper we use four of these general classes, see Table A2.2.

Table A0.2 General land cover classes, based on CLC2006 classes, used in mapping

Label	General class description	CLC classes grid codes	CLC classes codes	CLC classes description
HDR	High density residential areas	1	111	Continuous urban fabric
LDR	Low density residential areas	2	112	Discontinuous urban fabric
AGR	Agricultural areas	12 – 22	211 – 244	Agricultural areas
NAT	Natural areas	23 – 34	311 – 335	Forest and semi natural areas

Two aggregations are used, i.e. into 1x1 km grid and into the circle with radius of 5 km. For each general CLC class we spatially aggregated the high land use resolution into the 1x1 km EEA standard grid resolution. The aggregated grid square value represents for each general class the total area of this class as percentage of the total 1x1 km square area. For details, see Horálek (2017b).

Road type vector data

GRIP (Meijer et al., 2016) vector road type data base provided by PBL is used. The road types are distributed into 5 classes, from highways to local roads and streets. In agreement with Horálek et al. (2017b), the road classes No. 1 “Highways”, No. 2 “Primary roads” and No. 3 “Secondary roads” are used.

Percentage of the area influenced by traffic is represented by buffers around the roads: for the individual classes 1 – 3 and for classes 1 – 3 together, at all 1x1 grid cells; a buffer of 75 metres distance at each side from each road vector is taken for the roads of classes 1 and 2, while a buffer of 50 metres is taken for the roads of class 3. For motivation and calculation details, see Horálek et al. (2017b).

[3] Monaco: https://data.worldbank.org/country/Monaco; Andorra: http://www.estadistica.ad/serveiestudis/web/banc_dades4.asp?lang=4&codi_tema=2&codi_divisio=8&codi_subtemes=8; northern part of Cyprus: http://www.devplan.org/frame-eng.html

Annex 3 Technical details and mapping uncertainties

This annex contains technical details on the linear regression models and the residual kriging, including the performance. Furthermore, uncertainty estimates for the maps of the indicators are given.

A3.1 PM_{10}

Technical details on the interpolation model and uncertainty estimates for both PM_{10} indicators maps annual average (Map 2.1) and 90.4 percentile of daily means (Map 2.2) are presented in this section.

Technical details on the interpolation model

Table A3.1 presents the estimated parameters of the linear regression models (c, a_1, a_2, …) and of the residual kriging (nugget, sill, range) and includes the statistical indicators of both the regression and the kriging, for both PM_{10} indicators. The linear regression and ordinary kriging on its residuals is applied on the logarithmically transformed data of both measurement and modelled PM_{10} values. In Table A3.1 the standard error and variogram parameters (nugget, sill and range) refer to these transformed data, whereas RMSE and bias refer to the interpolation after a back-transformation.

For both the annual average and the 90.4 percentile of daily means (indicated further as 'P90.4'), surface solar radiation was found to be statistically non-significant and thus it was not used in the 2015 mapping.

The adjusted R^2 and standard error are indicators for the fit of the regression relationship, where the adjusted R^2 should be as close to 1 as possible and the standard error should be as small as possible. The adjusted R^2 for the rural areas was 0.58 at the annual average and 0.54 at the P90.4; for the urban areas 0.13 at the annual average and 0.11 at the P90.4.

RMSE (the smaller the better) and bias (the closer to zero the better), highlighted by orange, are the cross-validation indicators, showing the quality of the resulting map. The bias indicates to what extent the predictions are under- or overestimated on average. Further in this section, more detailed uncertainty analysis is presented. Annex 4 presents the comparison with results of the years 2005 – 2015.

Table A3.1 Parameters and statistics of linear regression model and ordinary kriging of PM_{10} indicators annual average and 90.4 percentile of daily means for 2015 in rural and urban areas for the final combined map

		Annual average		90.4 percentile of daily means	
		Rural areas	Urban areas	Rural areas	Urban areas
Linear regresion model (LRM, Eq. A1.3)	c (constant)	1.87	2.28	2.11	2.62
	a1 (log. EMEP model)	0.565	0.32	0.528	0.33
	a2 (altitude GTOPO)	-0.00041		-0.00038	
	a3 (wind speed)	-0.101		-0.086	
	a4 (s. solar radiation)	*non signif.*		*non signif.*	
	Adjusted R^2	**0.58**	**0.13**	**0.54**	**0.11**
	Standard Error [μg.m^{-3}]	**0.25**	**0.30**	**0.26**	**0.34**
Ordinary kriging (OK) of LRM residuals	nugget	0.035	0.023	0.028	0.023
	sill	0.063	0.037	0.068	0.097
	range [km]	1000	1000	1000	740
LRM + OK of its residuals	**RMSE [μg.m^{-3}]**	**3.2**	**4.5**	**6.2**	**10.8**
	Relative RMSE [%]	**19.4**	**19.2**	**21.1**	**25.6**
	Bias (MPE) [μg.m^{-3}]	**0.1**	**0.0**	**0.1**	**-0.1**

Uncertainty estimated by cross-validation

Using RMSE as the most common indicator, the *absolute mean uncertainty* of the final combined map at areas 'in between' the station measurements can be expressed in μg·m^{-3}. Table A3.1 shows that the absolute mean uncertainty of the final combined map of PM_{10} annual average resp. 90.4 percentile of daily means expressed by RMSE is 3.2 μg·m^{-3} resp. 6.2 μg·m^{-3} for the rural areas and 4.5 μg·m^{-3} resp. 10.8 μg·m^{-3} for the urban areas. Alternatively, one can express this uncertainty in relative terms by relating the absolute RMSE uncertainty to the mean air pollution indicator value for all stations. This *relative mean uncertainty* (Relative RMSE) of the final combined map of PM_{10} annual average resp. 90.4 percentile of daily means is 19.4 % resp. 21.1 % for rural areas and 19.2 % resp. 25.6 % for urban areas. These relative uncertainty values fulfil the data quality objectives for models as set in Annex I of the air quality Directive 2008/50/EC (EU, 2008). See Annex 4 (and specifically Table A4.1) for a further discussion on uncertainties over the previous eleven modelling years.

Figure A3.1 shows the cross-validation scatter plots, obtained according to Annex 1, for both rural and urban areas, for both PM_{10} indicators. The R^2 indicates that the variability is attributable to the interpolation for about 70-71 % at the rural areas and for about 69 % resp. 64 % at the urban areas.

Figure A3.1 Correlation between cross-validated predicted (y-axis) and measurement values for PM_{10} indicators annual average (top) and 90.4 percentile of daily means (bottom) for 2015 for rural (left) and urban (right) areas

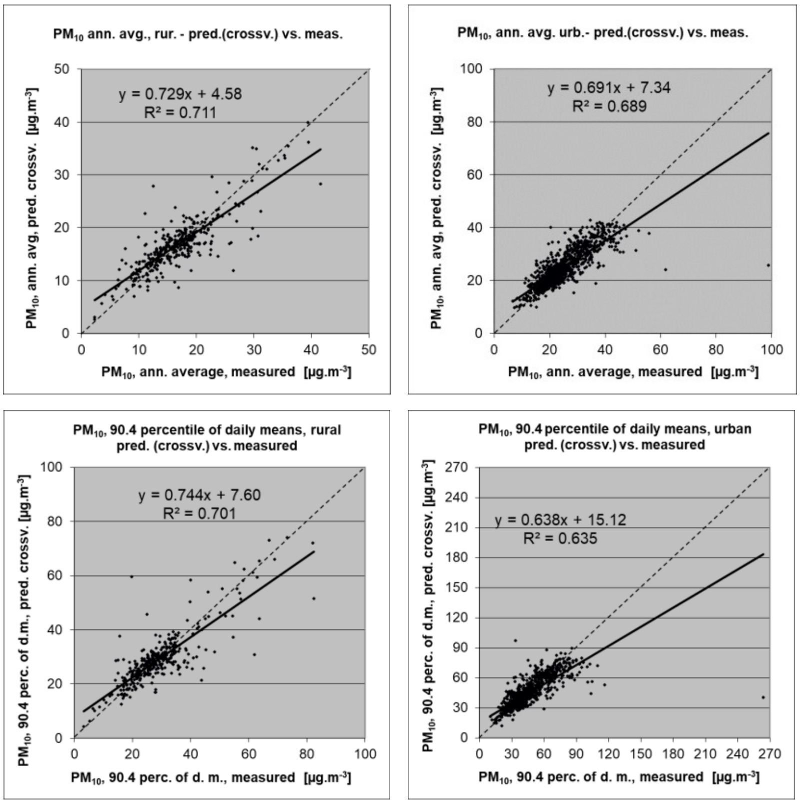

The trend line in the scatter-plots deviates at the lowest values somewhat above, and at the higher values under the symmetry axis, indicating that the interpolation methods tend to underestimate the high concentrations and overestimate the low concentrations. For example, in urban areas for annual average an observed value of 50 $\mu g \cdot m^{-3}$ is estimated in the interpolations to be about 42 $\mu g \cdot m^{-3}$, about 16 % lower. This underestimation at high values is common to all spatial interpolation methods. It could be reduced by either using a higher number of stations with an improved spatial distribution, or by introducing an improved regression that uses either other supplementary data or more advanced chemical transport model (resp. model in finer resolution).

Comparison of point measurement values with the predicted grid value

In addition to the above *point observation – point prediction* cross-validation, a simple comparison has been made between the point observation values and interpolated prediction values spatially averaged at grid cells. This *point observation – grid averaged prediction* comparison indicates to what extent the predicted value of a grid cell represents the corresponding measurement values at stations located in that cell. The comparison has been made primarily for the separate rural and urban background map at 10x10 km resolution. (One can directly relate this comparison result to the cross-validation results of Figure A3.1). Next to this, the comparison has been done also for the final combined maps at 1x1 km resolution. Figure A3.2 shows the scatterplots for these comparisons, for PM_{10} annual average only as an illustration.

Figure A3.2 Correlation between predicted grid values from rural 10x10 km (upper left), urban 10x10 km (bottom left) and final combined 1x1 km (upper and bottom right) map (y-axis) versus measurements from rural (top), resp. urban/suburban (bottom) background stations (x-axis) for PM_{10} annual average 2015

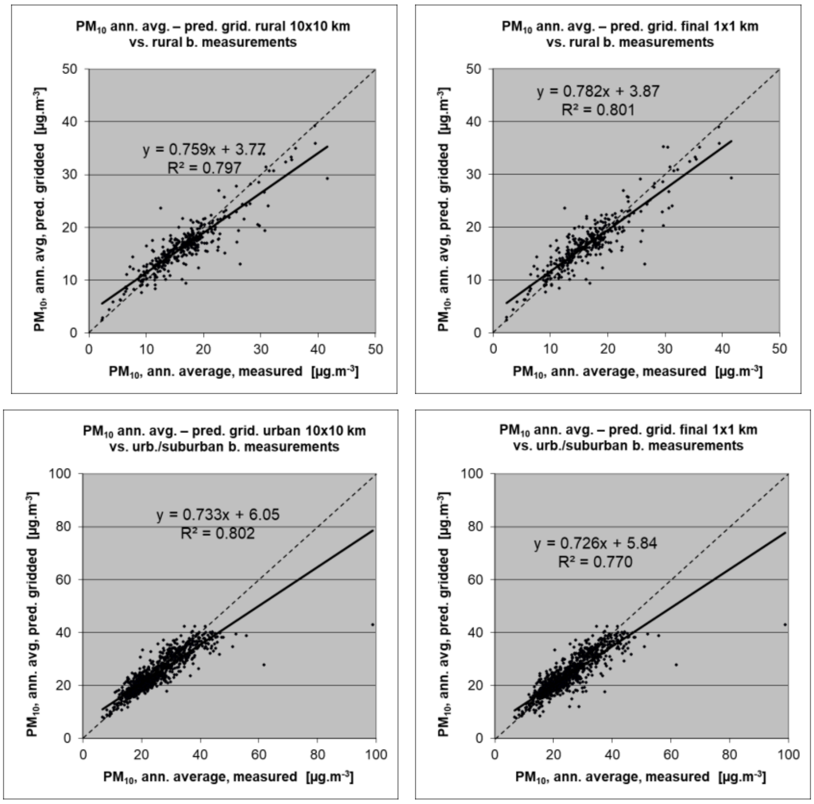

The results of the point observation – point prediction cross-validation of Figure A3.1 and those of the point observation – grid averaged prediction validation for separate rural and separate urban background maps, and for the final combined maps at both resolutions are summarised in Table A3.2 for both PM_{10} indicators.

By comparing the scatterplots and the statistical indicators for the separate rural and separate urban background map with the final combined maps in both resolutions, one can evaluate the level of representation of the rural resp. urban background areas in the final combined maps. Both the rural and the urban air quality are fairly well represented in the 1x1 km final combined map. This would not be the case in the urban areas for the aggregated final combined 10x10 km map (Horálek et al., 2016b). Therefore, we present the final combined maps just in the 1x1 km resolution, see Maps 2.1 and 2.2, contrary to the earlier reports up to Horálek et al. (2016b).

Table A3.2 Statistical indicators from the scatter plots for the predicted point values based on cross-validation and the predicted grid values from separate (rural resp. urban) 10x10 km and final combined 1x1 km map versus the measurement point values for rural (left) and urban (right) background stations for PM_{10} indicators annual average (top) and 90.4 percentile of daily means (bottom) for 2015

PM_{10}	rural backgr. stations				urban/suburban backgr. stations			
	RMSE	bias	R^2	lin. r. equation	RMSE	bias	R^2	lin r. equation
Annual average								
cross-valid. prediction, separate (r or ub) map	3.2	0.1	0.711	y = 0.729x + 4.58	4.5	0.0	0.689	y = 0.691x + 7.34
grid prediction, 10x10 km separate (r or ub) map	2.7	-0.2	0.797	y = 0.759x + 3.77	3.7	-0.3	0.802	y = 0.733x + 6.05
grid prediction, 1x1 km final combined map	2.7	0.3	0.801	y = 0.782x + 3.87	4.0	-0.6	0.770	y = 0.726x + 5.84
90.4 percentile of daily means								
cross-valid. prediction, separate (r or ub) map	6.2	0.1	0.701	y = 0.744x + 7.60	10.8	-0.1	0.635	y = 0.638x + 15.1
grid prediction, 10x10 km separate (r or ub) map	4.8	-0.3	0.821	y = 0.787x + 5.89	7.8	-0.6	0.819	y = 0.727x + 10.9
grid prediction, 1x1 km final combined map	4.7	0.4	0.828	y = 0.810x + 5.98	8.4	-1.3	0.792	y = 0.713x + 10.8

The Table A3.2 shows a better relation (i.e. lower RMSE, higher R^2, smaller intercept and slope closer to 1) between station measurements and the interpolated values of the corresponding grid cells at both rural and urban background map areas than it does at the point cross-validation predictions. That is because the simple comparison between point measurements and the gridded interpolated values shows the uncertainty at the actual station locations (points), while the point cross-validation prediction simulates the behaviour of the interpolation at point positions assuming no actual measurement would exist at that point. The uncertainty at measurement locations is introduced partly by the smoothing effect of the interpolation and partly by the spatial averaging of the values in the 10x10 km grid cells. The level of the smoothing effect leading to underestimation at areas with high values is there smaller than in situations where no measurement is represented in such areas. For example, in urban areas the predicted interpolation gridded annual average value in the separate urban background map will be about 43 $\mu g \cdot m^{-3}$ at the corresponding station point with the measurement value of 50 $\mu g \cdot m^{-3}$. This means an underestimation of about 15 %. It is a slightly less than the prediction underestimation of 16 % at the same point location, when leaving out this one actual measurement point and the interpolation is done without this station (see the previous subsection).

Probability of Limit Value exceedance

We constructed the map of probability of limit value exceedance. For this purpose, we used the final combined concentration map in the 1x1 km grid resolution. Based on this map, we derived, with support of the 1x1 km uncertainty map (Annex 1) and the limit value (40 $\mu g \cdot m^{-3}$), the probability of exceedance (PoE) map at that same resolution. It is important to emphasize that the exceedance of the spatial average of a 10x10 km grid cell (as presented in the previous reports, e.g. Horálek et al., 2016b) would show low probability even though some smaller (e.g. urban) areas inside such a grid cell would show high probability of exceedance (becoming visible in case one would present the map on a higher grid cell resolution).

It is needed to keep in mind that the interpolated maps refer to the rural or urban/suburban *background* situations only, i.e. it cannot be excluded that exceedances of limit values may occur at *hotspot* and traffic locations throughout Europe, which are not resolved by this type of map.

The map shows areas with a probability of limit value exceedance (PoE) above 66 % marked in red (large or high PoE) and areas below 33 % in green (low or little PoE). Red in two shades indicate areas for which exceedance is *likely* or *very likely* (above 90 %) to occur due to either high concentrations close to or already above the LV accompanied with such uncertainty that exceedance is very likely, or areas with lower concentrations accompanied with high uncertainty levels so that exceedance is very likely. Vice versa, in the green areas of two shades (below 33 %) it is *unlikely* to exceed the LV because we have predicted concentrations and accompanying uncertainties at levels that do not sum above the LV. The areas with 33–50 % and 50–66 % probability of LV exceedance are marked in yellow and orange respectively. Table A1.1 summarises the classes and terminology for probability (i.e. likelihood) that are used in this paper.

Maps A3.1 and A3.2 present the probability of the LV exceedance for PM_{10} indicators annual average and 90.4 percentile of daily means. In case of the annual average (Map A3.1), only limited areas do show increased probability of LV exceedance, namely the surrounding of Almeria in southern Spain, around Sophia in Bulgaria, around Milan in the Po Valley, around Katowice in southern Poland, and urbanised areas in the Balkans.

Map A3.1 Map with the probability of the limit value exceedance, PM_{10} annual average, 2015

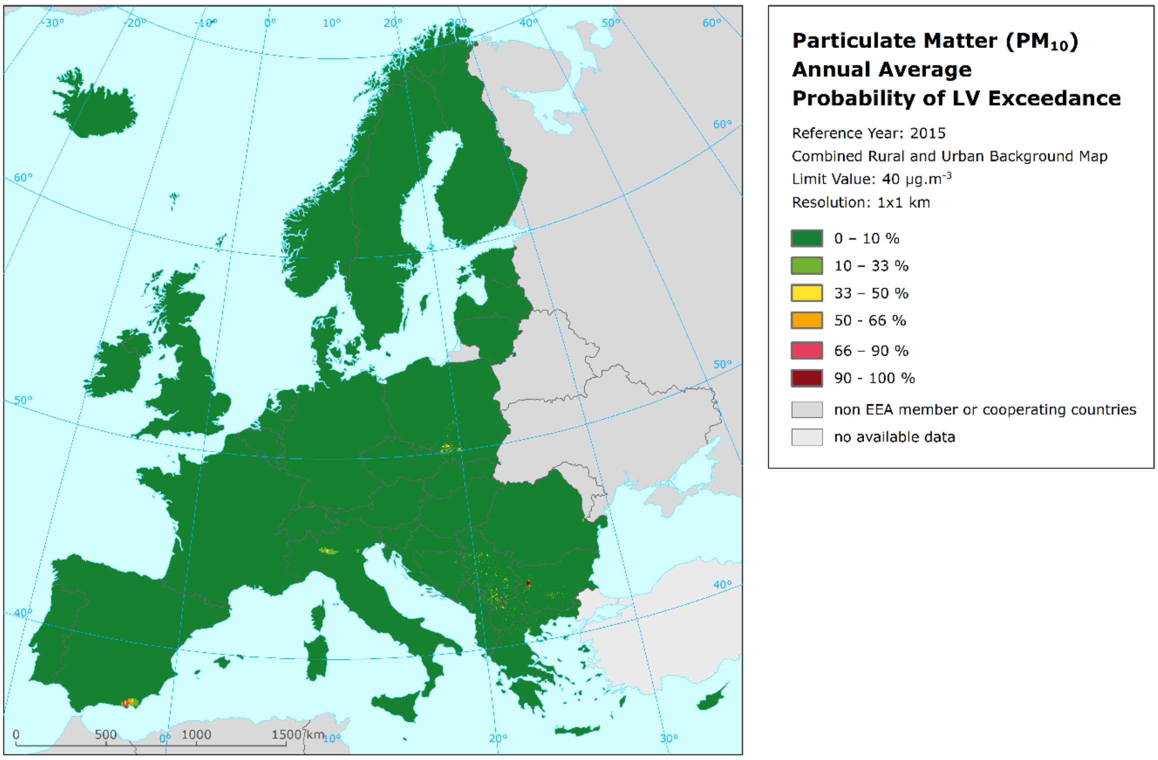

Note: Interpolation uncertainty is considered only, no other sources of uncertainty.

In case of the 90.4 percentile of daily means (Map A3.2), one observes considerably larger areas with relative quite high levels of PoE, namely the complete Po Valley in northern Italy, southern Poland and north-eastern Czech Republic (with industrial Ostrava–Katowice region), central part of Poland, eastern bordering areas of Slovakia and Hungary, northern Serbia and urbanised areas in the whole Balkan region, southern and eastern Romania, the Albanian coastal zone and also the region around Almería in southern Spain.

Map A3.2 Map with the probability of the limit value exceedance, PM_{10} indicator 90.4 percentile of daily means, 2015

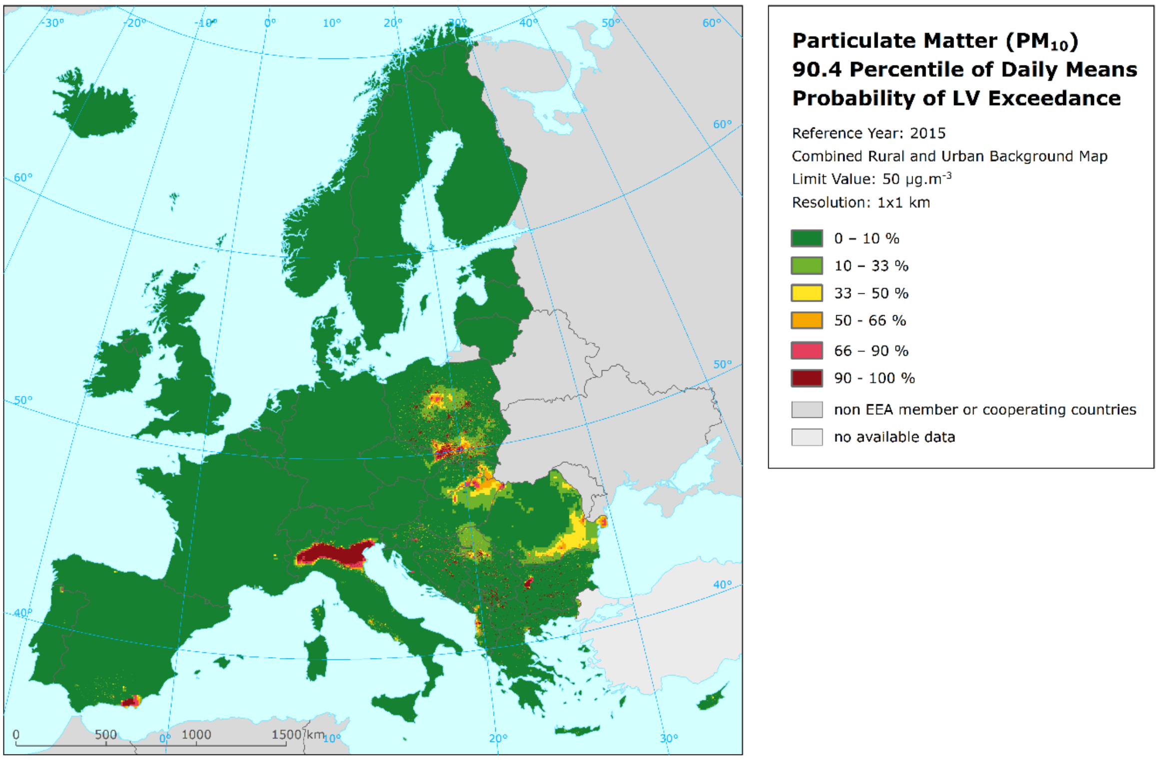

Note: Interpolation uncertainty is considered only, no other sources of uncertainty.

A3.2 $PM_{2.5}$

Technical details and uncertainty estimates for Map 3.1 with the $PM_{2.5}$ annual average are presented in this section.

Technical details on the interpolation model

Table A3.3 presents the regression coefficients determined for pseudo $PM_{2.5}$ stations data estimation, based on the 563 stations that have both $PM_{2.5}$ and PM_{10} measurements available (see Section 2.1.1).

Table A3.3 Parameters and statistics of linear regression model for generation of pseudo $PM_{2.5}$ data, regardless of rural or urban/suburban area, for $PM_{2.5}$ annual average 2015

		Both rural and urban areas
Linear regresion model (LRM, Eq. A1.1)	c (constant)	18.4
	b (PM_{10} measurement data)	0.744
	a1 (surface solar radiation)	-0.833
	a2 (latitude)	-0.236
	a3 (longitude)	0.067
	Adjusted R^2	**0.91**
	Standard Error [µg.m^{-3}]	**1.9**

The same supplementary data as in Denby (2011b) are used. However, the inclusion of the population density in the regression model was found not be significant (like in 2010 – 2014), thus it will not be further used.

Table A3.4 presents the estimated parameters of the linear regression models (*c*, a_1, a_2,…) and of the residual kriging (*nugget, sill, range*) and includes the statistical indicators of both the regression and the kriging of its residuals. Like in the case of PM_{10}, the linear regression is applied on the logarithmically transformed data of both measurement and modelled $PM_{2.5}$ values. Thus, the standard error and variogram parameters refer to these transformed data, whereas RMSE and bias refer to the interpolation after the back-transformation.

Surface solar radiation was not found to be statistically significant, like in 2010 – 2014, and is therefore not further used.

Table A3.4 Parameters and statistics of linear regression model and ordinary kriging of $PM_{2.5}$ annual average 2015 in rural and urban areas for final combined map

$PM_{2.5}$		Annual average	
		Rural areas	**Urban areas**
Linear regression model (LRM, Eq. A1.3)	c (constant)	1.24	1.65
	a1 (log. EMEP model)	0.654	0.46
	a2 (altitude GTOPO)	-0.00027	
	a3 (wind speed)	-0.065	
	a4 (s. solar radiation)	*non signif.*	
	a5 (log. population)	*non signif.*	
	Adjusted R^2	**0.61**	**0.24**
	Standard Error [μg.m^{-3}]	**0.27**	**0.34**
Ordinary kriging (OK) of LRM residuals	nugget	0.047	0.018
	sill	0.076	0.099
	range [km]	1000	1000
LRM + OK of its residuals	**RMSE [μg.m^{-3}]**	**2.5**	**2.6**
	Relative RMSE [%]	**21.9**	**16.6**
	Bias (MPE) [μg.m^{-3}]	**0.0**	**0.1**

The adjusted R^2 (the closer to 1 the better) and standard error (the smaller the better) are indicators for the *quality of the fit of the regression relation*. The adjusted R^2 is 0.61 for the rural areas and 0.24 for urban areas.

RMSE and bias – highlighted in orange – are the cross-validation indicators, showing the *quality of the resulting map*; the bias indicates to what extent the predictions are under- or overestimated on average. Only stations with $PM_{2.5}$ measurement data are used for calculating the RMSE and the bias (i.e. only non-pseudo $PM_{2.5}$ stations are used). These statistical inidcators are calculated excluding the pseudo stations because they are estimated values only, not actual measurement values. According Denby et al (2001b), the pseudo $PM_{2.5}$ data does not satisfy the quality objectives for fixed monitoring alone. The pseudo stations are used as they improve the mapping estimate. Whereas the actual measurements can be used for evaluating the *quality of the map*. For the future, we consider to quit the application of the $PM_{2.5}$ pseudo stations as the current number of the actual $PM_{2.5}$ measurement stations has increased over time such that the use of pseudo $PM_{2.5}$ stations may not contribute enough any longer to improve the mapping estimates.

Uncertainty estimated by cross-validation

Table A3.4 shows that the absolute mean uncertainty of the final combined map of $PM_{2.5}$ annual average expressed as RMSE is 2.5 $\mu g \cdot m^{-3}$ for the rural areas and 2.6 $\mu g \cdot m^{-3}$ for the urban areas. On the other hand, the *relative mean uncertainty* (Relative RMSE) of the final combined map of $PM_{2.5}$ annual average is 21.9 % for rural areas and 16.6 % for urban areas. These relative uncertainty values fulfil the data quality objectives for models as set in Annex I of the air quality Directive 2008/50/EC (EU, 2008). Annex 4 (and specifically Table A4.5) summarises both the absolute and relative uncertainties of different years.

Figure A3.3 shows the cross-validation scatter plots, obtained according to Section A1.3, for both the rural and urban areas. The R^2 indicates that about 78 % of the variability is attributable to the interpolation for the rural areas and 82 % for the urban areas.

Figure A3.3 Correlation between cross-validated predicted and measurement values for $PM_{2.5}$ annual average 2015 for rural (left) and urban (right) areas

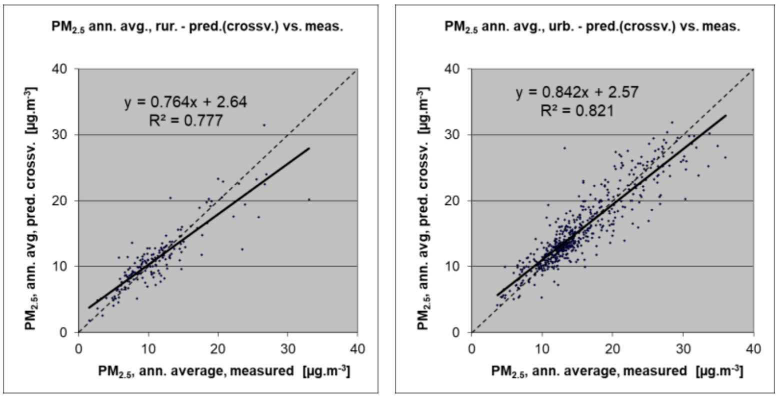

The scatter plots indicate that in areas with high concentrations the interpolation methods tend to underestimate the levels. For example, in rural areas an observed value of 25 $\mu g \cdot m^{-3}$ is estimated in the interpolations to be almost 22 $\mu g \cdot m^{-3}$, which is an underestimated prediction of about 13 %. This underestimation at high values is an inherent feature of all spatial interpolations. It could be reduced by either using a higher number of the stations at improved spatial distribution, or by introducing a closer regression that uses other supplementary data.

Comparison of point measurement values with the predicted grid value

Next to the cross-validation comparison, a simple comparison has been made between the point observation values and interpolated prediction values spatially averaged in grid cells. This point-grid comparison indicates to what extent the predicted value of a grid cell represents the corresponding measurement values at stations located in that cell. The comparison has been made primarily for the separate rural and urban map at 10x10 km resolution. Next to this, the comparison has been done also for the final combined maps at 1x1 km resolution. Figure A3.4 shows the scatterplots for these comparisons.

The results of the point observation – point prediction cross-validation of Figure A3.3 and those of the point observation – grid averaged prediction validation of Figure A3.4 for separate rural and separate urban background maps, and for the final combined maps at both resolutions are summarised in Table A3.5.

By comparing the scatterplots and the statistical indicators for the separate rural and separate urban background map with the final combined maps, one can evaluate the level of representation of the rural resp. urban background areas in the final combined maps. Similar results as for PM_{10} can be observed: both the rural and urban air quality are fairly well represented in the 1x1 km final combined map.

Figure A3.4 Correlation between predicted grid values from rural 10x10 km (upper left), urban 10x10 km (bottom left) and final combined 1x1 km (both right) map (y-axis) versus measurements from rural (top), resp. urban/suburban (bottom) background stations (x-axis) for $PM_{2.5}$ annual average 2015

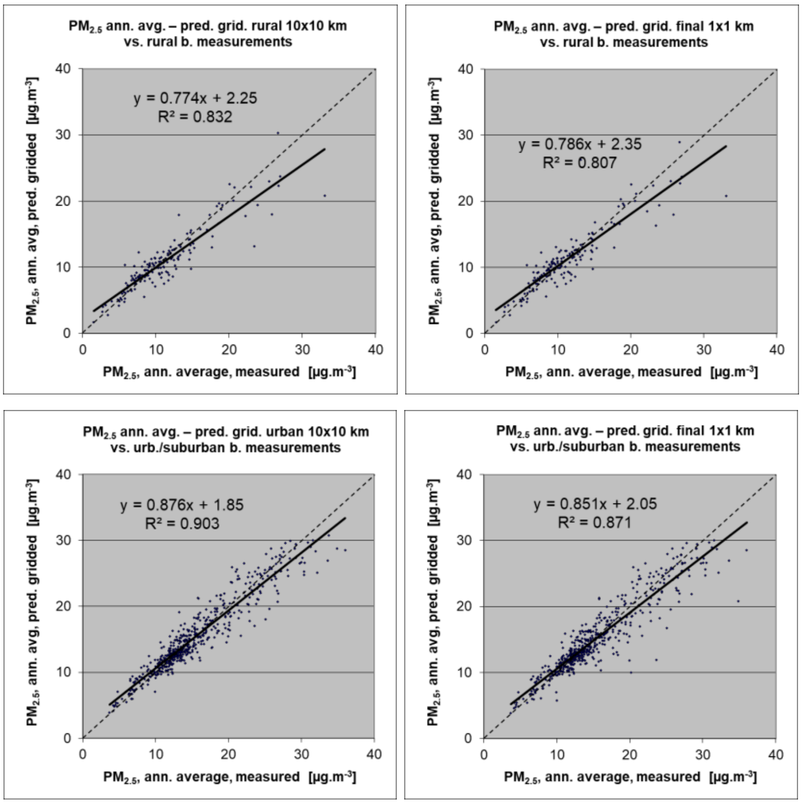

Like in the case of PM_{10}, Table A3.5 shows a better correlated relation with the station measurements (i.e. lower RMSE, higher R^2, smaller intercept and slope closer to 1) for the simply interpolated gridded values than for the point cross-validation predictions, at both rural and urban background map areas. That is because the simple comparison shows the uncertainty at the actual station locations, while the cross-validation prediction simulates the behaviour of the interpolation (within the area covered by measurements) at point positions assuming no actual measurements would exist at these points.

Table A3.5 Statistical indicators from the scatter plots for the predicted point values based on cross-validation and the predicted grid values from separate (rural resp. urban) 10x10 km and final combined 1x1 km versus the measurement point values for rural (left) and urban (right) background stations for $PM_{2.5}$ annual average 2015

$PM_{2.5}$	rural backgr. stations				urban/suburban backgr. stations			
	RMSE	bias	R^2	lin. r. equation	RMSE	bias	R^2	lin r. equation
cross-valid. prediction, separate (r or ub) map	2.5	0.0	0.777	y = 0.764x + 2.64	2.6	0.1	0.821	y = 0.842x + 2.57
grid prediction, 10x10 km separate (r or ub) map	2.2	-0.3	0.832	y = 0.774x + 2.25	1.9	-0.1	0.903	y = 0.876x + 1.85
grid prediction, 1x1 km final combined map	2.3	-0.1	0.807	y = 0.786x + 2.35	2.2	-0.2	0.871	y = 0.851x + 2.05

The uncertainty at measurement locations is caused partly by the smoothing effect of the interpolation and partly by the spatial averaging of the values in the 10x10 km grid cells. For example, in urban areas the predicted interpolation gridded value in the separate urban background map will be about 28 $\mu g \cdot m^{-3}$ at the corresponding station point with the measurement value of 30 $\mu g \cdot m^{-3}$ (calculated based on the linear regression equation), which coincides with an underestimation of about 6 %.

Probability of Limit Value exceedance

The probability of target value exceedance map was created for the $PM_{2.5}$ indicator in a similar way as the PoE maps for the PM_{10} indicators and presented at 1x1 km resolution with the Limit Value (LV) of 25 $\mu g \cdot m^{-3}$.

Map A3.3 Map with the probability of the limit value exceedance, $PM_{2.5}$ annual average, 2015

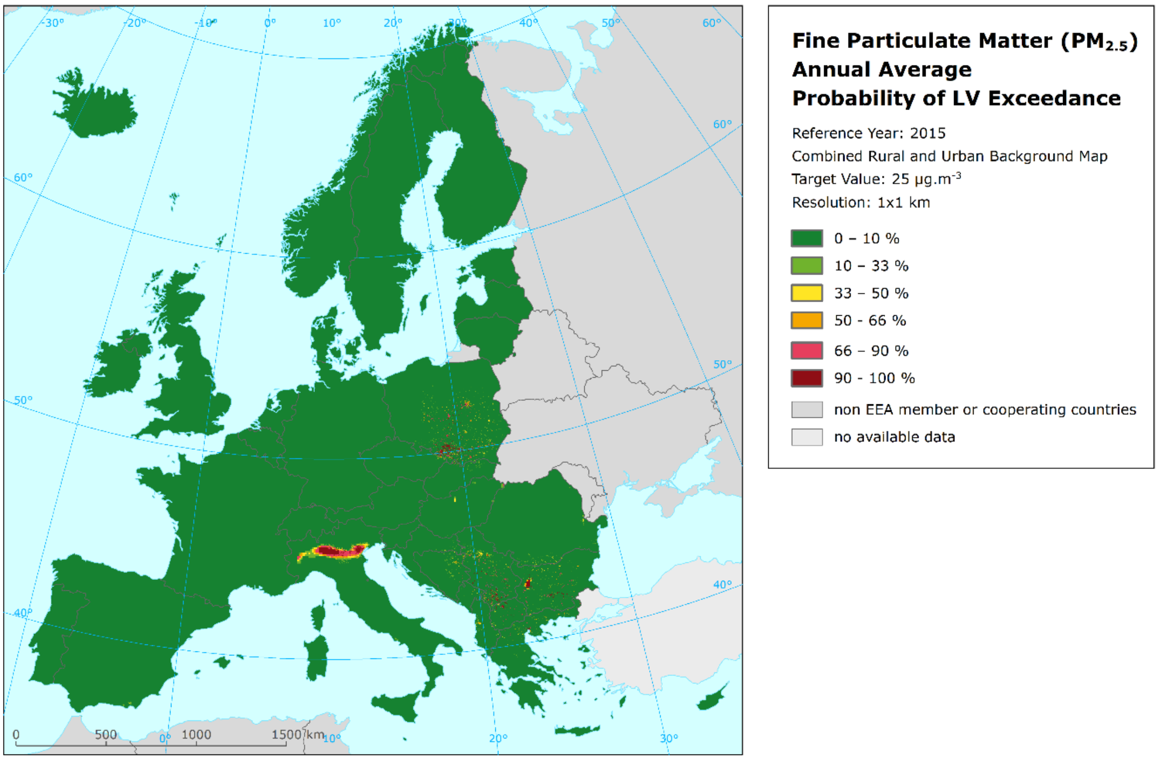

Note: Interpolation uncertainty is considered only, no other sources of uncertainty.

The areas with the highest probability of LV exceedance include most prominently the Po Valley in Italy, the area around Bulgaria's capital Sophia and locations around the Balkan cities, the region of southern Poland – north-eastern Czech Republic with the industrial zones of Krakow, Katowice and Ostrava, and the cities in the central part of Poland.

In the other parts of Europe, there is little to no likelihood of LV exceedance, at the level of 1x1 km grids.

One should bear in mind that the map is based on rural and urban/suburban *background* station data only. As such the map reflects rural and urban background situations only. Therefore, this type of map will not resolve the exceedances of limit values that may occur at the many *hotspot* and traffic locations throughout Europe.

A3.3 Ozone

In this section, we present the technical details and the uncertainty estimates for the maps of ozone health-related indicators 93.2 percentile of maximum daily 8-hour means and SOMO35 (Maps 4.1 and 4.2), as well as for the maps of ozone vegetation-related indicators AOT40 for vegetation and AOT40 for forests (Maps 4.3 and 4.4).

Technical details on the interpolation model

Table A3.6 presents the estimated parameters of the linear regression models and of the residual kriging, including the statistical indicators of both the regression and the kriging.

The adjusted R^2 and standard error show the quality of the fit of the regression relation. The SOMO35 shows a somewhat weaker adjusted R^2 (0.63 resp. 0.58) compared to the other indicators, both for rural and for urban areas. For the rural areas, the other three indicators show the same value of 0.69. For the urban areas, the adjusted R^2 for 93.2 percentile of daily 8-hour maximums is 0.65. For the vegetation-related indicators the urban maps are not constructed.

Table A3.6 Parameters and statistics of linear regression model and ordinary kriging for ozone indicators 93.2 percentile of maximum daily 8-hourly means and SOMO35 in rural and urban areas for the final combined map and for O_3 indicators AOT40 for vegetation and for forests in rural areas for 2015

		93.2 perc. of dmax 8h		SOMO35		AOT40v	AOT40f
		Rur. areas	Urb. areas	Rur. areas	Urb.areas	Rur. areas	Rur. areas
Linear regresion model (LRM, Eq. A1.3)	c (constant)	-44.5	29.4	-1964	534	-12317	-17772
	a1 (EMEP model)	1.38	0.89	0.62	0.45	0.89	0.75
	a2 (altitude GTOPO)	0.0066		1.61		3.74	8.50
	a3 (wind speed)		-4.75		-419.33		
	a4 (s. solar radiation)	1.03	0.62	322.7	290.6	1635.7	2287.7
	Adjusted R^2	**0.69**	**0.65**	**0.63**	**0.58**	**0.69**	**0.69**
	Stand. Err. [μg.m^{-3}.x]*	**11.2**	**12.0**	**1673**	**1481**	**6202**	**10111**
Ord. krig. (OK) of LRM	nugget	43	41	2.1E+06	8.7E+05	1.8E+07	6.0E+07
	sill	102	100	2.7E+06	6.4E+05	3.5E+07	9.4E+07
	range [km]	440	180	400	100	210	210
LRM + OK of its residuals	**RMSE [μg.m^{-3}.x]***	**9.0**	**8.6**	**1578**	**1221**	**5256**	**9141**
	Relative RMSE [%]	**7.5**	**7.4**	**27.1**	**25.6**	**28.7**	**29.1**
	Bias (MPE) [μg.m^{-3}.x]*	**0.1**	**0.2**	**21**	**43**	**120**	**165**

*) Units – 93.2 percentile of daily 8-h maximums: [μg·m^{-3}], SOMO35: [μg·m^{-3}·d], AOT40v and AOT40f: [μg·m^{-3}·h].

RMSE and bias – highlighted by orange – are the cross-validation indicators, showing the quality of the resulting map.

Uncertainty estimated by cross-validation

The basic uncertainty analysis is provided by cross-validation. Table A3.6 shows both absolute and relative mean uncertainty, expressed by RMSE and Relative RMSE. The relative mean uncertainty of the 2015 ozone map is at the 93.2 percentile of daily 8-h maximums about 7.5 % for both rural and urban areas, around 26 % for both rural and urban areas at the SOMO35, about 29 % at AOT40 for both vegetation and forests. The small level of the relative uncertainty for the 93.2 percentile of maximum daily 8-h means is induced by the concentration level of this indicator. Annex 4 (and specifically Table A4.9) summarises both the absolute and relative uncertainties of different years.

Figure A3.5 shows the cross-validation scatter plots for both the rural and urban areas of the 2015 map for the two health-related ozone indicators.

Figure A3.5 Correlation between cross-validated predicted (y-axis) and measurement values for ozone indicators 93.2 percentile of max. daily 8-hourly means (top) and SOMO35 (bottom) for 2015 for rural (left) and urban (right) areas

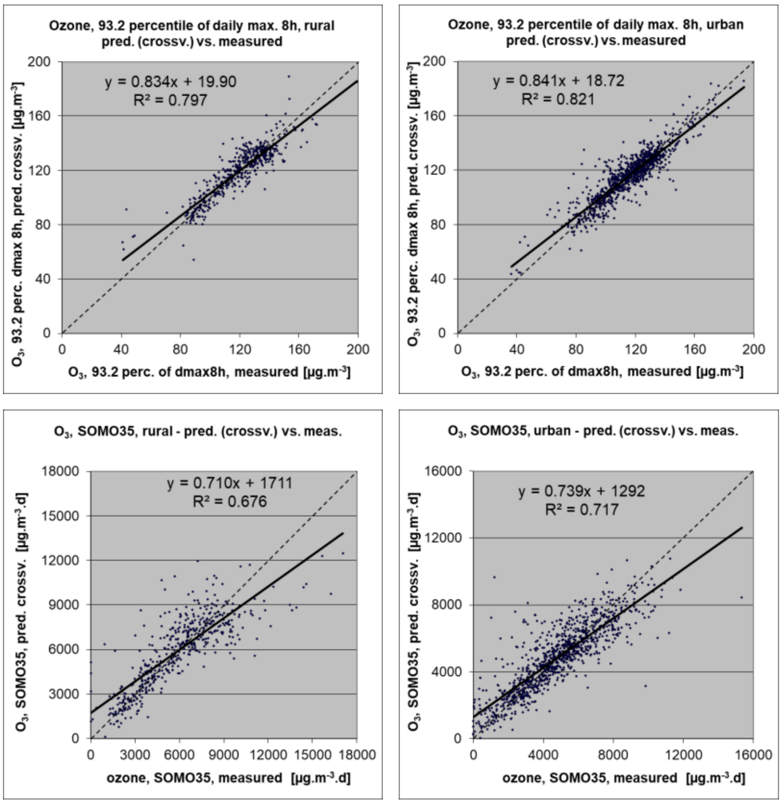

The R^2, an indicator for the interpolation correlation with the observations, shows at the 93.2 percentile of daily 8-h maximums that about 80 – 82 % is attributable to the interpolation, while at SOMO35 it is in the range of 68 – 72 %.

The scatter plots indicate that the higher values are underestimated and the lower values somewhat overestimated by the interpolation method; a typical smoothing effect inherent to the interpolation method with the linear regression and its residuals kriging. For example, in the case of the 93.2 percentile of daily 8-h maximums, in rural areas (Figure A.3.5, upper left panel) an observed value of 160 $\mu g \cdot m^{-3}$ is estimated in the interpolation as 153 $\mu g \cdot m^{-3}$, which is 4 % lower. Or, in the case of SOMO35, in urban areas (Figure A.3.5, bottom right panel) an observed value of 10 000 $\mu g \cdot m^{-3} \cdot d$ is estimated in the interpolation as about 8 700 $\mu g \cdot m^{-3} \cdot d$, which is 13 % lower.

Figure A3.6 shows the cross-validation scatter plots of the AOT40 for both vegetation and forests. R^2 indicates that about 78 % (in the case of AOT40 for vegetation) resp. 75 % (in the case of AOT40 for forests) of the variability is attributable to the interpolation.

The cross-validation scatter plots show again that in areas with higher accumulated ozone concentrations the interpolation methods tend to deliver underestimated predicted values. For example, in agricultural areas (Figure A3.6, left panel) an observed value of 45 000 $\mu g \cdot m^{-3} \cdot h$ is estimated in the interpolation as about 40 000 $\mu g \cdot m^{-3} \cdot h$, i.e. an underestimation of about 11 %. In addition, an overestimation at the lower end of predicted values occurred. One could reduce this under- and overestimation by extending the number of measurement stations and by optimising the spatial distribution of those stations, specifically in areas with elevated values over years.

Figure A3.6 Correlation between cross-validated predicted (y-axis) and measurement values for ozone indicators AOT40 for vegetation (left) and AOT40 for forests (right) for 2015 for rural areas

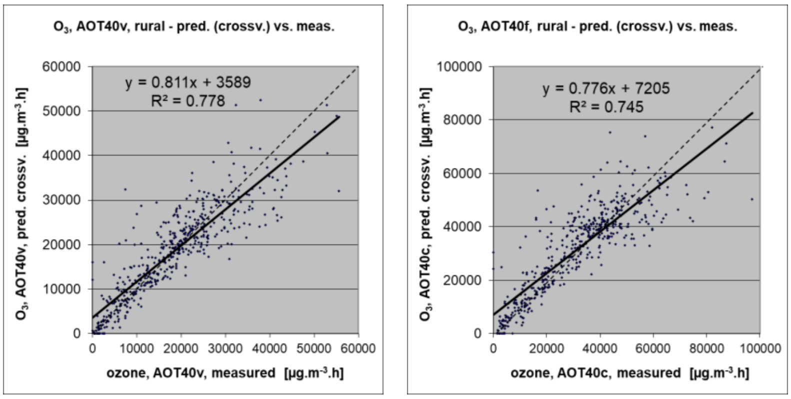

Comparison of point measurement values with the predicted grid value

In addition to the above point observation – point prediction cross-validation, a simple comparison was made between the point observation values and interpolated predicted grid values.

For health related indicators, the comparison has been made primarily for the separate rural and separate urban background maps at 10x10 km resolution. (One can directly relate this comparison result to the cross-validation of the previous section.) Next to this, the comparison has been done also for the final combined maps at 1x1 km resolution.

Figure A3.7 shows the scatterplots for these comparisons, for ozone indicator 93.2 percentile of maximum daily 8-hour means only, as an illustration.

The results of the point observation – point prediction cross-validation of Figure A3.6 and those of the point observation – grid averaged prediction validation for the separate rural and the separate urban background map, and for the final combined maps at both resolutions are summarised in Table A3.7.

By comparing the scatterplots and the statistical indicators for the separate rural and separate urban background map with the final combined maps, one can evaluate the level of representation of the rural resp. urban background areas in the final combined maps. Both the rural and the urban air quality are fairly well represented in the 1x1 km final combined map.

The uncertainty of the rural and urban background maps at measurement locations is caused partly by the smoothing effect of interpolation and partly by the spatial averaging of the values in the 10x10 km grid cells. The level of smoothing, which leads to underestimation in areas with high values, is weaker in areas where measurements exist than in areas where a measurement point is not available. For example, in the case of the SOMO35, in urban areas an observed value of 10 000 $\mu g \cdot m^{-3} \cdot d$ is estimated in the interpolation as about 9 000 $\mu g \cdot m^{-3} \cdot d$, which is almost 10 % lower. It is less than the cross-validation underestimation of 13 % at the same point location, when leaving out this one actual measurement point and the interpolation without this station is done (see the previous subsection).

Figure A3.7 Correlation between predicted grid values from rural 10x10 km (upper left), urban 10x10 km (bottom left) and final combined 1x1 km (both right) map (y-axis) versus measurements from rural (top), resp. urban/suburban (bottom) background stations (x-axis) for ozone indicator 93.2 percentile of daily max. 8-hourly means for 2015

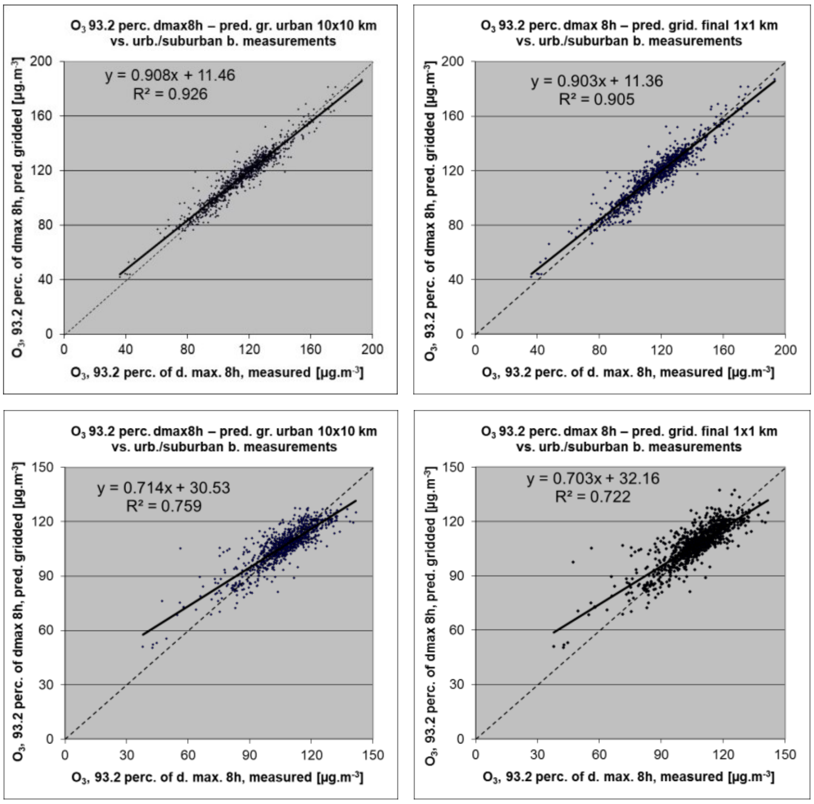

Table A3.7 Statistical indicators from the scatter plots for the predicted point values based on cross-validation and the predicted grid values from separate (rural resp. urban) 10x10 km and final combined 1x1 km map versus the measurement point values for rural (left) and urban (right) background stations for ozone indicators 93.2 percentile of daily max 8h means (top) and SOMO35 (bottom) for 2015

	rural backgr. stations				urban/suburban backgr. stations			
	RMSE	bias	R^2	lin. r. equation	RMSE	bias	R^2	lin r. equation
93.2 percentile of daily max. 8-hour means								
cross-valid. prediction, separate (r or ub) map	9.0	0.1	0.797	y = 0.834x + 19.9	8.6	0.2	0.821	y = 0.841x + 18.7
grid prediction, 10x10 km separate (r or ub) map	6.2	0.0	0.903	y = 0.892x + 12.9	5.5	0.0	0.926	y = 0.908x + 11.5
grid prediction, 1x1 km final merged map	6.4	0.2	0.897	y = 0.867x + 16.1	6.3	0.1	0.905	y = 0.903x + 11.4
SOMO35								
cross-valid. prediction, separate (r or ub) map	1578	21	0.676	y = 0.710x + 1711	1221	43	0.717	y = 0.739x + 1292
grid prediction, 10x10 km separate (r or ub) map	1348	13	0.762	y = 0.753x + 1452	830	17	0.872	y = 0.822x + 868
grid prediction, 1x1 km final merged map	1300	-58	0.781	y = 0.747x + 1415	992	38	0.813	y = 0.798x + 1002

Table A3.8 presents the results of the point observation – point prediction cross-validation of Figure A3.6 and those of the point-grid validation for the rural map, for vegetation related indicators AOT40 for vegetation and AOT40 for forests. Again, one can see for both indicators a better correlation between the station measurements and the averaged interpolated predicted values of the corresponding grid cells, than at the point cross-validation predictions, of Figure A3.6.

Table A3.8 Statistical indicators from the scatter plots for predicted point values based on cross-validation and predicted grid values from rural 2x2 km map versus measurement point values for rural background stations for O_3 indicators AOT40 for vegetation (top) and for forests (bottom) for 2015

	rural backgr. stations			
	RMSE	bias	R^2	linear regression equation
AOT40 for vegetation				
cross-valid. prediction, rural map	5256	120	0.778	y = 0.811x + 3589
grid prediction, 2x2 km rural map	3430	51	0.906	y = 0.880x + 2241
AOT40 for forests				
cross-valid. prediction, rural map	9141	165	0.745	y = 0.776x + 7205
grid prediction, 2x2 km rural map	6673	91	0.864	y = 0.839x + 5154

Probability of Target Value exceedance

Map A3.4 presents the gridded map of 1x1 km resolution showing the probability of target value exceedance for the 93.2 percentile of maximum daily 8-hour means. It was constructed on the basis of the 1x1 km gridded concentration map (Map 4.1), the 1x1 km gridded uncertainty map and the target value (TV) of 120 µg·m^{-3}. Table A1.1 explains the significance of the colour classes in the map.

Map A3.4 Map with the probability of the target value exceedance, ozone indicator 93.2 percentile of maximum daily 8-hour means, 2015

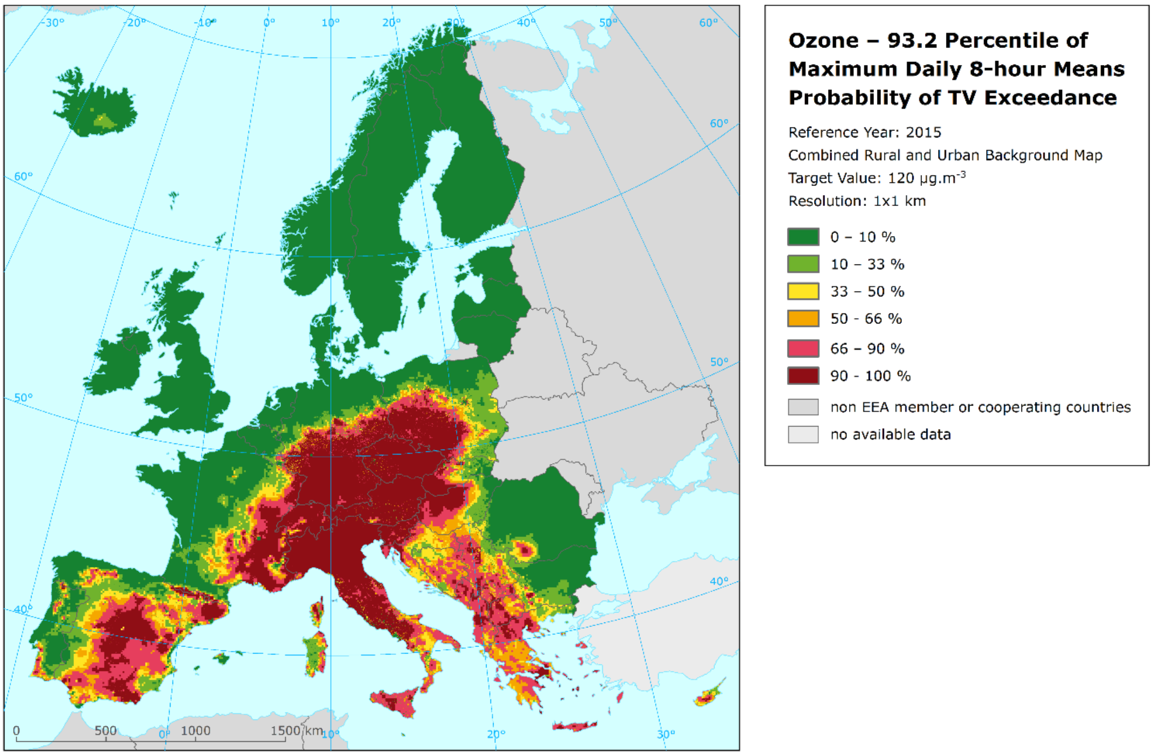

Note: Interpolation uncertainty is considered only, no other sources of uncertainty.

The PoE map for 2015 demonstrates the extended red and dark red areas (high or large PoE) in central Europe as a whole, Italy, the whole Balkan region and Greece, the central, south and eastern half part of Spain, the Pyrenees, Cyprus, western Bulgaria, and the Craiova region in Romania.

No Limit Value or Target Value is set for the WHO recommended ozone health indicator SOMO35, therefore no probability of exceedance map has been prepared.

A3.4 NO_2 and NO_x

In this section, the technical details and the uncertainty estimates for the maps of NO_2 annual average and NO_x annual average, for Maps 5.1 and 5.2, are presented.

Technical details on the interpolation model

In agreement with Horálek et al. (2007) and Annex 1, the NO_x measurements are supplemented by the so-called *pseudo* NO_x stations. The pseudo NO_x data are calculated based on the NO_2 data, using quadratic regression Eq. A1.2. The regression coefficients were estimated based on the rural background stations with both NO_x and NO_2 measurements (see Section 2.1.1). The number of such type of stations is 318. The estimated coefficients of Eq. A1.2 are: a = 0.024, b = 1.0332, c = 0.3706. Adjusted R^2 is 0.93, the standard error is 2.0 $\mu g \cdot m^{-3}$.

Table A3.9 presents the estimated parameters of the linear regression models and of the residual kriging and includes the statistical indicators of both the regression and the kriging.

Only stations with actual measurement data of the relevant pollutant (i.e. not the pseudo stations) are used for calculating of the cross-validation parameters RMSE and bias.

Table A3.9 Parameters and statistics of linear regression model and ordinary kriging of NO_2 annual average for 2015 in rural and urban areas for the final combined map (left) and NO_x annual average for 2015 in rural areas (right)

		NO_2 Annual average			NO_x Annual average
		Rural areas	Urb. b. areas	Urb. tr. areas	Rural areas
Linear regresion model (LRM, Eq. A1.3)	c (constant)	12.8	23.6	28.06	22.8
	a1 (EMEP model)	0.516	0.326	0.331	0.658
	a2 (altitude_1km)	-0.0079	-0.0069	-0.0213	-0.0087
	a3 (altitude_5km_radius)	0.0066	0.0076	0.0219	
	a4 (wind speed)	-1.34	-2.75	-1.95	-3.23
	a5 (population*1000)	0.00135	0.00013		
	a6 (NAT_1km)		-0.0700		
	a7 (AGR_1km)		-0.0323		
	a8 (LDR_5km_radius)	0.00118	0.00124	0.00383	
	a9 (HDR_5km_radius)		*n. sign.*	0.00235	
	a10 (NAT_5km_radius)	-0.00068			
	a11 (T1buf75m_1km)		11.404	0.015	
	Adjusted R^2	**0.68**	**0.56**	**0.38**	**0.55**
	Standard Error [$\mu g.m^{-3}$]	**3.2**	**5.4**	**10.7**	**6.2**
Ordinary kriging (OK) of LRM residuals	nugget	6	17	69	25
	sill	11	25	114	41
	range [km]	540	280	130	300
LRM + OK of its residuals	**RMSE [$\mu g.m^{-3}$]**	**2.9**	**4.6**	**9.2**	**4.9**
	Relative RMSE [%]	**31.9**	**22.2**	**25.3**	**42.5**
	Bias (MPE) [$\mu g.m^{-3}$]	**0.0**	**0.1**	**0.1**	**0.3**

Uncertainty estimated by cross-validation

Table A3.9 shows both absolute and relative mean uncertainty, expressed by RMSE and Relative RMSE. The absolute mean uncertainty of the final combined map of NO_2 annual average expressed as RMSE is 2.9 $\mu g \cdot m^{-3}$ for the rural areas, 4.6 $\mu g \cdot m^{-3}$ for the urban background areas and 9.2 $\mu g \cdot m^{-3}$ for the urban traffic areas. For the NO_x rural map it is 4.9 $\mu g \cdot m^{-3}$.

The relative mean uncertainty of the NO_2 annual average map is 32 % for rural, 22 % for urban background areas and 25 % for the urban traffic areas. The NO_x annual average rural map has a relative mean uncertainty of 43 %.

Figure A3.8 shows the point observation – point prediction cross-validation scatter plots for NO_2 annual average. The R^2 indicates that about 74 % of the variability is attributable to the interpolation for the rural areas, while for the urban background areas it is 67 % and for the urban traffic 54 %.

Figure A3.8 Correlation between cross-validated predicted and measurement values for NO_2 annual average 2015 for rural (left), urban background (middle) and urban traffic (right) areas

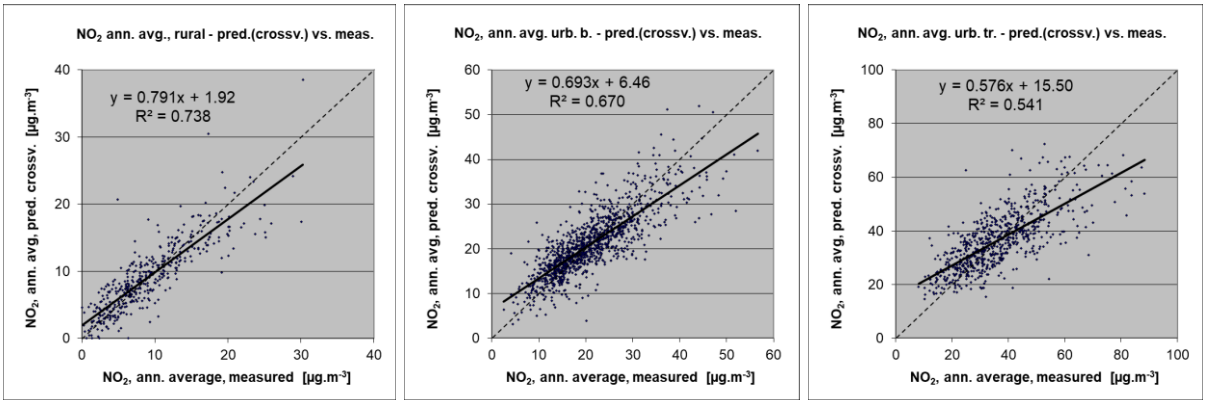

Like in the case of other pollutants, the cross-validation scatter plots show the underestimation of predictions at high concentrations at locations with no measurements. For example, in urban areas an observed value of 40 $\mu g \cdot m^{-3}$ is estimated in the interpolations to be about 34 $\mu g \cdot m^{-3}$, which is an underestimated prediction of almost 15 %.

Figure A3.9 shows the cross-validation scatter plot for NO_x annual average rural map. The R^2 indicates that about 65 % of the variability is attributable to the interpolation.

Figure A3.9 Correlation between cross-validated predicted and measurement values for NO_x annual average 2015 for rural areas

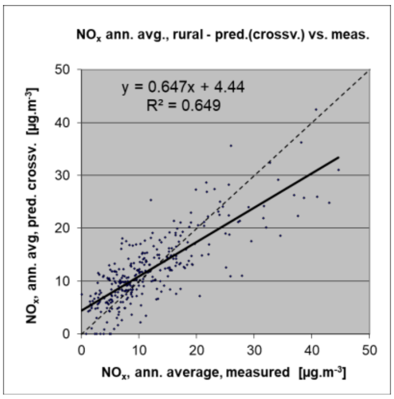

Comparison of point measurement values with the predicted grid value

Next to the above presented cross-validation, a simple comparison was made between the point observation values and interpolated predicted 1x1 km grid values.

For NO_2 annual average, the comparison has been made primarily for the separate rural, separate urban background and separate urban traffic map layers at 1x1 km resolution. Besides, the comparison has been done also for the final combined map. Table A3.10 presents the results of this comparison, together with the results of cross-validation prediction of Figure A3.8. One can conclude that the final combined map in 1x1 km resolution is representative for rural and urban background areas, but not for urban traffic areas.

Table A3.10 Statistical indicators from the scatter plots for the predicted grid values from separate (rural, urban background or urban traffic) map layers and final combined map versus the measurement point values for rural (upper left), urban background (upper right) and urban traffic (bottom left) stations for NO_2 annual average 2015

	rural backgr. stations				urban/suburban backgr. stations			
	RMSE	bias	R^2	lin. r. equation	RMSE	bias	R^2	lin r. equation
cross-valid. prediction, separate (r or ub) map	2.9	0.0	0.738	y = 0.791x + 1.92	4.6	0.1	0.670	y = 0.693x + 6.46
grid prediction, 1x1 km separate (r or ub) map	2.3	0.0	0.824	y = 0.830x + 1.55	4.0	0.0	0.759	y = 0.741x + 5.44
grid prediction, 1x1 km final merged map	2.8	0.2	0.757	y = 0.856x + 1.54	4.5	1.0	0.711	y = 0.787x + 5.41

	urban/suburban traffic stations			
	RMSE	bias	R^2	lin. r. equation
cross-valid. prediction, urban traffic map	9.2	0.1	0.541	y = 0.576x + 15.50
grid prediction, 1x1 km urban traffic map	6.7	0.1	0.762	y = 0.697x + 11.07
grid prediction, 1x1 km final merged map	15.5	-11.6	0.437	y = 0.386x + 10.61

Table A3.11 presents the cross-validation results of Figure A3.9 and those of the point observation – grid averaged prediction validation for the rural map of NO_x annual average.

Table A3.11 Statistical indicators from the scatter plots for predicted point values based on cross-validation and predicted grid values from rural 2x2 km map versus measurement point values for rural background stations for NO_x annual average 2015

	rural background stations			
	RMSE	bias	R^2	linear regression equation
cross-valid. prediction, rural map	4.9	0.3	0.649	y = 0.647x + 4.44
grid prediction, 2x2 km rural map	3.8	0.2	0.793	y = 0.729x + 3.37

Annex 4 Inter-annual changes

A4.1 PM10

Air concentrations

Map A4.1 presents the inter-annual difference between 2015 and 2014 for annual average and the 90.4 percentile of daily means for PM_{10}. Red areas show an increase of PM_{10} concentration in 2015, while blue areas show a decrease.

At the annual average PM_{10} difference map the highest increases are observed at the Po Valley, the Pyrenees, south-western Spain, Corsica, areas in the Balkan region, Romania and Bulgaria (Sophia). Other increases are at larger areas of France and south-western Spain with southern Portugal and the Balkan countries. More local increases are observed at a diversity of countries, such as Switzerland, Austria, Hungary, Romania, Bulgaria, the Balkan countries and at the island of Sardinia. Contrary to that, high decreases occur at other parts of Bulgaria and Romania, the countries and areas at the Baltic Sea, Poland and Denmark. Overall, the pattern of the 2015-2014 difference map seems to be for large part rather the opposite of that of the 2014-2013 difference in Horálek et al (2017b). The fluctuations over years seem to be mostly related to the annual meteorological variability. Besides the actual changes in the concentrations, the variability of the linear regression model and variogram parameters may cause minor differences in the concentration levels estimated.

Map A4.1 Difference concentrations between 2014 and 2015 for PM_{10} indicators annual average (left) and 90.4 percentile (right)

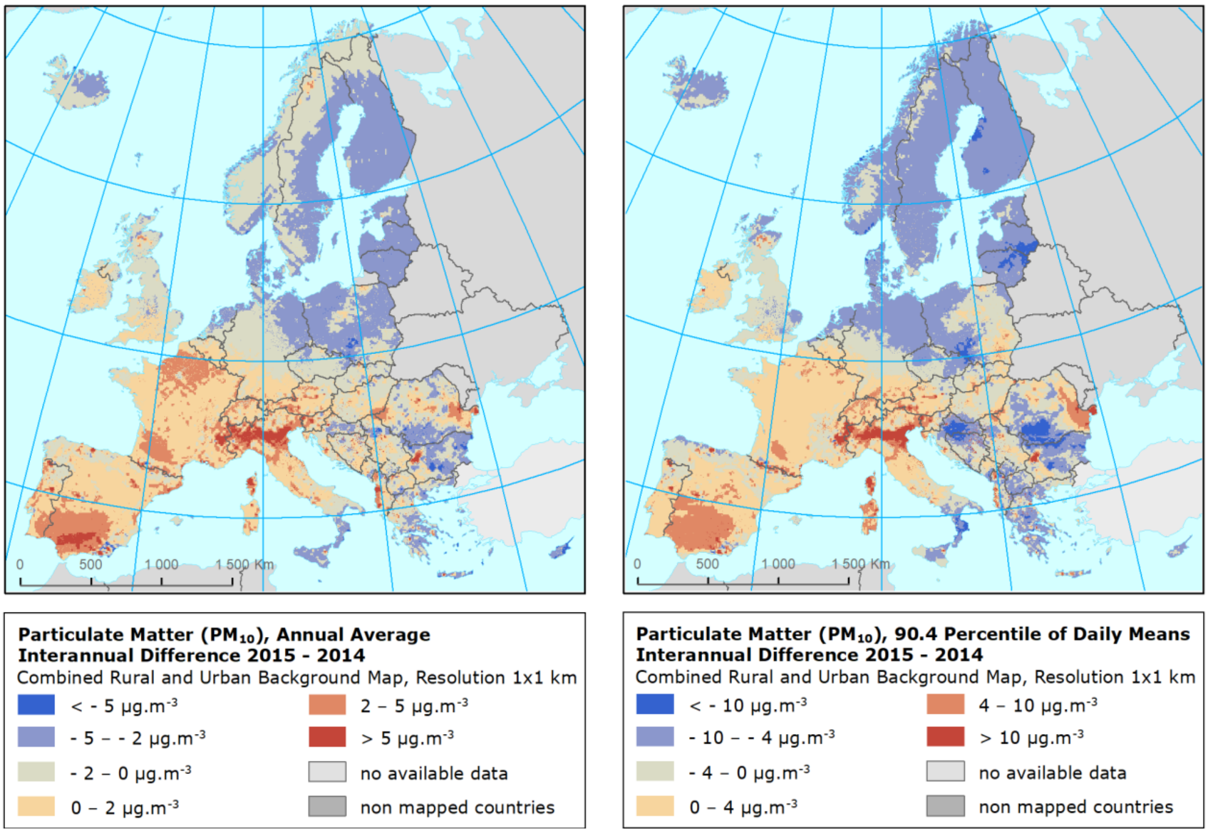

At the 90.4 percentile of daily means for PM_{10} the highest increases are observed again at the Po Valley and the Pyrenees, Corsica, Romania and Bulgaria (Sophia) and a few smaller areas in the Balkan region. Other increases are at larger areas quite similar to those at the annual average indicator. Decreases are observed at the countries around the Baltic Sea, as well as Denmark and the northern part of The Netherlands and Germany, the western half of Poland and part of Czech Republic, large part of Bulgaria, the northern Balkan area and South Italy.

Population exposure

The Tables A4.1 and A4.2 provide the inter-annual variation and trend analysis in population exposure for PM_{10} annual average and the 90.4 percentile of daily PM_{10} means over the eleven year period 2005 – 2015 and the inter-annual difference between the last two years (2014 and 2015) for individual countries and for Europe as a whole. Furthermore, there is the significance of a linear trend indicated and – if so – the slope of this trend.

In 2015, the overall average population-weighted annual mean PM_{10} concentration for the whole of Europe was 21.2 $\mu g \cdot m^{-3}$, about the same as in its previous year. This is together with year 2014 the lowest level of the eleven years period 2005 – 2015. One may observe a steady reduction of the population-weighted concentration over the period of time 2005 – 2011, with perhaps some flattening effect in 2011 – 2013 and further reduction in 2014. The steepest decrease of population-weighted concentration per country compared to 2014 took place in Latvia, Lithuania, Bulgaria, and Iceland. The highest increase was detected in Bosnia and Herzegovina, Albania, and Croatia.

For most of the countries, significant downward trend is detected. It is detected for almost all countries of northern and western Europe (i.e. apart from France, Luxemburg, Ireland and Iceland), for the most of the southern Europe (e.g. for Portugal, Spain and Italy) and the most of the Balkan countries. Contrary to this, no significant trend is detected e.g. for Poland, Czech Republic, Baltic countries, Greece and Cyprus.

The overall picture of the population-weighted concentration for the total of 40 European countries demonstrates a downward trend for the years 2005 – 2015. This trend is statistically significant, the slope is about -0.7 $\mu g \cdot m^{-3}$ per year, which means the mean decrease of 0.7 $\mu g \cdot m^{-3}$ per year. For the EU-28, the slope is also about -0.7 $\mu g \cdot m^{-3}$ per year.

Table A4.2 shows the evolution of the annual population exposure in the period 2005-2014, the inter-annual difference between 2014 and 2015, and the results of the trend analysis in relation to the PM_{10} daily limit value. For the period 2005 – 2011, the results of the 36th highest daily mean are presented, while the results of the 90.4 percentile of daily means are given for the period 2012 – 2015. Both statistics are related with the PM_{10} daily limit value according to the AQ Directive (EU, 2008), however the 36th highest daily mean results are somewhat underestimated due to the incompleteness in time series of the measurement data. The level of the underestimation of the population exposure for the whole Europe is almost 1 $\mu g \cdot m^{-3}$ (see Table 6.1), and can explain the most of the increase in 2012 with respect to 2011.

In Table A4.2 the European-wide population-weighted 90.4 percentile of the daily mean PM_{10} concentrations is estimated for 2015 at 36.9 $\mu g \cdot m^{-3}$, slightly lower compared to 2014 and the lowest in the period of 2005 – 2015 (even if until 2011 the underestimated 36th highest daily mean was used instead of the more realistic percentile approach that accounts for measurement incompleteness in time series).

The overall picture of the population-weighted concentration of both the overall European totals (i.e. totals of 40 European countries) and the EU-28 demonstrates a downward trend of -1.0 $\mu g \cdot m^{-3}$ per year for the years 2005 – 2015, which is statistically significant and means an average decrease of 1.0 $\mu g \cdot m^{-3}$ per year. Due to the underestimation of the values for the 36th highest daily mean, one may conclude the slope is in fact slightly steeper.

The steepest decrease of population-weighted concentration per country compared to 2014 took place in Iceland, Finland, Latvia, and Bulgaria. The highest increase was detected in Bosnia and

Herzegovina, Albania, Italy, and Slovenia. The results are similar to those obtained for the annual mean.

Table A4.1 Evolution and trend in 2005–2014 and difference between 2015 and 2014 for population-weighted concentration, PM_{10} annual average. Trend estimates are only given when a significant trend is observed (p >0.1).

Country		Population-weighted conc. [μg·m^{-3}]											Differ. '15 - '14	Trend of pop.-weighted conc. 2005–2015	
		2005	2006	2007	2008	2009	2010	2011	2012	2013	2014	2015		Signific.	Slope [μg·m^{-3}·yr^{-1}]
Albania	AL	36.3	31.8	31.6	33.3	35.3	45.5	26.5	32.0	32.5	25.7	30.2	4.5		
Andorra	AD	19.5	22.5	20.5	18.7	17.7	17.9	18.0	33.2	25.0	21.3	24.7	3.3		
Austria	AT	25.4	26.0	22.1	21.3	21.6	22.7	20.8	20.0	20.2	17.8	18.7	0.8	**	-0.7
Belgium	BE	29.2	31.3	24.8	23.9	26.5	25.7	24.8	23.2	23.6	20.2	20.4	0.1	**	-0.9
Bosnia-Herzegovina	BA	34.3	33.1	32.4	29.3	37.2	30.8	22.3	27.2	23.1	22.1	26.8	4.7	**	-1.2
Bulgaria	BG	42.6	41.6	40.2	44.2	39.8	38.0	27.3	36.6	36.7	36.2	33.1	-3.1	**	-0.9
Croatia	HR	33.6	31.5	30.0	28.1	29.0	27.3	25.0	24.7	23.5	21.7	25.1	3.4	***	-1.2
Cyprus	CY	38.9	35.4	33.9	76.1	41.0	50.2	31.1	42.9	35.8	32.1	31.4	-0.7		
Czech Republic	CZ	32.9	33.5	25.6	24.2	25.3	28.3	23.7	25.4	25.6	25.5	23.3	-2.2		
Denmark	DK	21.3	23.5	20.8	18.8	16.3	15.7	18.4	16.3	16.3	18.5	17.1	-1.5	+	-0.5
Estonia	EE	17.7	19.7	15.7	12.9	13.4	14.1	9.8	12.1	13.5	14.8	12.1	-2.7		
Finland	FI	14.2	17.0	13.7	12.5	11.7	12.2	9.5	10.2	10.5	12.0	9.1	-2.9	**	-0.6
France	FR	19.3	20.4	24.6	22.6	24.0	23.0	21.8	21.4	20.7	16.7	18.2	1.5		
Germany	DE	23.0	24.2	20.7	19.6	20.7	21.2	19.6	18.4	19.0	18.7	17.8	-0.9	**	-0.5
Greece	GR	38.0	33.6	33.5	39.7	35.3	37.3	24.6	30.3	34.6	27.4	28.7	1.3	+	-0.9
Hungary	HU	34.8	32.9	28.7	26.8	27.6	28.1	29.1	26.1	25.3	25.4	26.3	0.9	*	-0.7
Iceland	IS	13.8	17.4	12.2	15.2	9.0	10.7	9.3	9.6	11.8	12.7	9.7	-3.0		
Ireland	IE	12.7	14.9	14.7	15.4	12.8	13.7	12.8	12.4	15.1	13.7	11.9	-1.8		
Italy	IT	34.9	33.9	33.2	30.1	28.7	26.4	27.7	27.0	27.0	24.0	26.6	2.6	**	-1.0
Latvia	LV	19.8	21.9	17.8	19.1	18.8	21.5	14.6	18.0	19.5	20.3	16.5	-3.9		
Liechtenstein	LI	23.4	24.9	20.7	20.6	18.3	17.3	11.3	14.3	15.5	13.1	16.3	3.2	**	-1.1
Lithuania	LT	20.7	22.5	18.5	17.3	19.0	22.0	14.8	18.1	20.4	21.7	18.5	-3.2		
Luxembourg	LU	18.7	20.8	19.5	18.2	21.0	19.4	16.4	17.2	18.8	17.4	18.5	1.1		
Macedonia, FYR of	MK	46.2	39.3	38.5	41.6	45.4	43.9	23.0	42.3	44.5	39.3	37.3	-2.0		
Malta	MT	37.1	29.4	27.0	27.5	27.2	32.5	27.8	25.4	35.7	28.9	26.4	-2.5		
Monaco	MC		36.7	34.5	29.5	26.8	24.0	22.8	28.0	22.7	22.3	23.2	0.9	**	-1.5
Montenegro	ME	35.1	33.1	33.1	33.6	35.0	32.8	21.5	28.3	27.0	24.6	26.7	2.1	*	-1.0
Netherlands	NL	29.2	29.1	25.8	24.0	24.3	24.3	25.1	21.1	20.7	20.2	18.7	-1.6	***	-1.0
Norway	NO	18.1	19.6	15.6	15.7	14.1	14.7	9.3	12.2	13.8	12.6	11.1	-1.5	**	-0.7
Poland	PL	32.7	37.0	28.8	28.3	30.8	35.2	27.2	32.4	30.4	31.5	29.5	-2.0		
Portugal	PT	30.9	28.4	27.0	21.8	22.9	21.7	20.8	19.9	20.3	16.9	18.7	1.8	***	-1.2
Romania	RO	42.7	39.1	35.0	30.8	28.9	25.2	27.2	28.9	26.0	25.9	25.7	-0.2	**	-1.5
San Marino	SM	31.7	33.9	31.2	29.6	26.0	25.0	20.9	25.8	22.1	21.2	24.6	3.4	**	-1.2
Serbia (incl. Kosovo*)	RS	44.2	41.8	39.4	40.1	39.5	33.1	30.1	34.9	31.8	32.1	32.7	0.6	**	-1.3
Slovakia	SK	34.3	33.8	29.1	26.7	26.9	30.2	27.4	27.9	26.8	27.2	26.3	-0.8	*	-0.5
Slovenia	SI	30.8	29.0	27.2	25.0	25.2	26.0	25.4	24.3	22.7	20.3	23.3	3.0	**	-0.8
Spain	ES	29.6	31.4	29.6	25.2	23.7	21.4	18.8	20.9	19.1	19.7	21.6	1.9	**	-1.2
Sweden	SE	16.9	19.0	15.7	16.3	13.8	12.8	12.3	12.4	13.2	13.8	13.3	-0.5	*	-0.5
Switzerland	CH	21.3	23.2	21.4	20.5	21.0	19.8	17.7	17.6	18.3	16.5	17.4	0.9	**	-0.6
United Kingdom	UK	21.4	23.2	21.6	19.5	18.4	18.2	17.5	16.5	17.0	16.6	15.1	-1.6	***	-0.7
Total		**28.0**	**28.5**	**26.2**	**24.8**	**24.6**	**24.3**	**22.1**	**22.7**	**22.2**	**21.1**	**21.2**	**0.1**	***	**-0.7**
EU-28		**27.6**	**28.3**	**26.0**	**24.4**	**24.2**	**24.0**	**22.1**	**22.4**	**22.1**	**20.9**	**20.9**	**0.0**	***	**-0.7**

*) under the UN Security Council Resolution 1244/99

A significant downward trend is detected for about sixty percent of the countries; for the rest no significant trend is detected. However, without the underestimation of the values for the 36th highest daily mean, probably the downward trend would be detected at more countries. This trend is detected for almost the same countries as for the annual average. Across Europe a similar pattern as for the annual average is observed here.

Table A4.2 Evolution and trend in 2005–2015 and difference between 2015 and 2014 for population-weighted concentration, PM_{10} indicator 36th highest daily mean / 90.4 percentile of daily means. Trend estimates are only given when a significant trend is observed (p >0.1).

Country		Population-weighted conc. [µg·m^{-3}]												Trend of pop.-weighted conc. 2005–2015	
		36th highest daily mean							90.4 perc. of daily means						
		2005	2006	2007	2008	2009	2010	2011	2012	2013	2014	2015	diff. '15 - '14	Signific.	Slope [µg·m^{-3}·year^{-1}]
Albania	AL	59.8	54.0	53.3	55.7	51.3	69.5	42.8	57.2	61.4	47.4	56.6	9.2		
Andorra	AD	31.1	35.7	32.1	29.3	29.4	28.5	29.2	78.4	47.6	41.9	45.7	3.8		
Austria	AT	45.7	47.1	39.9	36.9	36.7	42.8	38.7	36.1	37.0	32.4	32.4	0.0	**	-1.2
Belgium	BE	46.9	51.3	43.5	38.4	45.8	42.7	45.1	43.9	41.2	35.0	34.6	-0.3	*	-1.2
Bosnia-Herzegovina	BA	57.3	57.4	52.7	50.6	57.8	53.7	40.8	52.8	44.2	44.2	54.5	10.3		
Bulgaria	BG	73.3	74.2	67.5	78.2	70.3	69.2	46.6	66.9	67.9	68.4	62.2	-6.3	+	-0.9
Croatia	HR	57.6	53.7	49.6	48.6	46.9	50.5	46.6	45.5	44.6	42.1	46.8	4.7	**	-1.1
Cyprus	CY	63.7	58.2	54.4	130.7	68.6	74.5	46.2	62.0	56.9	47.4	45.2	-2.2	+	-2.2
Czech Republic	CZ	60.2	57.5	46.2	42.5	43.6	53.7	46.2	47.6	46.9	47.3	41.6	-5.7		
Denmark	DK	34.5	37.0	32.5	29.0	26.0	25.5	31.6	26.3	26.7	32.6	29.3	-3.4		
Estonia	EE	31.7	34.1	28.0	22.4	22.4	25.8	17.6	21.6	22.6	26.4	20.7	-5.8	+	-1.0
Finland	FI	24.2	29.5	23.9	21.9	19.4	22.7	16.9	18.3	18.0	22.4	15.0	-7.4	**	-0.9
France	FR	29.8	32.9	41.0	36.3	39.2	37.1	36.6	38.1	36.9	28.2	30.2	2.0		
Germany	DE	38.6	41.3	35.7	31.7	34.4	37.2	35.7	32.8	32.9	33.0	30.6	-2.4	*	-0.7
Greece	GR	59.9	54.3	53.0	64.9	54.7	64.8	37.6	47.8	61.2	46.4	48.2	1.8		
Hungary	HU	61.6	58.5	48.5	47.5	46.4	52.3	55.4	47.2	44.6	45.3	46.2	0.9	*	-1.1
Iceland	IS	19.0	27.2	21.4	25.4	15.8	16.8	15.8	17.6	20.1	22.3	14.5	-7.8		
Ireland	IE	17.8	24.1	24.8	25.8	21.7	23.2	23.2	21.8	26.3	23.6	21.3	-2.2		
Italy	IT	60.2	58.6	57.4	51.7	48.6	45.2	48.6	48.0	49.7	42.1	47.4	5.3	**	-1.3
Latvia	LV	35.9	40.0	31.9	32.7	33.4	37.8	26.7	33.7	33.0	36.1	29.0	-7.2		
Liechtenstein	LI	40.2	47.5	39.3	38.5	31.5	33.6	21.3	27.7	32.4	23.6	28.9	5.3	**	-1.8
Lithuania	LT	37.7	39.7	33.2	29.5	32.7	39.5	26.6	33.9	34.1	38.8	34.0	-4.8		
Luxembourg	LU	31.2	35.9	32.5	29.1	34.3	31.9	29.4	30.6	31.5	29.6	31.1	1.5		
Macedonia, FYR of	MK	77.5	69.9	57.8	71.5	75.6	80.1	37.9	80.4	93.1	80.9	78.1	-2.8	+	1.1
Malta	MT	62.7	44.8	42.6	40.3	38.7	49.4	39.7	37.8	62.2	42.4	41.7	-0.7		
Monaco	MC		59.7	46.2	46.0	41.5	36.1	37.0	46.0	39.0	34.8	35.0	0.2		
Montenegro	ME	58.7	57.9	53.6	56.7	51.8	54.0	36.2	55.9	53.6	49.2	52.9	3.7	*	-0.6
Netherlands	NL	47.5	46.1	41.9	37.7	39.0	40.2	44.0	35.8	34.2	34.5	30.2	-4.3	**	-1.5
Norway	NO	29.3	31.9	26.3	26.1	24.0	25.7	16.3	21.9	23.7	22.4	19.3	-3.1	**	-1.0
Poland	PL	58.6	64.0	50.8	48.6	55.4	65.7	51.4	62.7	55.4	58.0	55.7	-2.4		
Portugal	PT	52.0	48.3	45.0	35.5	38.5	35.6	35.4	35.8	34.5	29.9	31.8	2.0	**	-1.8
Romania	RO	73.4	65.4	57.7	53.1	49.0	45.2	48.1	50.0	45.4	45.4	43.8	-1.6	**	-2.3
San Marino	SM	51.7	57.4	54.1	48.9	40.6	44.0	35.9	44.3	40.2	38.5	43.7	5.3	*	-1.5
Serbia (incl. Kosovo*)	RS	73.1	73.1	61.8	68.6	67.6	60.1	54.6	65.9	61.3	63.3	65.7	2.4	+	-0.9
Slovakia	SK	60.9	58.5	50.5	47.5	46.2	56.0	51.5	51.6	47.5	48.7	47.4	-1.3	+	-1.2
Slovenia	SI	53.7	49.2	46.1	42.7	41.9	47.2	48.1	44.0	42.2	37.3	42.6	5.3	*	-0.9
Spain	ES	46.7	49.3	46.9	40.1	38.0	33.4	30.5	34.2	30.7	32.0	34.9	2.9	*	-1.9
Sweden	SE	27.7	32.0	25.8	26.4	23.3	22.1	21.1	21.2	22.5	24.3	22.4	-1.9	*	-0.7
Switzerland	CH	36.0	43.9	39.9	36.5	37.1	36.3	33.0	32.8	36.5	28.3	30.1	1.8	*	-1.2
United Kingdom	UK	32.5	35.5	34.7	32.1	30.1	28.8	30.3	29.6	29.0	28.7	25.3	-3.4	**	-0.7
Total		**46.8**	**47.8**	**44.1**	**41.3**	**41.2**	**41.9**	**39.0**	**40.6**	**39.4**	**37.1**	**36.9**	**-0.2**	*******	**-1.0**
EU-28		**46.1**	**47.2**	**43.8**	**40.5**	**40.5**	**41.3**	**39.0**	**40.0**	**38.8**	**36.6**	**36.2**	**-0.4**	******	**-1.0**

*) under the UN Security Council Resolution 1244/99

Next to the population-weighted concentration, another trend indicator is the evolution of the percentage of population living in areas with concentrations above the limit value. However, the percentage of population living above the limit value is not a very robust statistical parameter: just small changes in the level of concentrations closely around the threshold and over extended areas might result in large changes in exposed population. The evolution of this statistics for European area as a whole is presented in Table 6.1. In comparison with the previous ten years, the percentage of population living in areas above the LV is the lowest in 2015. The table showing the evolution of the percentage population in exceedance for individual countries is presented as supplementary material at the web page http://acm.eionet.europa.eu/reports/ETCACM_TP_2017_7_AQMaps2015, i.e. at the web page of this paper.

Uncertainties

Table A4.3 summarises the eleven-year evolution of the absolute and relative mean interpolation uncertainties, and also R^2 from cross-validation scatterplots, for the rural and maps, for both PM_{10} indicators.

In the year 2015, both the absolute and the relative uncertainty results show slightly better levels for rural areas and slightly worse levels for urban areas, compared to 2014.

The results for R^2 from cross-validation scatterplots show slightly better levels for rural areas and somewhat worse levels for urban areas, compared to previous four years.

Table A4.3 Absolute and relative mean uncertainty and R^2 from cross-validation scatterplot for the total European rural and urban areas, PM_{10} indicators annual average and 90.4 percentile of daily means, years 2005 – 2015

PM10			2005	2006	2007	2008	2009	2010	2011	2012	2013	2014	2015
Annual average													
rural areas	abs. mean uncertainty	RMSE [µg.m^{-3}]	5.5	5.8	4.6	5.0	4.6	4.5	4.1	3.8	3.4	3.5	3.2
	rel. mean uncertainty	RRMSE [%]	*25.9*	*26.6*	*23.5*	*27.2*	*23.9*	*22.7*	*21.1*	*21.4*	*19.6*	*20.7*	*19.4*
	coeff. of determinatio	R^2	*0.52*	*0.52*	*0.59*	*0.48*	*0.54*	*0.62*	*0.68*	*0.67*	*0.70*	*0.68*	*0.71*
urban areas	abs. mean uncertainty	RMSE [µg.m^{-3}]	5.5	6.1	5.0	6.3	6.7	6.6	6.1	6.1	4.3	4.2	4.5
	rel. mean uncertainty	RRMSE [%]	*20.0*	*20.9*	*18.4*	*22.4*	*23.0*	*22.5*	*20.7*	*22.1*	*17.3*	*17.7*	*19.2*
	coeff. of determinatio	R^2	*0.71*	*0.69*	*0.66*	*0.82*	*0.73*	*0.75*	*0.77*	*0.76*	*0.74*	*0.76*	*0.69*
36th max. daily mean (2005 - 2011) / 90.4 percentile of daily means (2012 - 2015)													
rural areas	abs. mean uncertainty	RMSE [µg.m^{-3}]	9.7	9.9	8.0	8.8	8.0	8.6	8.4	7.8	6.5	6.5	6.2
	rel. mean uncertainty	RRMSE [%]	*26.3*	*26.6*	*23.5*	*28.2*	*24.1*	*24.4*	*23.5*	*24.3*	*21.0*	*21.5*	*21.1*
	coeff. of determinatio	R^2	*0.55*	*0.56*	*0.60*	*0.52*	*0.56*	*0.64*	*0.66*	*0.64*	*0.69*	*0.69*	*0.70*
urban areas	abs. mean uncertainty	RMSE [µg.m^{-3}]	9.9	11.7	9.1	12.7	13.2	12.2	13.0	12.1	8.6	8.6	10.8
	rel. mean uncertainty	RRMSE [%]	*21.4*	*23.5*	*19.6*	*24.4*	*26.7*	*23.7*	*24.3*	*25.0*	*19.5*	*20.4*	*25.6*
	coeff. of determinatio	R^2	*0.75*	*0.65*	*0.65*	*0.79*	*0.72*	*0.77*	*0.75*	*0.75*	*0.75*	*0.76*	*0.64*

A4.2 $PM_{2.5}$

Air concentrations

Map A4.2 presents the inter-annual difference between 2015 and 2014 for annual average $PM_{2.5}$.

The highest increases are seen in Po Valley, south-western Spain, Corsica, the Sophia region, north-eastern and central Romania and extended Mediterranean coastal shores. Smaller increases over extended areas are observed at the Iberian Peninsula, in France, Italy, Switzerland, Austria, Slovakia and Hungary. The steepest decrease from 2014 to 2015 is observed in a large part of Poland, Lithuania, South Romania with North Bulgaria and large rural areas of the Western Balkans.

Map A4.2 Difference $PM_{2.5}$ annual average concentrations between 2015 and 2014

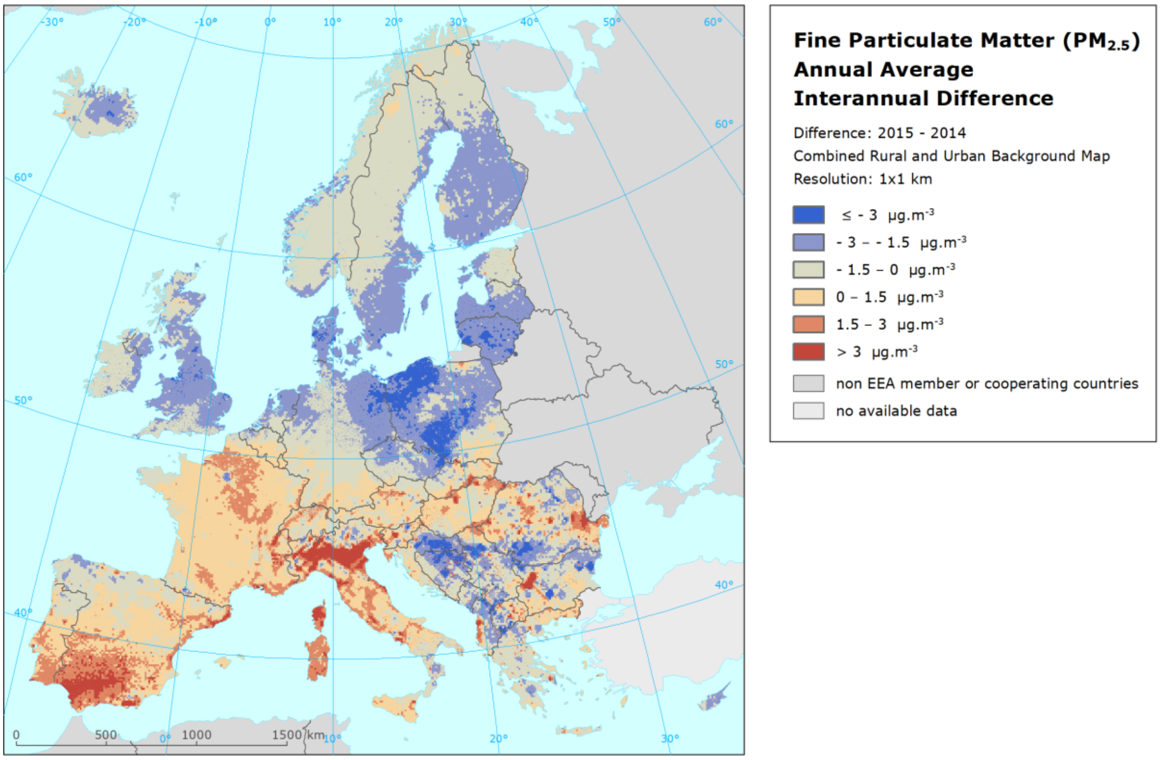

Population exposure

Table A4.4 shows the evolution of the population exposure for the years 2007 – 2015, with missing calculations for 2009, based on the results presented in Chapter 3.1 and in Horálek et al. (2017b) resp. references cited therein. Next to this, the inter-annual difference between 2014 and 2015, and the results of the trend analysis for 2007 – 2015 are presented in this table. It should be noted that this period for the trend analysis is shorter than for PM_{10} and ozone, leading to less robust results.

Considering Europe as a whole, Table A4.4 shows that the overall population-weighted annual mean $PM_{2.5}$ concentration in 2015 was 14.2 $\mu g \cdot m^{-3}$. This is the similar as in 2014. These two years show the lowest values for all the years presented.

One may observe similar levels in the population-weighted concentration across Europe as a whole in 2007 – 2008, an increase in 2010, slightly continuous reduction for the period 2010 – 2014 and stagnation in 2015. For the whole period 2007 – 2015, a slight downward trend is detected. The estimated slope is about -0.3 $\mu g \cdot m^{-3}$ per year for both Europe as a whole and the EU-28, which means a mean decrease of 0.3 $\mu g \cdot m^{-3}$ per year.

The steepest decrease of population-weighted concentration per country compared to 2014 took place in Lithuania, Latvia and Ireland. The highest increase was detected in Albania, Bosnia and Herzegovina, Andorra and Montenegro.

For seven countries, significant decreasing trend is detected at the significance level 0.95, and for additional three countries at the significance level 0.90. For most of the countries, no significant trend is detected. However, the examined period consists of eight years only, so the results of the trend analysis are less robust than for PM_{10} and ozone.

Table A4.4 Evolution and trend in 2007–2015 and difference between 2015 and 2014 for population-weighted concentration, $PM_{2.5}$ annual average. Trend estimates are only given when a significant trend is observed (p >0.1).

Country		Population-weighted conc. [µg·m^{-3}]										Trend of pop.-weighted conc. 2007–2015	
		2007	2008	2009	2010	2011	2012	2013	2014	2015	Differ. '14	Signific.	Slope [µg·m^{-3}·year^{-1}]
Albania	AL	20.8	19.6	not mapped	25.1	17.2	21.1	20.3	16.5	20.5	4.0		
Andorra	AD	11.5	11.3		12.4	13.7	15.9	11.9	10.0	13.3	3.2		
Austria	AT	16.3	16.4		17.7	16.3	14.8	15.7	12.9	13.3	0.4	*	-0.5
Belgium	BE	16.6	17.1		18.8	17.3	15.8	16.6	13.7	13.0	-0.6		
Bosnia-Herzegovina	BA	21.7	20.3		22.2	17.2	18.5	16.0	15.3	18.9	3.6		
Bulgaria	BG	28.8	28.4		24.5	18.3	24.9	24.1	24.0	24.1	0.1		
Croatia	HR	19.5	18.5		20.0	19.6	16.8	16.8	15.6	17.4	1.8		
Cyprus	CY	25.0	25.3		21.8	21.0	25.0	17.0	17.0	16.9	0.0	*	-1.1
Czech Republic	CZ	17.5	17.7		21.5	18.8	18.8	19.6	18.7	17.0	-1.6		
Denmark	DK	11.5	11.1		11.4	12.5	10.0	9.6	11.6	9.7	-1.9		
Estonia	EE	8.8	8.9		8.9	8.0	7.9	7.8	8.7	6.7	-2.0	+	-0.2
Finland	FI	7.7	7.4		7.8	7.4	7.1	5.9	7.4	5.3	-2.1	*	-0.3
France	FR	14.9	14.7		16.2	15.3	14.7	14.5	11.0	11.9	0.8	*	-0.5
Germany	DE	14.0	14.1		16.3	14.8	13.3	14.2	13.4	12.3	-1.2		
Greece	GR	22.0	21.7		20.0	16.8	19.2	19.7	17.0	19.1	2.0	+	-0.4
Hungary	HU	19.3	19.4		20.3	23.1	18.9	18.2	17.3	18.9	1.6		
Iceland	IS	7.1	7.1		6.9	4.6	4.7	6.5	6.6	5.5	-1.2		
Ireland	IE	8.5	9.6		10.3	7.9	8.1	9.2	9.0	6.5	-2.5		
Italy	IT	19.0	19.1		17.5	19.8	18.9	18.2	15.8	18.5	2.6		
Latvia	LV	15.3	16.4		14.7	11.1	12.4	12.8	14.1	10.6	-3.5		
Liechtenstein	LI	15.5	15.5		15.3	8.5	10.2	11.4	9.0	11.0	2.0		
Lithuania	LT	13.8	15.5		15.6	12.7	12.9	13.9	15.5	11.7	-3.7		
Luxembourg	LU	13.9	14.5		15.8	13.3	12.6	14.3	11.9	12.0	0.2		
Macedonia, FYR of	MK	24.4	23.6		27.5	15.8	29.2	30.4	27.4	28.7	1.2		
Malta	MT	14.9	14.9		13.8	15.6	12.4	12.5	12.0	12.8	0.9		
Monaco	MC	16.5	16.5		14.9	16.4	18.2	13.8	12.9	14.4	1.5		
Montenegro	ME	21.4	19.9		24.6	15.1	18.7	17.1	15.6	18.5	2.9		
Netherlands	NL	16.9	17.0		17.6	17.1	13.7	14.3	13.8	12.3	-1.5		
Norway	NO	8.6	8.2		8.8	6.3	7.2	7.1	7.2	5.9	-1.3		
Poland	PL	20.8	21.1		26.4	21.8	23.9	22.8	22.9	21.6	-1.4		
Portugal	PT	11.5	10.9		10.5	10.5	9.9	10.0	8.7	9.8	1.1	**	-0.2
Romania	RO	22.4	21.8		17.0	20.5	20.8	18.5	17.5	18.1	0.6		
San Marino	SM	18.2	18.2		16.3	14.7	16.7	15.1	13.5	16.2	2.7		
Serbia (incl. Kosovo*)	RS	26.6	25.4		22.7	21.2	24.3	22.5	22.4	23.9	1.5		
Slovakia	SK	20.2	20.6		21.3	21.8	20.5	20.1	19.2	19.1	-0.1		
Slovenia	SI	18.5	18.0		19.0	19.4	17.7	17.4	15.1	17.4	2.3		
Spain	ES	14.1	13.6		11.8	11.1	11.9	11.0	10.7	12.7	1.9		
Sweden	SE	9.2	8.8		8.1	8.1	7.2	6.0	7.6	5.9	-1.6	**	-0.4
Switzerland	CH	14.9	14.8		15.5	12.6	12.6	13.9	11.6	11.8	0.3	+	-0.4
United Kingdom	UK	12.2	12.5		13.0	12.4	11.9	11.8	11.6	9.4	-2.2	*	-0.2
Total		**16.3**	**16.3**		**16.8**	**15.9**	**15.6**	**15.3**	**14.1**	**14.2**	**0.0**	**	**-0.3**
EU-28		**16.1**	**16.1**		**16.7**	**15.9**	**15.5**	**15.1**	**14.0**	**14.0**	**-0.1**	**	**-0.3**

*) under the UN Security Council Resolution 1244/99

The evolution of the percentage population living in areas with concentrations above the $PM_{2.5}$ limit value in Europe as a whole is presented in Table 6.2. In 2015, the percentage is slightly below average of the limited time series. Throughout the years, fluctuations do occur. However, as stated earlier, the percentage population living in areas with concentrations above the limit value is not statistically a very robust parameter.

The table showing the evolution of the percentage population in exceedance for individual countries is presented as a supplementary material at the web page of this paper, see http://acm.eionet.europa.eu/reports/ETCACM_TP_2017_7_AQMaps2015.

Uncertainties

Table A4.5 presents the uncertainty results for $PM_{2.5}$ maps for the years 2007 – 2015 (excluding the 'not-mapped' year 2009). Both absolute and relative uncertainties show for 2015 similar results as in 2014. In the case of the absolute uncertainties, the 2014 and 2015 results are the lowest, compared to all the previous years; this is related to the lowest concentration (see e.g. Table 6.2). In the case of the relative uncertainties, the 2015 results are among the better results throughout the years.

The results for R^2 from cross-validation scatterplots show quite similar levels to the previous years.

Table A4.5 Absolute and relative mean uncertainty and R^2 from cross-validation scatterplot for the total European rural and urban areas, $PM_{2.5}$ annual average, years 2007 – 2015

PM2.5			2007	2008	2009	2010	2011	2012	2013	2014	2015
Annual average											
rural areas	abs. mean uncertainty	RMSE [μg.m^{-3}]	3.3	3.5	not mapped	3.4	2.8	3.0	2.7	2.5	2.5
	rel. mean uncertainty	RRMSE [%]	*27.4*	*29.8*		*25.0*	*16.8*	*24.9*	*22.1*	*22.4*	*21.9*
	coeff. of determinatio	R^2				*0.74*	*0.82*	*0.78*	*0.78*	*0.78*	*0.78*
urban areas	abs. mean uncertainty	RMSE [μg.m^{-3}]	4.1	3.6	not mapped	3.1	3.2	3.3	2.9	2.6	2.6
	rel. mean uncertainty	RRMSE [%]	*23.7*	*20.0*		*16.8*	*16.7*	*18.7*	*17.5*	*16.4*	*16.6*
	coeff. of determinatio	R^2				*0.81*	*0.80*	*0.78*	*0.78*	*0.81*	*0.82*

A4.3 Ozone

Air concentrations

Map A4.3 presents the inter-annual difference between 2014 and 2015 for health related ozone indicators, i.e. for 93.2 percentile of maximum daily 8-hour means and SOMO35; and for vegetation related ozone indicators, i.e. for AOT40 for vegetation and AOT40 for forests. In all the maps, red areas show an increase of ozone concentrations, while blue areas show a decrease.

Most of the European continent and Iceland show a quite steep increase for 93.2 percentile of maximum daily 8-hour means from 2014 to 2015. The steepest decrease can be seen in the Romanian-Bulgarian region. Somewhat smaller decreases occur at Scandinavia, Ireland and the Pyrenees

The difference pattern for SOMO35 is quite similar to that of the percentile indicator, however, the extremes are less elevated or prominent, except for central Italy, some areas around the Alps and the Balkan region, where elevated increases are observed. Decreases are only observed in the Romanian-Bulgarian region, and a few location in Scandinavia, such as south-western Norway.

In the case of AOT40 for vegetation, increases are observed in the large extend of south-western, south, central and south-eastern of Europe. Contrary to that, the largest decreases are observed in limited areas of south-western Norway and the central part of Denmark. Less prominent decreases are observed in the most of Scandinavia and the regions bordering the Baltic Sea, as well as northern Germany and the Netherlands, the rest of Denmark, south-eastern UK and parts in Slovakia, Hungary, Romania and Bulgaria. In the case of AOT40 for forests, the whole continental area except Scandinavia shows high increases. The main decrease is visible in in a limited area in both south-eastern Norway and central Denmark. Less prominent decreases occur in most of the rest of Scandinavia.

Map A4.3 **Difference concentrations between 2014 and 2015 for ozone indicators 93.2 percentile of daily 8-hour maximums (top left), SOMO35 (top right), AOT40v (bottom left) and AOT40f (bottom right)**

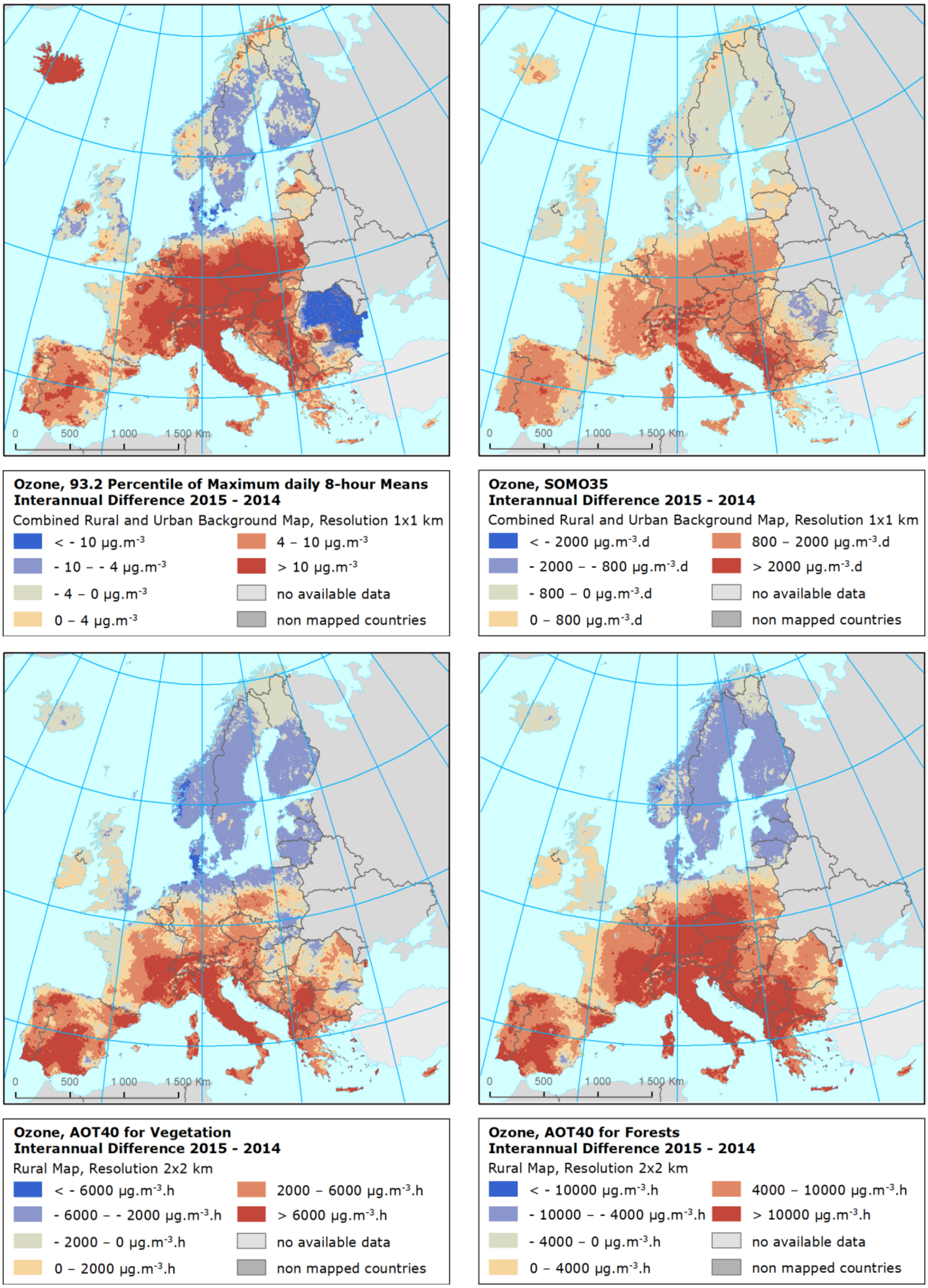

Population exposure

Table A4.6 provides the evolution of the annual population exposure in the period 2005–2015, the inter-annual difference between 2014 and 2015, and the results of the trend analysis. For the period 2005 – 2011, the results of the 26th highest maximum daily 8-hour mean are presented, while the results of the 93.2 percentile of maximum daily 8-hour means are given for the period 2012 – 2015. Both statistics are related to the ozone target value threshold for the protection of health according to the AQ Directive (EU, 2008), however the 26th highest maximum daily 8-hour mean results are somewhat underestimated due to the incomplete time series of the measurement data. The level of the underestimation of the population exposure for the whole Europe is about 0.6 $\mu g \cdot m^{-3}$ (see Table 6.3).

In 2015 the overall population-weighted concentration for ozone indicator 93.2 percentile of maximum daily 8-hour means for whole of Europe was 110.4 $\mu g \cdot m^{-3}$. This is one of the highest values of the whole eleven years period (however, be aware that for 2005–2011 the 26th highest value of the maximum daily eight-hour mean was considered instead). Examining the time series 2005 – 2015, one could conclude that 2006 was an exceptional year with highly elevated ozone, which was followed by the decrease of concentration levels in 2007 – 2010 and some increase and flattening in 2011 – 2013, further reduction in 2014, and increase in 2015.

The overall picture of the population-weighted concentration for the totals of 40 European countries shows a slightly downward trend for the years 2005 – 2015. This trend is statistically significant, the slope is about -0.5 $\mu g \cdot m^{-3}$ per year for Europe and about -0.7 $\mu g \cdot m^{-3}$ for the EU-28, which means an average decrease of about 0.5 $\mu g \cdot m^{-3}$ resp. 0.7 $\mu g \cdot m^{-3}$ per year. Due to the underestimation of the 26th highest maximum daily 8-hour mean values, one may suppose the slope is in fact slightly steeper.

The highest increase of population-weighted concentration per country compared to 2014 is seen in Serbia, Hungary, Albania, Czech Republic, and Austria. The steepest decrease was detected in Malta, Denmark, Sweden and Norway.

For three countries, significant decreasing trend is detected at the significance level 0.95, and for additional five countries at the significance level 0.90. For most of the countries, no significant trend is detected. This is influenced by quite large inter-annual fluctuations of the ozone concentrations caused by the different meteorological conditions.

Table A4.7 provides the evolution of the annual population exposure in the period 2005–2015, the inter-annual difference between 2014 and 2015, and the results of the trend analysis, for the ozone indicator SOMO35, based on the results presented in Chapter 4.2 and in Horálek et al. (2017b). In 2015 the overall population-weighted value of ozone indicator SOMO35 for whole of Europe was 4312 $\mu g \cdot m^{-3} \cdot d$. This is of about 810 $\mu g \cdot m^{-3} \cdot d$ more than in 2014, and it is among the highest values of the whole eleven years period. The overall evolution of the population-weighted concentration for the totals of 40 European countries shows a slightly downward trend for the years 2005 – 2015. This trend is statistically significant; the slope is about -95, which means an average decrease of about 95 $\mu g \cdot m^{-3} \cdot d$ per year. For the EU-28, the slope is about -96 $\mu g \cdot m^{-3} \cdot d$ per year.

The highest increase of population-weighted concentration per country compared to 2014 was detected in the Balkan countries, namely FYR of Macedonia, Albania, Montenegro, and Serbia. The steepest decrease took place in Malta, Andorra, Denmark and Norway.

For nine countries, significant decreasing trend is detected at the significance level 0.90. For most of the countries, no significant trend is detected. This is influenced by quite large inter-annual fluctuations of the ozone concentrations caused by the different meteorological conditions.

Next to the population weighted concentration evolution, the evolution of the percentage European population living in areas with concentrations above the ozone target value for the 93.2 percentile of maximum daily 8-hour means resp. above a level of 6 000 $\mu g \cdot m^{-3} \cdot d$ for SOMO35 is presented in Table

6.3. In 2015, 34 % of the population was exposed to ozone level above the target value, which is among the highest numbers of eleven years period. For SOMO35, the population living in areas above 6 000 μg·m^{-3}·d fluctuates from about 17 % to 25 % in the period of 2008 – 2015, except 2014 with about 9 %.

Table A4.6 Evolution and trend in 2005–2015 and difference between 2015 and 2014 for population-weighted concentration, ozone indicator 26th highest maximum daily 8-hour mean / 93.2 percentile of maximum daily 8-hour means. Trend estimates are only given when a significant trend is observed (p >0.1).

Country		Population-weighted conc. [μg·m^{-3}]												Trend of pop.-weighted conc. 2005–2015	
		26th highest daily maximum 8-hour							93.2 perc. of d. max. 8-h m.						
		2005	2006	2007	2008	2009	2010	2011	2012	2013	2014	2015	Differ. '14	Signific.	Slope [μg·m^{-3}·year^{-1}]
Albania	AL	122.7	117.9	126.9	115.3	114.7	109.5	121.1	134.4	117.8	107.4	127.3	19.9		
Andorra	AD	127.2	119.1	118.6	122.0	115.6	122.4	120.6	122.5	122.4	117.4	114.3	-3.1		
Austria	AT	120.6	124.9	122.8	114.8	116.4	118.4	118.6	118.7	121.4	112.0	131.1	19.2		
Belgium	BE	104.0	126.0	98.9	103.6	101.5	97.7	104.4	94.7	102.5	99.0	104.3	5.3		
Bosnia-Herzegovina	BA	119.9	118.1	122.5	113.7	114.5	107.4	109.9	126.3	116.2	105.6	118.2	12.6		
Bulgaria	BG	109.9	105.0	115.7	114.4	112.0	103.8	105.1	116.5	103.5	94.6	106.5	11.8		
Croatia	HR	122.8	124.8	124.7	115.5	115.6	114.3	118.3	125.7	119.4	109.5	121.4	11.9		
Cyprus	CY	114.5	102.1	116.9	115.2	120.8	109.8	112.0	116.2	110.9	104.6	110.3	5.7		
Czech Republic	CZ	121.6	126.5	121.0	114.6	113.5	114.1	114.8	116.7	113.9	109.6	129.2	19.6		
Denmark	DK	95.0	104.9	95.2	102.6	95.5	91.4	96.9	95.7	96.7	96.6	89.1	-7.5		
Estonia	EE	94.2	105.1	94.1	96.3	90.8	97.2	94.8	93.3	97.6	92.8	89.3	-3.6		
Finland	FI	92.9	100.7	89.0	94.3	90.6	92.2	93.0	88.8	92.6	89.1	85.3	-3.8	+	-0.6
France	FR	113.8	122.0	109.0	107.3	107.3	111.6	112.8	104.7	113.2	105.6	110.0	4.4		
Germany	DE	113.8	125.8	113.3	113.5	108.8	112.8	111.5	107.1	110.2	107.9	118.5	10.7	+	-0.6
Greece	GR	125.4	115.8	126.5	131.1	122.8	119.4	126.5	133.1	123.5	112.2	121.4	9.2		
Hungary	HU	119.7	121.7	125.0	117.5	124.2	110.9	117.1	122.3	113.9	103.2	123.9	20.8		
Iceland	IS	85.2	93.3	81.1	90.8	81.4	78.3	83.6	81.1	87.8	69.0	70.1	1.1	+	-1.6
Ireland	IE	86.5	90.2	84.2	92.1	84.9	85.6	84.4	87.1	91.6	58.1	56.1	-1.9		
Italy	IT	131.1	135.1	129.5	123.2	125.8	124.3	127.7	130.5	126.1	116.2	130.9	14.7		
Latvia	LV	91.3	104.5	95.8	94.9	91.9	93.2	96.3	99.0	98.0	91.8	98.5	6.6		
Liechtenstein	LI	106.9	127.3	119.9	119.4	118.9	123.3	116.4	118.0	124.8	113.4	128.2	14.8		
Lithuania	LT	103.0	110.1	98.1	102.0	95.8	96.9	101.4	101.4	98.8	96.5	100.5	4.0		
Luxembourg	LU	119.9	130.0	111.7	112.1	108.6	111.4	110.4	99.0	109.5	105.5	114.1	8.6	+	-1.1
Macedonia, FYR of	MK	117.5	110.3	121.1	121.0	111.3	109.0	117.4	136.3	118.1	102.0	119.6	17.6		
Malta	MT	105.9	115.6	109.1	108.4	107.7	109.4	112.6	116.7	112.0	115.8	107.1	-8.6		
Monaco	MC		142.4	127.3	123.1	127.2	124.0	126.6	118.9	122.5	116.3	122.9	6.5	*	-1.2
Montenegro	ME	120.8	114.3	122.3	118.1	111.7	108.6	115.1	127.1	113.2	105.6	120.6	15.0		
Netherlands	NL	93.7	116.1	94.1	98.4	94.7	90.7	98.6	94.1	99.5	97.5	101.4	3.9		
Norway	NO	98.1	101.7	91.3	99.0	94.0	88.8	93.7	90.9	94.5	88.7	83.8	-4.9	*	-1.1
Poland	PL	113.6	120.4	112.9	109.7	107.8	106.6	109.5	112.0	109.4	107.2	117.9	10.7		
Portugal	PT	119.0	119.4	111.0	102.7	112.4	112.0	108.4	106.0	113.5	101.0	103.4	2.4	+	-1.6
Romania	RO	112.1	105.7	116.9	110.1	108.8	94.0	91.1	103.1	86.5	83.3	89.8	6.5	**	-2.9
San Marino	SM	130.8	120.8	130.4	119.0	118.1	116.1	117.9	121.2	110.7	118.4	129.3	10.9		
Serbia (incl.	RS	115.6	108.5	122.5	117.3	115.8	102.5	112.0	124.1	110.5	95.6	117.0	21.4		
Slovakia	SK	121.3	122.2	122.2	116.4	122.7	112.8	118.5	121.2	117.4	110.2	120.3	10.1		
Slovenia	SI	122.6	132.6	126.6	116.9	119.7	122.1	125.5	125.8	125.5	115.0	126.3	11.3		
Spain	ES	117.7	116.2	115.4	110.7	113.1	115.4	112.1	112.7	114.9	112.2	114.1	1.9		
Sweden	SE	97.6	104.5	93.5	97.6	94.2	91.2	96.1	94.0	94.8	95.4	89.7	-5.7		
Switzerland	CH	122.6	132.6	120.1	116.8	117.3	124.7	120.8	117.3	124.2	113.8	131.1	17.3		
United Kingdom	UK	87.2	98.0	83.3	93.1	86.8	81.6	87.8	84.0	89.7	84.1	83.2	-1.0		
Total		**112.1**	**118.2**	**110.7**	**109.8**	**108.1**	**106.8**	**108.9**	**108.5**	**108.9**	**102.9**	**110.4**	**7.5**	**+**	**-0.5**
EU-28		**111.8**	**118.3**	**110.2**	**109.5**	**107.8**	**106.8**	**108.7**	**107.7**	**108.6**	**103.0**	**110.0**	**7.0**	*****	**-0.7**

*) under the UN Security Council Resolution 1244/99

However, as stated earlier, the percentage population living in areas with concentrations above the target value threshold is not statistically a very robust parameter. The table showing the evolution of the percentage population in exceedance (resp. above the specific SOMO35 threshold) for individual countries is presented as a supplementary material at the web page of this paper, see http://acm.eionet.europa.eu/reports/ETCACM_TP_2017_7_AQMaps2015.

Table A4.7 Evolution and trend in 2005–2014 and difference between 2015 and 2014 for population-weighted concentration, ozone indicator SOMO35. Trend estimates are only given when a significant trend is observed (p >0.1).

Country		Population-weighted conc. [μg·m^{-3}·d]												Trend of pop.-weighted conc.	
		2005	2006	2007	2008	2009	2010	2011	2012	2013	2014	2015	Differ. '15 - '14	Signific.	Slope [μg·m^{-3}·d·year^{-1}]
Albania	AL	7 911	7 193	7 817	7 668	6 754	5 617	7 769	8 760	7 179	4 376	7 215	2 839		
Andorra	AD	7 520	6 587	7 121	6 319	7 186	7 282	7 891	8 058	7 303	6 692	6 050	-642		
Austria	AT	5 946	6 237	5 874	5 099	5 050	4 969	5 452	5 419	5 389	4 423	6 169	1 745		
Belgium	BE	2 775	4 017	2 235	2 520	2 599	2 401	2 714	2 050	2 520	2 297	2 792	495		
Bosnia-Herzegovina	BA	6 714	6 571	6 938	5 972	5 536	4 879	5 702	7 322	5 670	3 852	6 053	2 201		
Bulgaria	BG	5 311	4 896	6 064	5 797	5 686	4 377	5 215	5 960	4 082	2 519	4 182	1 663	+	-189
Croatia	HR	6 324	6 928	6 756	5 899	5 491	5 419	6 470	7 143	5 989	4 503	6 239	1 736		
Cyprus	CY	7 155	5 759	7 739	8 027	8 788	7 374	8 773	8 369	7 909	5 426	6 390	964		
Czech Republic	CZ	5 845	6 097	5 123	4 576	4 487	4 160	4 743	4 806	4 266	3 822	5 556	1 734		
Denmark	DK	2 519	3 578	2 440	3 080	2 440	2 245	2 752	2 662	2 749	2 611	2 200	-411		
Estonia	EE	2 437	3 594	2 061	2 363	1 762	2 646	2 516	2 310	2 545	1 991	1 775	-216		
Finland	FI	2 275	3 141	1 332	1 938	1 623	1 925	2 052	1 650	2 011	1 615	1 358	-257		
France	FR	4 591	4 972	3 686	3 563	4 025	4 139	4 439	3 635	4 098	3 786	4 245	460		
Germany	DE	3 940	4 860	3 648	3 822	3 507	3 652	3 668	3 357	3 506	3 287	4 300	1 014		
Greece	GR	8 321	6 657	8 330	8 969	8 330	7 483	9 182	9 378	8 532	5 926	6 908	982		
Hungary	HU	5 751	5 738	6 547	5 751	6 631	4 408	5 828	6 342	4 604	3 620	5 553	1 933		
Iceland	IS	1 329	2 265	1 168	2 224	833	775	1 094	1 242	1 473	218	258	40	+	-114
Ireland	IE	1 701	2 453	1 412	2 096	1 487	1 419	1 353	1 479	2 043	868	856	-12	*	-78
Italy	IT	7 634	8 205	7 506	6 386	6 986	6 302	7 532	7 328	6 576	5 569	6 856	1 287	+	-146
Latvia	LV	2 391	3 734	2 262	2 347	1 837	2 304	2 708	3 103	2 614	2 213	2 562	350		
Liechtenstein	LI	5 233	6 258	4 826	4 930	5 271	5 244	5 128	5 132	5 221	4 360	5 802	1 442		
Lithuania	LT	3 671	4 535	2 744	3 059	2 291	2 608	3 131	3 358	2 703	2 457	2 804	347		
Luxembourg	LU	4 769	5 090	3 424	3 557	3 500	3 505	3 527	2 561	3 167	2 872	3 461	589	*	-126
Macedonia, FYR of	MK	7 069	6 297	6 690	7 133	6 229	5 081	7 110	8 472	6 326	3 215	6 197	2 982		
Malta	MT	6 971	7 797	7 209	6 582	6 634	6 722	7 127	8 022	7 403	6 946	5 791	-1 154		
Monaco	MC		8 903	8 381	7 246	8 325	8 028	8 354	6 979	7 795	7 112	8 015	904	+	-99
Montenegro	ME	7 608	6 554	7 379	7 120	6 237	5 653	6 970	8 584	6 674	4 012	6 793	2 781		
Netherlands	NL	1 901	3 245	1 816	2 104	1 922	1 916	2 283	1 949	2 410	2 244	2 678	435		
Norway	NO	2 580	3 496	1 705	2 514	2 000	1 803	2 395	2 128	2 443	2 113	1 764	-349		
Poland	PL	4 784	5 416	4 179	3 951	3 747	3 278	4 065	4 045	3 792	3 425	4 528	1 102		
Portugal	PT	5 510	5 257	4 863	3 851	5 003	5 133	4 552	4 240	5 091	3 519	3 989	470	*	-141
Romania	RO	5 238	4 798	5 882	5 039	5 044	3 033	3 276	3 967	2 221	1 842	2 952	1 110	**	-366
San Marino	SM	7 540	6 321	7 296	5 863	5 860	5 331	6 220	6 048	5 067	5 949	7 176	1 227		
Serbia (incl.	RS	5 947	5 239	6 768	6 378	6 118	4 001	5 793	6 844	4 738	2 762	5 449	2 687		
Slovakia	SK	6 141	6 261	6 098	5 455	6 348	4 748	6 051	6 103	5 116	4 344	5 456	1 111	+	-101
Slovenia	SI	6 242	7 480	6 671	5 761	5 775	5 998	7 062	7 092	6 540	5 086	6 649	1 563		
Spain	ES	6 139	5 813	5 992	5 110	5 983	6 088	5 858	5 850	5 895	5 436	5 820	385		
Sweden	SE	2 682	3 635	1 795	2 387	2 100	2 025	2 628	2 233	2 317	2 318	2 084	-233		
Switzerland	CH	5 740	6 321	5 114	4 619	5 139	5 127	5 435	4 990	4 919	4 417	6 174	1 757		
United Kingdom	UK	1 551	2 676	1 174	2 044	1 433	1 072	1 471	1 183	1 606	1 337	1 287	-50		
Total		**4 706**	**5 167**	**4 411**	**4 275**	**4 275**	**3 917**	**4 414**	**4 279**	**4 089**	**3 500**	**4 312**	**813**	**+**	**-95**
EU28		**4 613**	**5 128**	**4 319**	**4 178**	**4 208**	**3 888**	**4 339**	**4 154**	**4 040**	**3 506**	**4 249**	**743**	*****	**-96**

*) under the UN Security Council Resolution 1244/99

Vegetation exposure

Table A4.8 provides the evolution of the annual vegetation exposure for AOT40 for vegetation in the period 2005–2015, the inter-annual difference between 2014 and 2015, and the results of the trend analysis. In 2015 the overall agricultural-weighted concentration for whole Europe was 14 223 $\mu g.m^{-3}\cdot h$, which is within the average range of most of the eleven year period.

Table A4.8 Evolution and trend in 2005–2014 and difference between 2015 and 2014 for agricultural-weighted concentration, ozone indicator AOT40v. Trend estimates are only given when a significant trend is observed (p >0.1).

Country		Agricultural-weighted conc. [$\mu g\cdot m^{-3}\cdot h$]												Trend of agric.-weighted conc.	
		2005	2006	2007	2008	2009	2010	2011	2012	2013	2014	2015	Differ. '15 - '14	Signif.	Slope [$\mu g.m^{-3}\cdot h\cdot year^{-1}$]
Albania	AL	28 831	39 959	40 051	20 388	41 766	16 335	22 561	28 949	36 337	18 063	25 781	7 718		
Austria	AT	21 123	27 496	21 558	18 494	14 296	18 477	17 201	18 631	16 949	17 251	21 542	4 290		
Belgium	BE	12 764	24 201	6 538	11 609	7 404	12 324	8 158	8 005	9 110	9 144	10 122	977		
Bosnia-Herzegovina	BA	21 866	19 086	28 503	19 769	24 333	17 931	17 968	22 534	17 068	15 738	17 842	2 104	*	-600
Bulgaria	BG	21 523	18 607	22 707	15 221	20 752	11 471	14 728	17 335	11 731	12 552	13 450	898	*	-977
Croatia	HR	20 016	24 168	26 847	19 415	20 809	18 987	19 391	23 193	17 520	15 445	19 052	3 607	*	-508
Cyprus	CY	31 742	22 820	28 080	12 000	29 579	21 092	22 690	23 482	26 761	21 667	26 572	4 905		
Czech Republic	CZ	19 006	27 909	19 825	19 571	11 341	16 047	15 508	16 979	13 173	15 857	18 462	2 605		
Denmark	DK	7 411	16 411	6 887	13 615	6 393	7 579	7 146	7 355	6 043	8 357	3 169	-5 189		
Estonia	EE	5 198	12 873	4 631	7 117	3 317	4 312	6 068	5 275	5 226	3 959	1 771	-2 188		
Finland	FI	4 267	11 373	3 447	6 399	2 993	4 138	5 151	3 275	4 039	3 486	680	-2 807	+	-386
France	FR	16 973	22 759	7 614	12 202	9 448	13 855	12 510	9 112	11 712	10 630	12 715	2 085		
Germany	DE	14 946	25 938	12 510	18 715	8 888	15 831	12 898	11 182	10 878	13 745	13 817	72		
Greece	GR	27 613	25 433	29 271	19 689	27 723	17 700	19 869	26 543	23 529	19 991	24 499	4 508		
Hungary	HU	19 070	22 325	25 664	19 652	20 434	14 493	16 245	20 710	15 192	14 890	14 962	73	+	-670
Iceland	IS	367	4 748	177	5 310	3 332	237	125	160	30	9	1	-8	**	-53
Ireland	IE	2 619	5 454	1 978	5 212	2 222	1 843	1 109	2 211	2 015	718	927	209	*	-216
Italy	IT	31 334	35 407	25 987	22 407	27 302	22 171	22 928	27 365	24 241	22 028	30 626	8 598		
Latvia	LV	6 304	13 023	5 434	6 446	3 924	4 691	6 765	7 259	5 310	4 958	2 498	-2 460		
Liechtenstein	LI	16 781	27 422	12 479	17 409	12 394	17 226	17 126	15 241	14 632	13 324	20 189	6 865		
Lithuania	LT	7 297	12 390	6 800	7 582	4 950	5 626	7 680	8 681	5 205	6 340	3 594	-2 746		
Luxembourg	LU	18 878	28 422	9 749	15 471	11 244	17 259	12 858	9 079	12 423	13 993	13 414	-579		
Macedonia, FYR of	MK	26 298	38 217	37 041	20 139	41 337	14 858	18 713	27 086	34 364	17 385	21 857	4 471		
Malta	MT	24 698	24 162	20 604	24 373	24 935	18 815	26 442	27 327	30 088	28 986	28 982	-4	*	674
Monaco	MC		35 762	20 979	17 071	26 212	32 986	27 282	21 969	26 572	21 361	23 960	2 600		
Montenegro	ME	27 800	30 608	35 559	21 588	33 770	16 514	19 684	24 728	27 676	17 933	22 231	4 299		
Netherlands	NL	7 966	18 087	5 201	8 781	3 826	8 350	6 764	6 363	6 108	8 572	7 512	-1 061		
Norway	NO	4 084	12 296	3 553	7 841	2 586	2 913	4 186	3 596	2 595	4 103	824	-3 279		
Poland	PL	13 558	24 487	14 751	15 869	9 341	10 298	13 374	13 283	10 269	11 921	11 400	-521	+	-484
Portugal	PT	22 127	20 634	8 585	13 191	11 083	16 715	13 007	10 919	15 847	9 400	13 921	4 520		
Romania	RO	17 654	14 435	23 657	15 372	15 373	9 472	12 085	15 782	7 595	10 419	11 224	805	+	-761
San Marino	SM	32 857	39 916	29 665	21 844	26 414	23 088	24 630	29 244	21 972	25 774	32 517	6 744		
Serbia (incl.	RS	22 588	22 768	30 064	18 958	28 406	14 677	17 081	22 737	17 931	13 591	17 687	4 096	+	-894
Slovakia	SK	19 408	24 674	23 750	19 471	18 344	14 609	15 615	19 746	15 970	15 576	14 374	-1 202	*	-798
Slovenia	SI	20 368	32 119	26 452	19 608	20 176	23 787	22 145	25 103	22 809	18 445	24 054	5 609		
Spain	ES	27 207	25 913	14 800	18 045	16 172	19 040	17 204	19 213	20 399	17 882	23 126	5 244		
Sweden	SE	6 356	15 201	5 951	9 398	3 992	6 197	7 021	5 515	5 626	5 640	2 213	-3 427	+	-414
Switzerland	CH	23 807	33 834	15 170	19 476	15 354	22 349	17 432	15 522	18 032	16 109	23 953	7 844		
United Kingdom	UK	4 437	12 629	1 929	7 808	4 535	3 869	3 066	3 570	3 304	3 385	2 485	-900	+	-266
Total		**17 481**	**22 344**	**14 597**	**15 214**	**13 157**	**13 310**	**13 255**	**14 041**	**12 838**	**12 427**	**14 223**	**1 796**	*****	**-335**
EU28		**17 313**	**22 245**	**13 981**	**15 081**	**12 512**	**13 259**	**13 116**	**13 719**	**12 536**	**12 378**	**14 084**	**1 706**	**+**	**-290**

*) under the UN Security Council Resolution 1244/99

The overall picture of the agricultural-weighted concentration for the totals of 40 European countries shows a slightly downward trend for the years 2005 – 2015. This trend is statistically significant, the slope is about -335, which means an average decrease of about 335 $\mu g \cdot m^{-3} \cdot h$ per year. The highest increase of agricultural-weighted concentration per country compared to 2014 is seen in Italy, Switzerland, and Albania. The steepest decrease was detected in Denmark, Sweden, and Norway.

Table A4.9 provides the similar data as presented in Table A4.8, but for AOT40 for forests.

Table A4.9 Evolution and trend in 2005–2014 and difference between 2015 and 2014 for forest-weighted concentration, ozone indicator AOT40f. Trend estimates are only given when a significant trend is observed (p >0.1).

Country		Forest-weighted conc. [$\mu g \cdot m^{-3} \cdot h$]												Trend of forest-weighted conc.	
		2005	2006	2007	2008	2009	2010	2011	2012	2013	2014	2015	Differ. '15 - '14	Signif.	Slope [$\mu g \cdot m^{-3} \cdot h \cdot year^{-1}$]
Albania	AL	60 607	61 982	65 662	43 220	87 193	33 340	49 630	55 361	85 847	29 463	47 249	17 787		
Austria	AT	35 595	41 055	38 212	30 098	31 444	31 533	32 660	33 264	34 596	25 863	42 247	16 384		
Belgium	BE	21 612	31 473	16 478	16 062	17 678	18 564	19 011	14 020	17 632	13 912	20 597	6 685		
Bosnia-Herzegovina	BA	42 195	36 956	50 356	36 609	51 704	32 849	37 877	45 680	40 787	24 565	36 818	12 253		
Bulgaria	BG	43 105	40 043	48 421	32 861	47 861	29 283	34 407	39 810	32 232	23 880	32 992	9 112	+	-1450
Croatia	HR	35 742	42 453	46 583	34 999	41 730	32 875	39 051	44 435	39 110	23 758	38 425	14 667		
Cyprus	CY	63 155	43 595	59 808	31 069	65 009	44 352	51 896	55 212	59 206	39 387	49 998	10 612		
Czech Republic	CZ	32 597	39 537	33 821	29 839	26 662	25 399	27 988	29 594	26 850	23 293	38 374	15 081		
Denmark	DK	13 463	22 648	12 207	17 567	13 125	10 888	12 510	12 148	12 862	13 942	7 837	-6 105		
Estonia	EE	10 502	20 025	6 905	11 790	7 610	7 424	9 721	9 417	10 663	9 166	3 680	-5 486		
Finland	FI	8 173	16 269	3 669	8 501	5 802	4 119	5 828	4 315	6 541	5 869	1 037	-4 831		
France	FR	33 155	36 827	24 669	22 423	25 406	28 948	28 480	23 250	24 851	19 582	28 443	8 862		
Germany	DE	27 043	34 988	24 881	26 204	22 792	23 842	24 645	21 298	21 595	20 573	30 044	9 471	+	-640
Greece	GR	53 769	47 853	52 992	40 147	56 584	35 623	43 629	46 622	48 333	32 627	43 974	11 347		
Hungary	HU	30 852	36 583	43 380	33 923	41 478	26 384	31 155	39 635	33 702	23 031	32 198	9 167		
Iceland	IS	1 250	7 384	585	9 832	5 932	839	1 426	1 162	1 001	415	2	-413	*	-337
Ireland	IE	5 064	9 940	4 002	8 279	4 304	5 084	4 367	4 820	5 226	2 367	3 227	860		
Italy	IT	53 285	57 440	51 128	40 702	45 537	41 607	47 253	47 981	43 513	34 575	52 978	18 403		
Latvia	LV	12 820	19 956	7 491	11 195	8 888	9 267	11 226	14 436	10 190	10 859	5 520	-5 339		
Liechtenstein	LI	31 218	43 271	34 987	31 307	30 688	32 476	34 267	32 540	32 446	24 101	42 159	18 059		
Lithuania	LT	16 029	20 167	10 807	13 171	11 167	11 995	13 367	16 938	8 727	13 128	9 138	-3 990		
Luxembourg	LU	25 981	33 147	20 525	18 920	23 181	22 183	22 834	15 562	20 543	17 723	23 110	5 386		
Macedonia, FYR of	MK	58 866	63 450	70 095	42 569	86 656	33 254	43 696	52 315	85 248	29 275	44 629	15 354		
Malta	MT	66 996	46 492	47 217	42 969	53 717	42 815	54 429	51 481	51 800	47 687	50 585	2 898		
Monaco	MC	0	47 644	36 743	29 096	42 620	47 582	44 467	33 083	41 118	28 905	34 712	5 807		
Montenegro	ME	56 716	51 440	55 227	43 867	72 376	33 764	42 272	51 198	64 979	28 071	44 266	16 195		
Netherlands	NL	11 607	22 894	9 580	10 649	9 261	10 928	13 333	10 975	12 036	10 942	13 966	3 024		
Norway	NO	8 666	19 301	7 897	11 541	7 391	5 731	7 758	6 145	8 027	8 719	3 880	-4 839		
Poland	PL	25 243	34 212	24 306	24 709	22 048	18 833	23 343	23 275	20 748	18 931	24 684	5 753	+	-562
Portugal	PT	40 217	37 193	24 072	23 473	27 949	34 640	26 004	21 550	30 994	15 245	24 378	9 133	+	-1261
Romania	RO	33 840	30 684	43 702	30 270	36 887	23 858	26 452	28 586	14 966	19 749	26 336	6 587	*	-1566
San Marino	SM	49 031	54 866	49 275	37 902	43 800	37 732	51 272	46 136	37 606	34 782	50 773	15 991		
Serbia (incl.	RS	46 891	43 047	52 348	35 582	64 808	28 951	36 589	46 627	50 338	22 935	39 388	16 453		
Slovakia	SK	33 953	40 634	41 135	34 174	38 330	26 906	32 984	36 307	34 092	23 784	31 278	7 494	+	-965
Slovenia	SI	33 853	47 136	46 330	34 709	40 996	38 197	44 032	48 996	47 292	27 386	43 600	16 214		
Spain	ES	45 027	43 398	32 909	31 045	33 479	34 380	33 390	34 679	34 785	27 458	34 409	6 950		
Sweden	SE	9 918	18 646	6 799	10 833	7 608	5 860	8 124	5 762	9 270	8 592	2 833	-5 760		
Switzerland	CH	42 076	48 933	40 157	30 734	34 665	36 640	34 872	31 854	35 076	26 016	40 890	14 874		
United Kingdom	UK	6 533	14 595	3 961	11 214	6 985	5 513	6 538	5 958	6 244	4 489	3 804	-685	+	-499
Total		**25 900**	**31 154**	**23 744**	**21 951**	**23 532**	**19 625**	**21 892**	**21 580**	**21 753**	**17 124**	**21 150**	**4 027**	**	**-617**
EU28		**25 849**	**31 110**	**23 130**	**21 806**	**22 407**	**19 902**	**21 915**	**21 252**	**20 855**	**17 255**	**21 272**	**4 018**	**	**-656**

*) under the UN Security Council Resolution 1244/99

Considering Europe as a whole, Table A4.9 shows that the overall forest-weighted ozone concentration for AOT40 for forests in 2015 was 21 150 μg·m^{-3}·h. This value appears to be in the midrange of values for the eleven years period.

The overall picture of the forest-weighted concentration for the totals of 40 European countries shows a slightly downward trend for the years 2005 – 2015. This trend is statistically significant, the slope is about -617, which means an average decrease of about 617 μg·m^{-3}·h per year. The highest increase of forest-weighted concentration per country compared to 2014 is seen in Italy, Albania, Liechtenstein, Serbia, and Austria. The steepest decrease was detected in Denmark, Sweden and Estonia.

The evolution of the agricultural land (*crops*) exposed to accumulated ozone concentrations (AOT40 for vegetation) exceeding the target value (TV) threshold and the long-term objective (LTO) for Europe as a whole in the eleven years period 2005 – 2015 is presented in Table 6.4. The same table also shows the evolution of the *forest* land exposed to accumulated ozone concentrations (AOT40 for forests) exceeding the level of 20 000 μg·m^{-3}·h (earlier used Reporting Value, RV) and Critical Level (CL) for Europe as a whole. The results are discussed in Chapter 6. The table showing the evolution of the percentage land in exceedance for individual countries, for both AOT40 indicators, is presented as supplementary material at http://acm.eionet.europa.eu/reports/ETCACM_TP_2017_7_AQMaps2015.

Uncertainties

Table A4.10 shows the evolution of the absolute and relative mean interpolation uncertainties and also R^2 from cross-validation scatterplots for the maps of all four ozone indicators, in the period 2005 – 2015.

Table A4.10 Absolute and relative mean uncertainty and R^2 from cross-validation scatterplot for the total European areas, ozone indicators 93.2 percentile of maximum daily 8-hour means, SOMO35, AOT40 for vegetation and AOT40 for forests, years 2005 – 2015

Ozone			2005	2006	2007	2008	2009	2010	2011	2012	2013	2014	2015
26th highest daily max. 8-hr mean (2005 - 2011) / 93.2 percentile of daily max. 8-hr means (2012 - 2015)													
rural areas	abs. mean uncertainty	RMSE [μg.m^{-3}]	12.3	11.2	8.8	8.7	8.2	8.9	8.4	8.5	8.5	7.4	9.0
	rel. mean uncertainty	RRMSE [%]	*10.3*	*8.9*	*7.5*	*7.6*	*7.2*	*7.7*	*7.2*	*7.4*	*7.3*	*6.7*	*7.5*
	coeff. of determination	R^2	*0.51*	*0.49*	*0.71*	*0.56*	*0.69*	*0.68*	*0.67*	*0.71*	*0.72*	*0.65*	*0.73*
urban areas	abs. mean uncertainty	RMSE [μg.m^{-3}]	10.0	10.2	8.9	8.8	9.3	9.2	9.1	9.1	9.1	7.9	8.6
	rel. mean uncertainty	RRMSE [%]	*8.9*	*8.4*	*7.9*	*7.9*	*8.4*	*8.2*	*8.1*	*8.3*	*8.1*	*7.4*	*7.4*
	coeff. of determination	R^2	*0.50*	*0.53*	*0.66*	*0.61*	*0.64*	*0.71*	*0.66*	*0.68*	*0.70*	*0.64*	*0.82*
SOMO35													
rural areas	abs. mean uncertainty	RMSE [μg.m^{-3}.d]	2 173	2 077	1 801	1 609	1 635	1 608	1 747	1 633	1 596	1 414	1 578
	rel. mean uncertainty	RRMSE [%]	*35.5*	*31.6*	*33.3*	*30.7*	*29.7*	*29.6*	*29.6*	*29.2*	*29.2*	*29.2*	*27.1*
	coeff. of determination	R^2	*0.55*	*0.47*	*0.63*	*0.63*	*0.63*	*0.62*	*0.63*	*0.68*	*0.61*	*0.61*	*0.68*
urban areas	abs. mean uncertainty	RMSE [μg.m^{-3}.d]	1 459	1 472	1 260	1 293	1 475	1 278	1 374	1 362	1 194	1 133	1 221
	rel. mean uncertainty	RRMSE [%]	*32.0*	*29.2*	*29.5*	*31.3*	*33.1*	*29.6*	*29.7*	*31.7*	*28.1*	*29.3*	*25.6*
	coeff. of determination	R^2	*0.58*	*0.49*	*0.67*	*0.54*	*0.62*	*0.65*	*0.66*	*0.67*	*0.66*	*0.62*	*0.72*
AOT40 for vegetation													
rural areas	abs. mean uncertainty	RMSE [μg.m^{-3}.h]	7 677	7 674	5 876	5 283	5 138	5 198	5 263	5 062	5 179	4 518	5 256
	rel. mean uncertainty	RRMSE [%]	*40.7*	*29.6*	*39.6*	*31.3*	*37.7*	*30.8*	*34.9*	*32.9*	*34.6*	*30.5*	*28.7*
	coeff. of determination	R^2	*0.58*	*0.53*	*0.63*	*0.53*	*0.69*	*0.67*	*0.62*	*0.70*	*0.68*	*0.67*	*0.78*
AOT40 for forests													
rural areas	abs. mean uncertainty	RMSE [μg.m^{-3}.h]	12 474	11 990	10 190	8 750	9 304	8 384	9 341	8 847	9 257	7 354	9 141
	rel. mean uncertainty	RRMSE [%]	*41.5*	*33.6*	*37.1*	*34.0*	*33.9*	*31.4*	*32.7*	*32.8*	*34.7*	*33.8*	*29.1*
	coeff. of determination	R^2	*0.55*	*0.49*	*0.67*	*0.56*	*0.68*	*0.69*	*0.67*	*0.70*	*0.68*	*0.62*	*0.75*

The absolute mean interpolation uncertainty results of 2015 fit within the fluctuation of the previous years. The results are influenced by high levels of ozone concentration values in this year. The relative uncertainties and R^2 from cross-validation scatterplots of 2015 maps show mostly the best levels for all the eleven years period. The main reason probably is in the finer resolution of the EMEP model used.

A4.4 NO_2 and NO_x

Air concentrations

Map A4.4 presents the inter-annual difference between 2015 and 2014 for NO_2 and NO_x annual averages. Red areas show an increase of concentration in 2015, while blue areas show a decrease.

The highest increases for NO_2 are seen in Greece, Ireland and in some large cities like Madrid, Rome, Napoli, Milan or Paris. The steepest decreases are shown in southern England, in Benelux and in broader surroundings of large cities. However, it should be mentioned that both increases and decreases near large cities are strongly influenced by the shift of the EMEP model resolution from cc. 50x50 km to cc. 10x10 km. In 2015 map, more realistic patterns near large cities can be seen.

In the case of NO_x, highest increases are observed in north-eastern Spain, in north-eastern France, in southern Italy, and near large cities. The steepest decreases are seen in Benelux, in rural areas of Po valley and in broader surroundings of large cities. Again, the results are influenced by the model resolution shift.

Map A4.4 Difference concentrations between 2014 and 2015 for NO_2 annual average (left) and NO_x annual average (right)

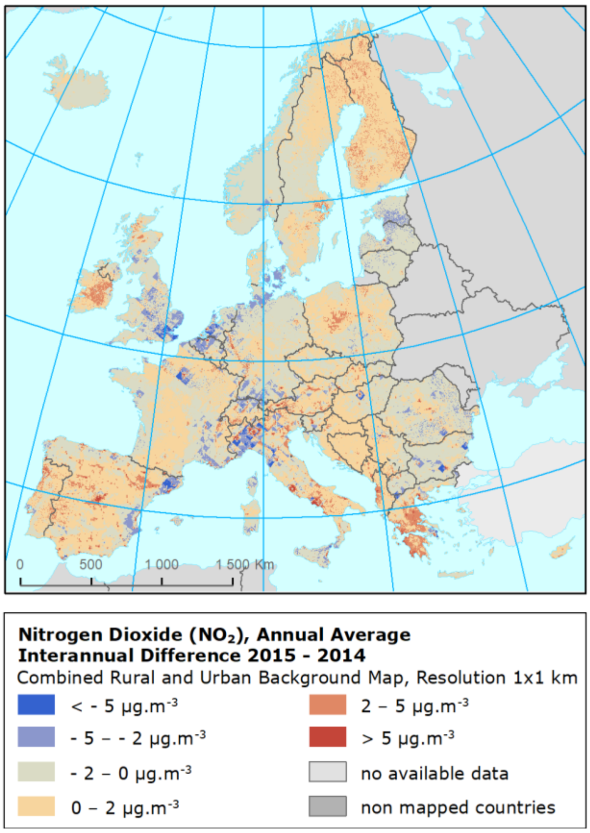

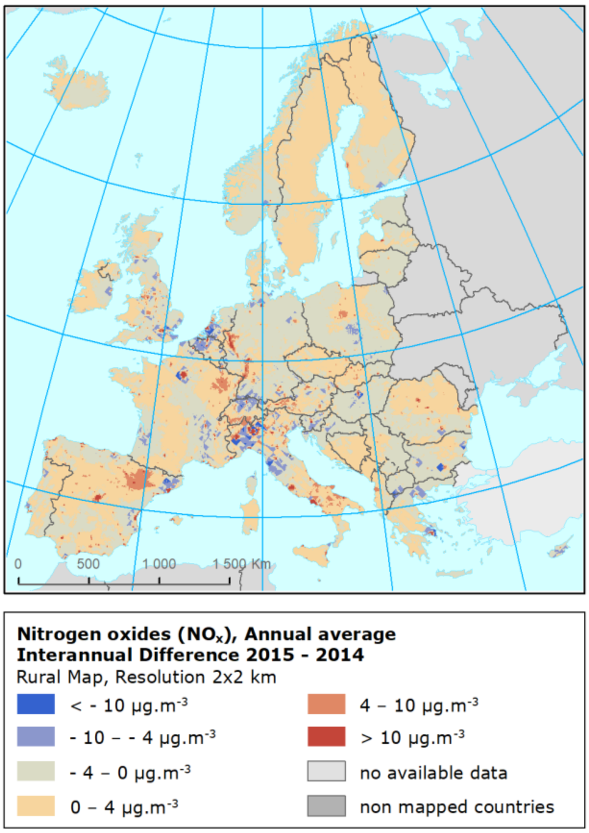

Population exposure

Table A4.11 provides the evolution of the annual population exposure for NO_2 annual average in the period 2013–2015 and the inter-annual difference between 2014 and 2015. In 2015 the overall population-weighted concentration for NO_2 annual average for whole of Europe was 18.8 µg·m^{-3}, i.e. slightly more than in 2014 and slightly less than in 2013. The highest increase of population-weighted concentration per country compared to 2014 is seen in Andorra, Monaco, Albania, and Greece. The steepest decrease was detected in the United Kingdom, Romania, and the Netherlands.

Table A4.11 Evolution in 2013–2015 and difference between 2015 and 2014 for population-weighted concentration, NO_2 annual average.

Country		Population-weighted conc. [µg.m^{-3}]				Country		Population-weighted conc. [µg.m^{-3}]			
		2013	2014	2015	diff. '15 - '14			2013	2014	2015	diff. '15 - '14
Albania	AL	17.5	14.8	18.1	3.3	Lithuania	LT	12.4	12.5	12.2	-0.3
Andorra	AD	14.0	15.0	20.5	5.5	Luxembourg	LU	23.0	19.9	19.9	0.0
Austria	AT	20.2	19.2	19.8	0.6	Macedonia, FYR of	MK	20.3	16.0	18.1	2.2
Belgium	BE	24.0	21.9	20.9	-1.0	Malta	MT	15.2	16.0	16.5	0.5
Bosnia-Herzegovina	BA	14.4	15.1	16.2	1.1	Monaco	MC	30	24.5	29.7	5.2
Bulgaria	BG	17.0	16.5	16.1	-0.4	Montenegro	ME	16.4	13.9	16.4	2.5
Croatia	HR	15.8	15.7	17.3	1.6	Netherlands	NL	22.0	21.9	20.5	-1.4
Cyprus	CY	10.5	12.8	14.1	1.3	Norway	NO	14.4	12.4	12.3	-0.1
Czech Republic	CZ	17.2	16.8	16.6	-0.2	Poland	PL	16.0	15.1	15.6	0.5
Denmark	DK	12.6	11.0	10.5	-0.5	Portugal	PT	15.7	13.7	15.7	2.0
Estonia	EE	10.0	9.0	8.2	-0.9	Romania	RO	18.6	16.5	14.9	-1.6
Finland	FI	9.3	8.3	8.8	0.5	San Marino	SM	12.0	14.7	16.2	1.4
France	FR	19.0	17.7	17.9	0.2	Serbia (incl. Kosovo*)	RS	18.8	18.5	17.9	-0.6
Germany	DE	20.7	20.2	20.0	-0.3	Slovakia	SK	16.4	15.2	16.9	1.7
Greece	GR	16.0	14.9	18.1	3.1	Slovenia	SI	16.8	14.9	16.7	1.7
Hungary	HU	17.0	17.1	18.0	0.8	Spain	ES	19.1	19.9	21.2	1.3
Iceland	IS	13.4	10.9	11.9	1.0	Sweden	SE	10.9	9.9	10.8	0.9
Ireland	IE	11.8	6.1	7.6	1.4	Switzerland	CH	21.6	20.9	21.4	0.5
Italy	IT	23.8	22.5	24.9	2.4	United Kingdom	UK	22.5	22.2	19.7	-2.5
Latvia	LV	13.8	12.3	12.1	-0.2	**Total**		**19.4**	**18.6**	**18.8**	**0.2**
Liechtenstein	LI	20.6	18.5	20.5	2.0	**EU-28**		**19.5**	**18.7**	**18.9**	**0.2**

*) under the UN Security Council Resolution 1244/99

Uncertainties

Table A4.12 presents the uncertainty results for NO_2 maps for the years 2013 – 2015 and for and NO_x maps for 2014 – 2015. For NO_2, all indicators show for 2015 similar results as in 2013 and 2014. For NO_x, all indicators show for 2015 better results compared to 2014.

Table A4.12 Absolute and relative mean uncertainty and R^2 from cross-validation scatterplot for the total European rural and urban areas, NO_2 and NO_x annual average, years 2013 – 2015

NO2 / NOx			2013	2014	2015
NO2 Annual average					
rural areas	abs. mean uncertainty	RMSE [μg.m^{-3}]	2.8	3.3	2.9
	rel. mean uncertainty	RRMSE [%]	*29.2*	*36.6*	*31.9*
	coeff. of determination	R^2	*0.78*	*0.68*	*0.74*
urban background areas	abs. mean uncertainty	RMSE [μg.m^{-3}]	4.6	4.8	4.6
	rel. mean uncertainty	RRMSE [%]	*21.3*	*23.6*	*22.2*
	coeff. of determination	R^2	*0.65*	*0.61*	*0.67*
urban traffic areas	abs. mean uncertainty	RMSE [μg.m^{-3}]	9.2	8.9	9.2
	rel. mean uncertainty	RRMSE [%]	*24.3*	*25.5*	*25.3*
	coeff. of determination	R^2	*0.51*	*0.53*	*0.54*
NOx Annual average					
rural areas	abs. mean uncertainty	RMSE [μg.m^{-3}]	not mapped	5.7	4.9
	rel. mean uncertainty	RRMSE [%]		*47.0*	*42.5*
	coeff. of determination	R^2		*0.52*	*0.65*

Annex 5 Concentration maps including station points

Throughout the report, the concentration maps presented do not include station points, contrary to the previous reports up to Horálek et al. (2016b). The reason is to better visualise the health related indicators with their distinct concentration levels at the more fragmented and smaller urban areas in predominant rural areas. The allocation of these smaller ‘patches’ is better discriminated now that the map is presented in a 1x1 km grid resolution, as the smoothing effect of the formerly used 10x10 km grid resolution does not play a role any longer.

As presented in Annex 3, the kriging interpolation methodology somewhat smooths the concentration field. Therefore, it is valuable to present in this Annex 5 the indicator maps *including* the concentration values resulting from the measurement data at the station points. These points provide important additional visual information on the smoothing effect caused by the interpolation. For instance, maps A5.1 and A5.2 present PM_{10} indicators annual average and 90.4 percentile of daily means and include the stations points used in the interpolation. They correspond to Maps 2.1 and 2.2 of the main report, but without station points. Table A5.1 provides an overview on the maps of the main report and the corresponding maps including stations point values as presented in this annex.

Both the rural and the urban/suburban background stations are included in the maps of the health related indicators, while the rural stations only are shown in the maps of vegetation related indicators. For $PM_{2.5}$ and NO_x, only the stations with relevant measured data (i.e. not the pseudo stations) are presented.

Table A5.1 Overview of maps presented in this Annex 5 and their relation with the maps presented in the main report

Air pollutant	Indicator	Map including station points	Map without station points
PM_{10}	Annual average	A5.1	2.1
	90.4 percentile of daily means	A5.2	2.2
$PM_{2.5}$	Annual average	A5.3	3.1
Ozone	93.2 percentile of maximum daily 8-hour means	A5.4	4.1
	SOMO35	A5.5	4.2
	AOT40 for vegetation ([a])	A5.6	4.3
	AOT40 for forests ([a])	A5.7	4.4
NO_2	Annual average	A5.8	5.1
NO_x	Annual average ([a])	A5.9	5.2

([a]) Rural map, applicable for rural areas only.

Map A5.1 **Concentration map of PM_{10} annual average including station points, 2015**

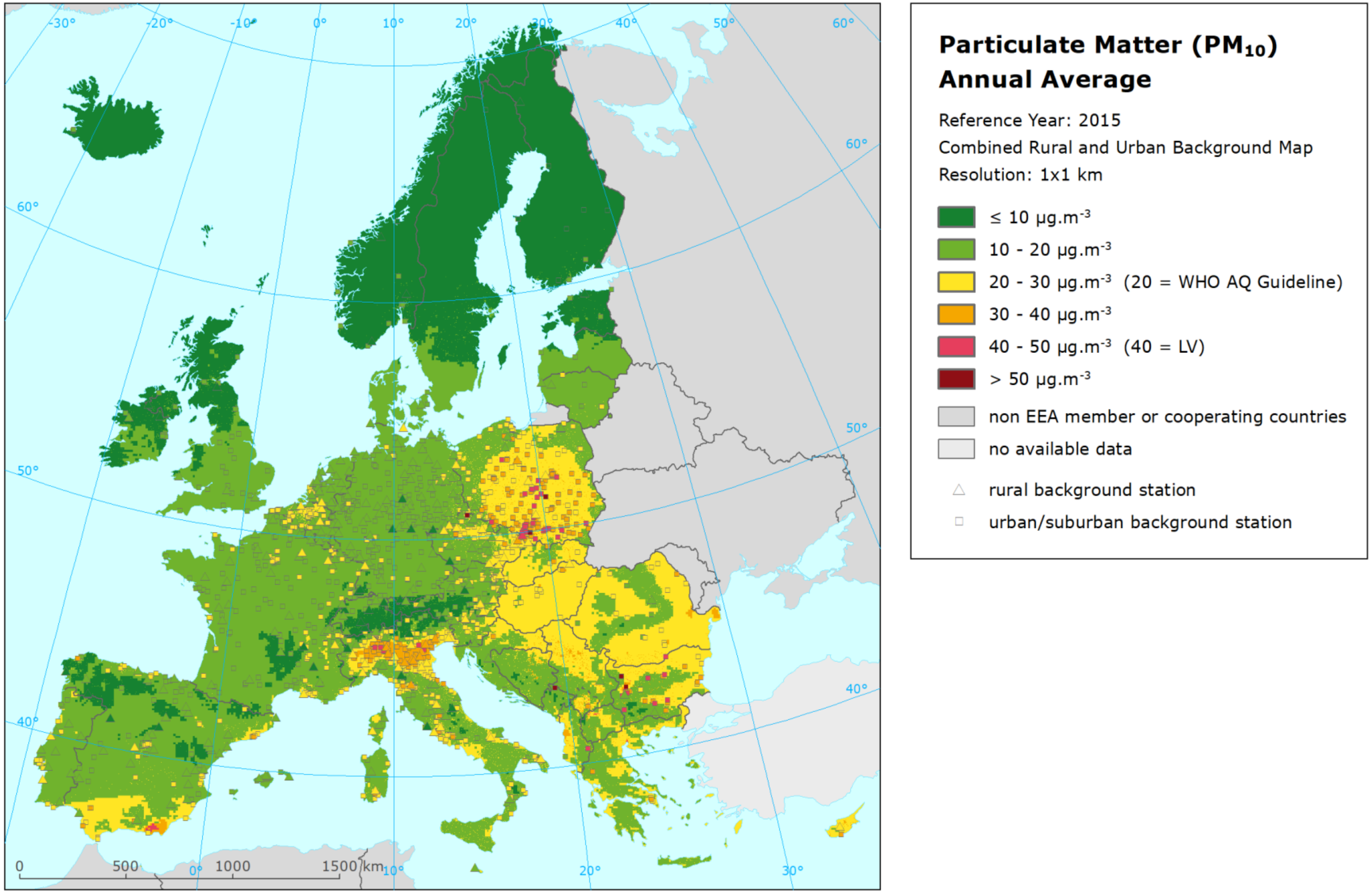

Map A5.2 Concentration map of PM_{10} indicator 90.4 percentile of daily means including station points, 2015

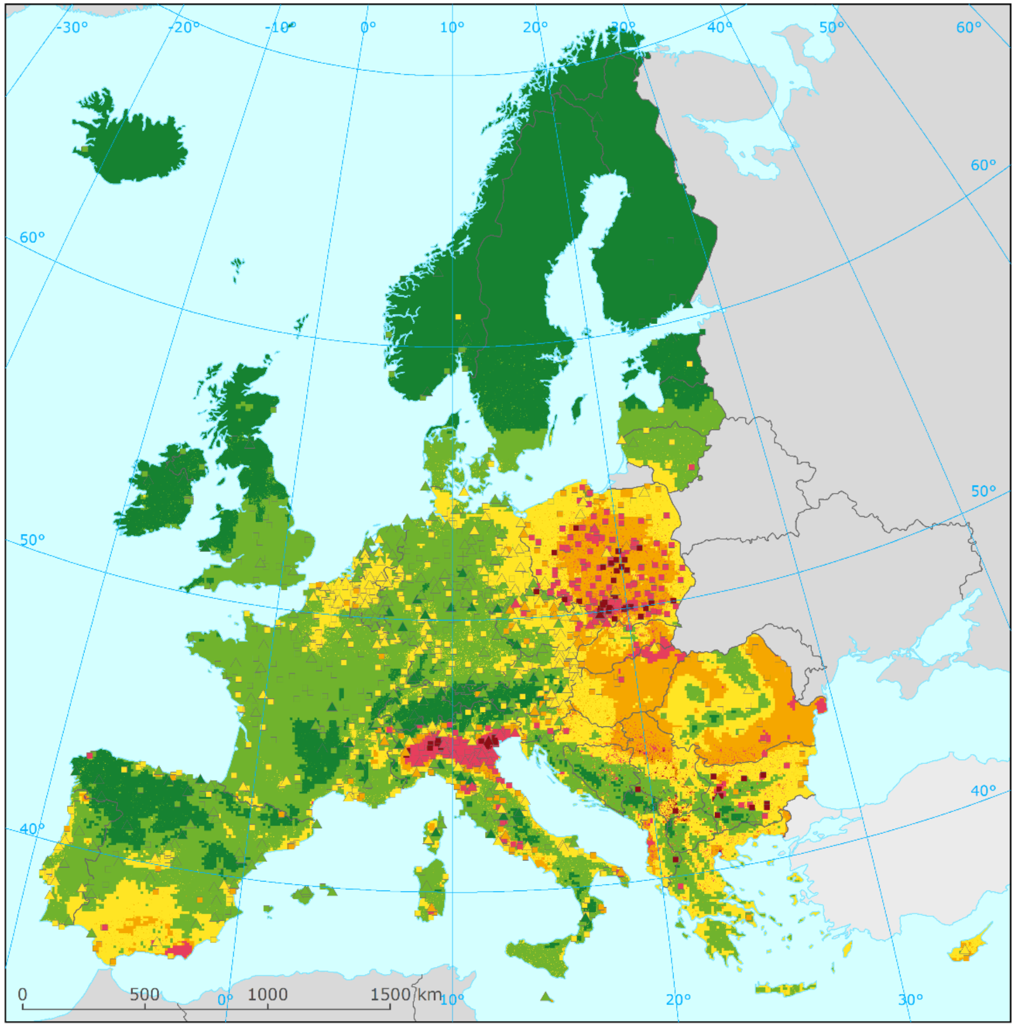

Particulate Matter (PM_{10})
90.4 Percentile of Daily Means

Reference Year: 2015
Combined Rural and Urban Background Map
Resolution: 1x1 km

- ≤ 20 $\mu g.m^{-3}$
- 20 - 30 $\mu g.m^{-3}$
- 30 - 40 $\mu g.m^{-3}$
- 40 - 50 $\mu g.m^{-3}$
- 50 - 75 $\mu g.m^{-3}$ (50 = LV)
- > 75 $\mu g.m^{-3}$
- non EEA member or cooperating countries
- no available data
- rural background station
- urban/suburban background station

Map A5.3 Concentration map of $PM_{2.5}$ annual average including station points, 2015

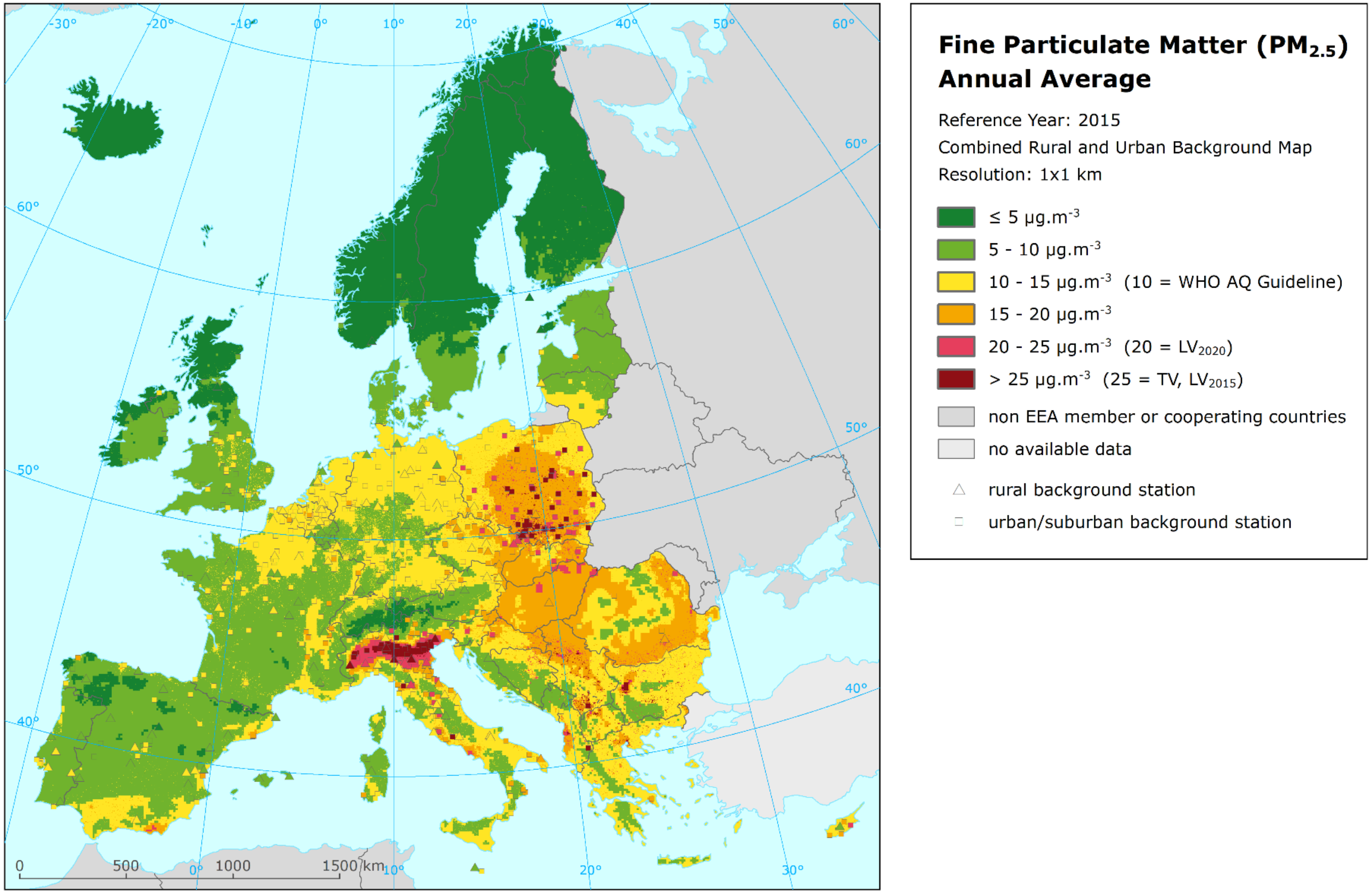

Map A5.4 Concentration map of ozone indicator 93.2 percentile of maximum daily 8-hour means including station points, 2015

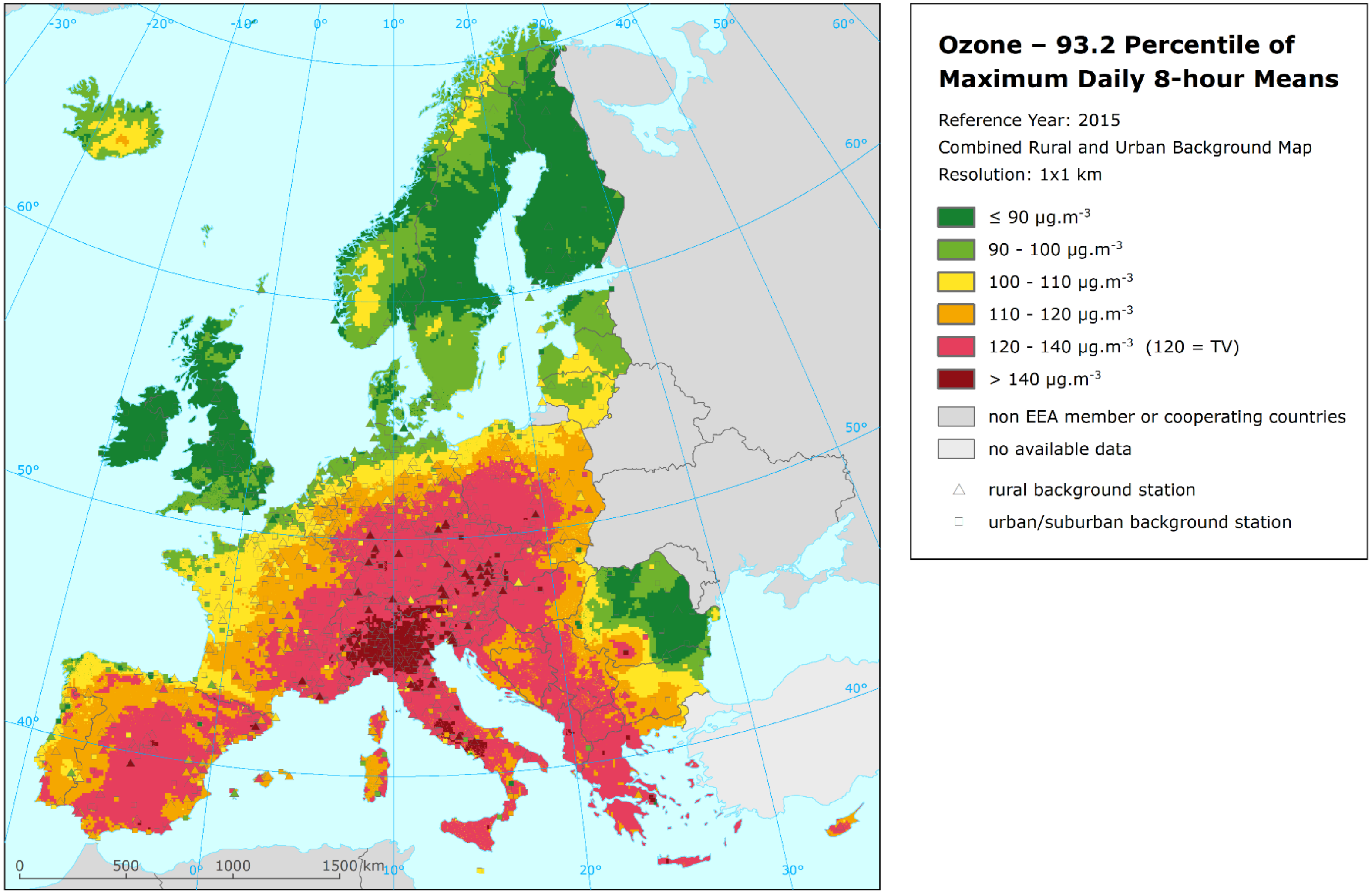

Map A5.5 Concentration map of ozone indicator SOMO35 including station points, 2015

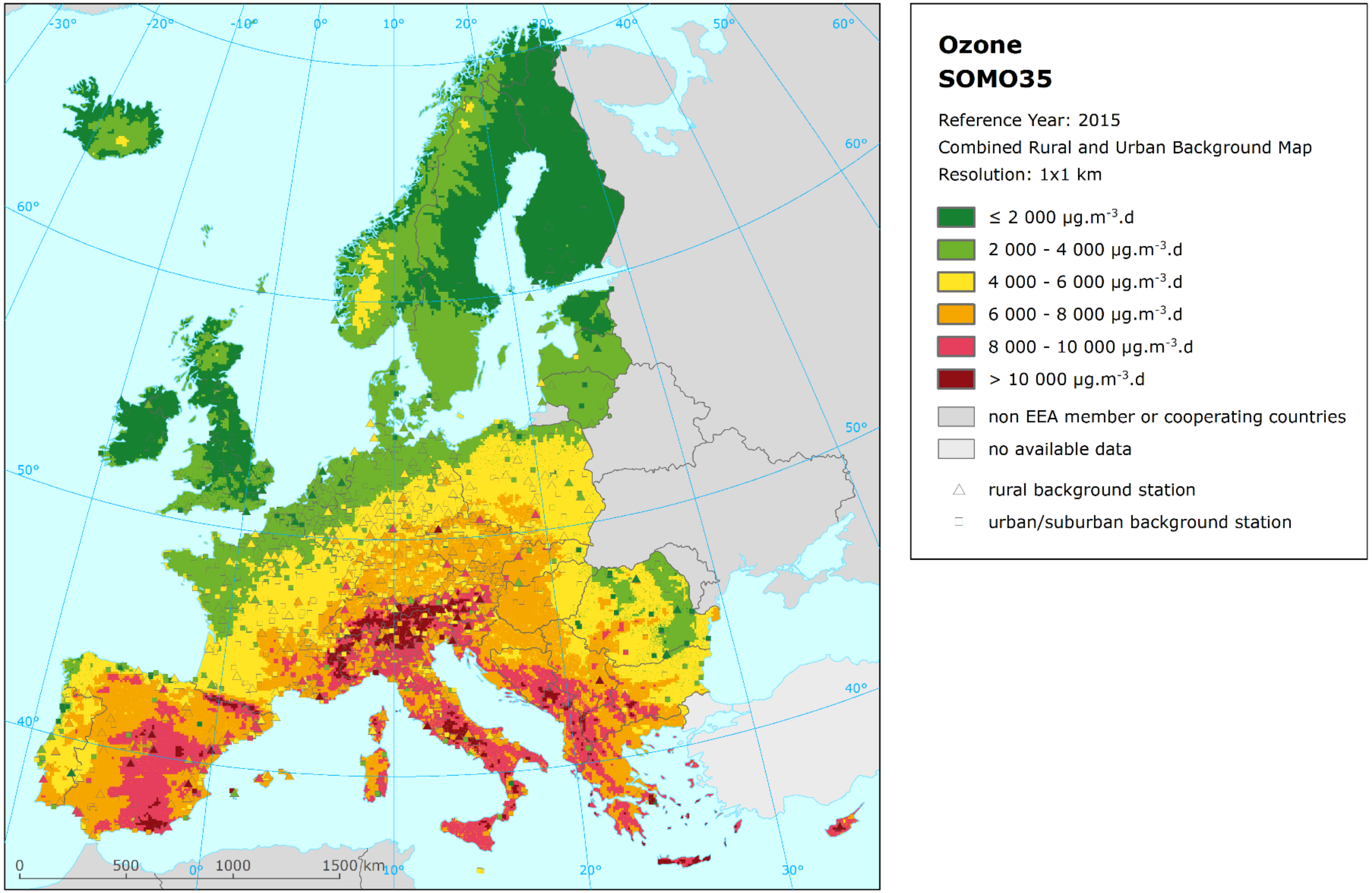

Map A5.6 Concentration map of ozone indicator AOT40 for vegetation including station points, rural air quality, 2015

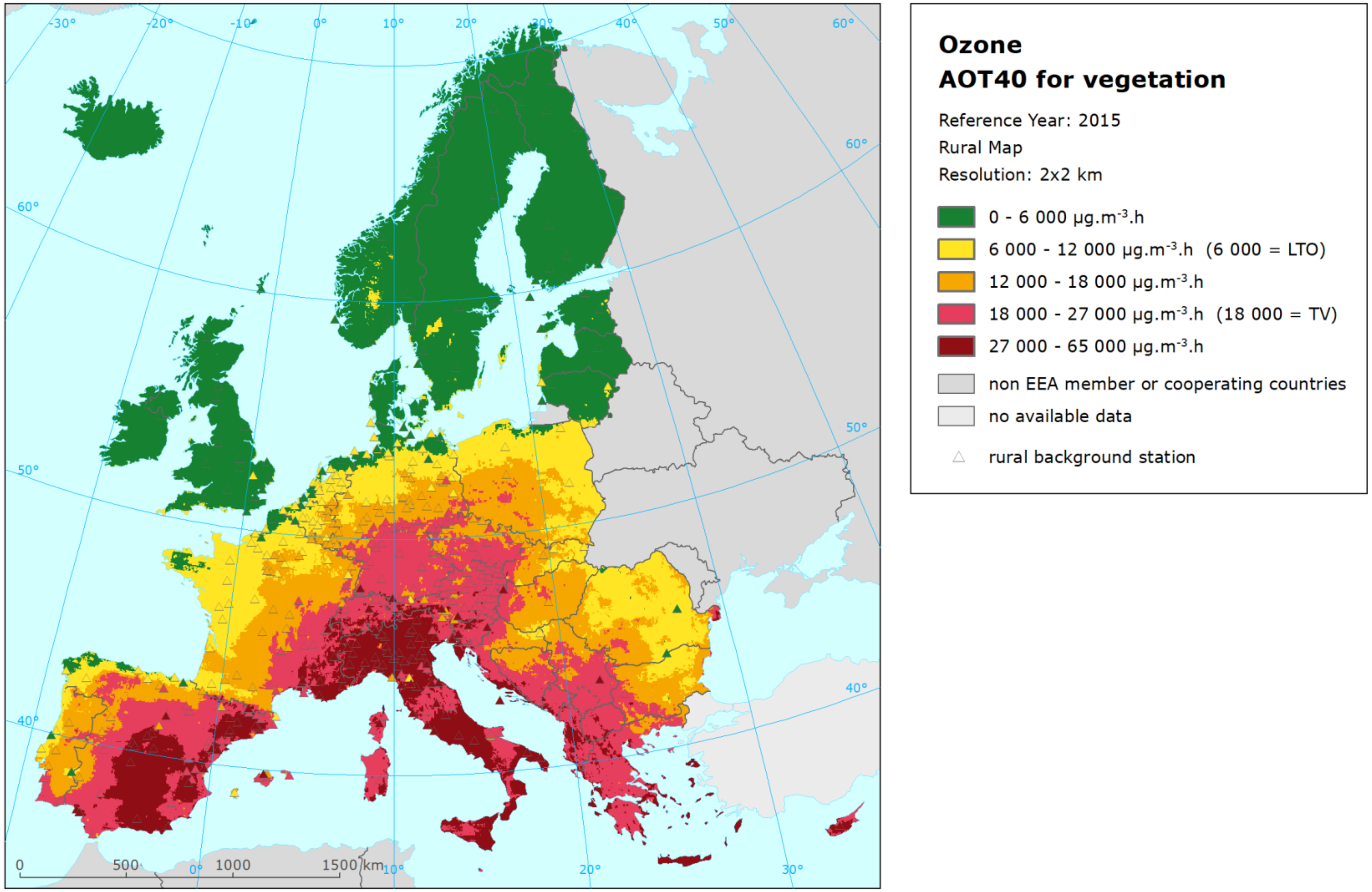

Map A5.7 Concentration map of ozone indicator AOT40 for forests including station points, rural air quality, 2015

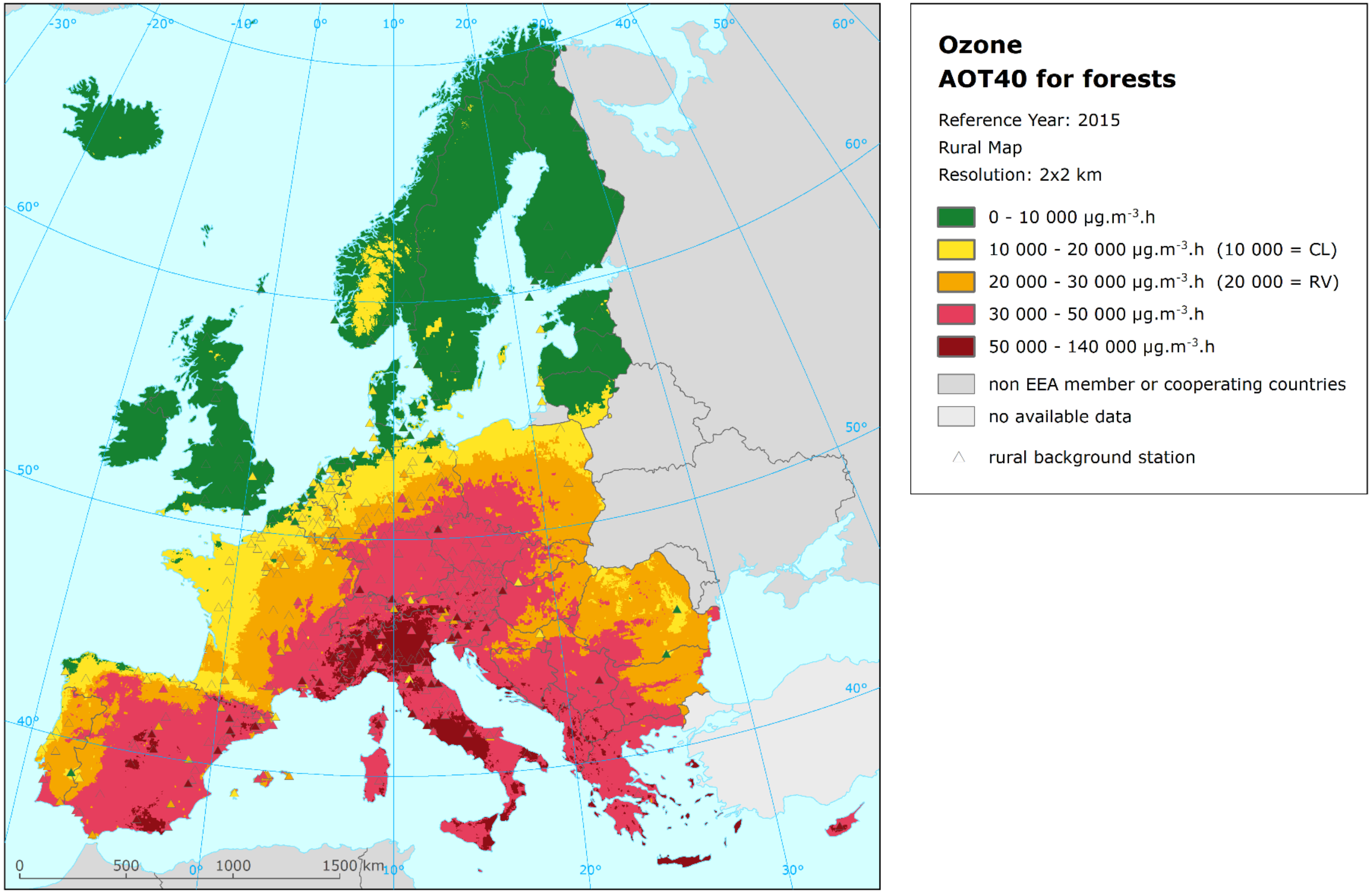

Map A5.8 Concentration map of NO_2 annual average including station points, 2015

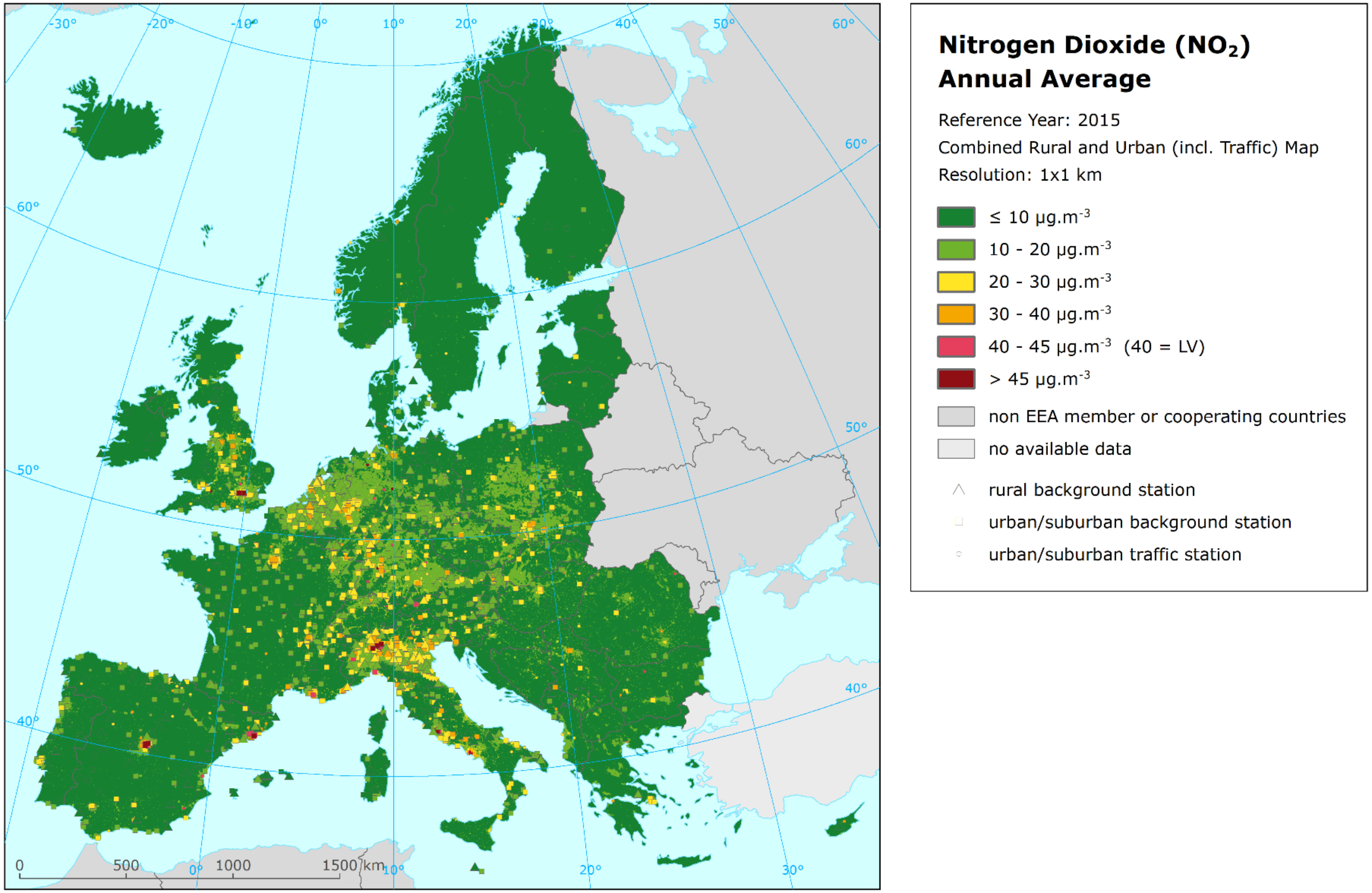

Map A5.9 Concentration map of NO_x annual average including station points, rural air quality, 2015